A&A 462, 481–494 (2007)
DOI: 10.1051/0004-6361:20053774

Astronomy & Astrophysics

New response functions for absorption-line indices from high-resolution spectra⋆

R. Tantalo, C. Chiosi, and L. Piovan

Department of Astronomy, University of Padova, Vicolo dell'Osservatorio 2, 35122 Padova, Italy
e-mail: [tantalo;chiosi;piovan]@pd.astro.it

Received 6 July 2005 / Accepted 4 August 2006

ABSTRACT

Using a huge library of 1-Å resolution spectra over a wide range of $\log T_{\rm eff}$, $\log g$ and [Fe/H] and for both solar and α-enhanced abundance ratios [α/Fe], we present theoretical absorption-line indices in the Lick system. First we derive the response functions ($\mathcal{RF}$s) for a wide range of $\log T_{\rm eff}$, $\log g$, [Fe/H], and [α/Fe] = +0.4 dex. The $\mathcal{RF}$s are commonly used to correct indices with solar [α/Fe] ratios to indices with [α/Fe] > 0. The $\mathcal{RF}$s vary not only with the type of star but also with metallicity. Second, with the aid of this and the fitting functions ($\mathcal{FF}$s), we derive the indices for single stellar populations and compare them with those obtained by previous authors. The new $\mathcal{RF}$s not only supersede the old ones, but also show that Hβ increases with the degree of enhancement. The new indices for single stellar populations are used with aid of the recursive minimum-distance method to derive the age, metallicity, and degree of enhancement of a sample of Galactic globular clusters for which these key parameters have been independently derived from the colour–magnitude diagram and/or spectroscopic studies. The agreement is remarkably good.

Key words. galaxies: abundances – galaxies: evolution – galaxies: formation

1. Introduction

The Lick system of absorption-line indices developed over the years by Burstein et al. (1984), Faber et al. (1985), Worthey (1992), Worthey et al. (1992, 1994), and Worthey (1994) was designed to infer the age and the metallicity of stellar systems, and of early-type galaxies in particular.

The Lick indices seem to have the potential of partially resolving the age-metallicity degeneracy that has long been known to affect the spectral energy distribution of stellar populations (Renzini & Buzzoni 1986)[1]. Thanks to it, the Lick system of indices has been extensively used by many authors (Bressan et al. 1996; Tantalo 1998; Tantalo et al. 1998; Trager et al. 2000b,a; Kuntschner 1998; Kuntschner & Davies 1998; Jørgensen 1999; Kuntschner 2000; Poggianti et al. 2001; Kuntschner et al. 2001; Vazdekis et al. 2001; Davies et al. 2001; Maraston et al. 2003; Thomas et al. 2003a,b; Thomas & Maraston 2003; Tantalo & Chiosi 2004a). The main result of all those studies is that, even in early-type galaxies, some recent episodes of star formation ought to occur so that we can explain the large scatter shown by the observational data for indices like Hβ commonly thought to be sensitive to the turn-off stars and consequently to their age.

The problem is, however, complicated further by a third parameter, i.e. the abundance ratios [α/Fe] (where α stands for all chemical elements produced by α-captures on lighter nuclei). Absorption-line indices like Mg2 and ⟨Fe⟩ measured in the central regions of galaxies are known to vary, passing from one galaxy to another (González 1993; Trager et al. 2000b,a). Looking at the correlation between Mg2 and ⟨Fe⟩ (or similar indices) for the galaxies in the above-quoted samples, Mg2 increases faster than ⟨Fe⟩, which is interpreted as due to the enhancement of α-elements in some galaxies. Since the classical paper by Burstein et al. (1988), the index Mg2 is also known to increase with the velocity dispersion (and hence mass and luminosity) of the galaxy. Based on this body of data, the conviction arose that the degree of enhancement in α-elements ought to increase, as the source passed from dwarf to massive early-type galaxies (Faber et al. 1992; Worthey et al. 1994; Matteucci 1994, 1997; Matteucci et al. 1998). These findings strongly affect the theory of galaxy formation, because super-solar [α/Fe] ratios require rather short star-formation time-scales, (see for instance the discussion of this topic by Chiosi & Carraro 2002), whereas the correlation with the velocity dispersion requires that the star formation time scale should get longer with decreasing galaxy mass. This does not agree with the predictions of the supernova-driven galactic wind model by Larson (1974), and instead agrees with those of N-Body-Tree-SPH models of early-type galaxies by Chiosi & Carraro (2002).

In the presence of α-enhanced chemical compositions, the ages and metallicities of early-type galaxies should be derived from indices in which α-enhancement is included. As noticed long ago by Worthey et al. (1992) and Weiss et al. (1995), indices for α-enhanced chemical mixtures of a given total metallicity are expected to differ from those of the standard case. On one hand, this spurred new generations of stellar models, isochrones, and SSPs with α-enhanced mixtures (Salasnich et al. 2000) and, on the other hand, led to many increasingly complex attempts to simultaneously derive, the age, metallicity, and degree of enhancement by fitting the observational indices to their theoretical counterparts (Tantalo et al. 1998; Trager et al. 2000b,a; Maraston et al. 2003; Thomas et al. 2003a,b; Thomas & Maraston 2003; Tantalo & Chiosi 2004a). The formal solution for ages, metallicities, and [α/Fe] ratios based on large samples of galaxies, e.g. the Trager et al. (1998) list, once more yields a wide range of

⋆ Appendix A is only available in electronic form at http://www.aanda.org

[1] An old metal-poor stellar population may happen to have the same spectral energy distribution as a young metal-rich one.

ages, metallicities, and abundance ratios, as amply discussed by Tantalo & Chiosi (2004a, hereafter TC04).

Although the picture emerging from the above studies is a convincing one, there are still several points of weakness intrinsic to even the state-of-the-art theoretical indices, which forces us to reconsider the whole problem. Let us examine in some detail (i) the foundations of the Lick indices; (ii) the various steps that are required to derive theoretical indices and their dependence on age, metallicity, and degree of enhancement; (iii) the current method of estimating these parameters from the indices; (iv) and, finally, comment briefly on a few points of controversy among different groups.

- The information contained in the stellar spectra concerning the effective temperature ($\log T_{\rm eff}$), gravity ($\log g$), and chemical composition (usually the parameter [Fe/H]) was in a system of indices measuring the strength of atomic and molecular lines (see Sect. 2). The Lick indices are defined and measured on a finite sample of stellar spectra with a fixed mean resolution of 8.4 Å, which in most cases differs from the resolution of theoretical spectra used in population synthesis.
- In order to make the general use of the Lick indices possible, Worthey et al. (1994) introduced the concept of the so-called fitting functions ($\mathcal{FF}$s). The indices for a large sample of stars with known atmospheric parameters ($\log T_{\rm eff}$, $\log g$, and [Fe/H]) are measured and then expressed as empirical polynomial fits that are in turn functions of these parameters. The major drawback of these $\mathcal{FF}$s is that they encompass a limited range of values as far as [Fe/H] is concerned. The sample of stars was indeed collected from the solar vicinity even if attempts to extend it to lower metallicities have been made (Idiart & de Freitas-Pacheco 1995; Cenarro et al. 2001, 2002). Metallicities that are much higher than those in the solar vicinity are simply not included for obvious reasons. A new library with an unprecedented coverage of atmospheric parameters is currently in progress by Sánchez-Blázquez et al. (2003) and Sanchez-Blázquez et al. (in preparation).
- Despite is being known that magnesium is perhaps enhanced with respect to iron ([Mg/Fe] > 0) in giant elliptical galaxies (see e.g. Worthey et al. 1992, and above), the collection of stellar spectra and $\mathcal{FF}$s did not allow for non-standard abundance ratios in the chemical composition. $\mathcal{FF}$s have been proposed to include the effect of non-standard abundance ratios have been proposed by Borges et al. (1995) limited to a few indices, e.g. Mg2 and NaD.
- A milestone was achieved by Tripicco & Bell (1995) who have modeled synthetic spectra of high-resolution (0.1 Å), degraded them to the mean 8.4 Å resolution of the Lick system, and derived from them the indices for three prototype stars, namely a cool-dwarf, a turn-off, and a cool-giant along a 5 Gyr isochrone matching the CMD of M 67 (in other words for three different combinations of $\log T_{\rm eff}$ and $\log g$). Even more important here, they studied the response of the indices to changes in the abundance ratios of individual elements. In other words, thanks to their $\mathcal{RF}$s, it was possible to evaluate the effect of abundance ratios that were different from solar.
- With the aid of the Tripicco & Bell (1995) $\mathcal{RF}$s and suitable algorithms, the indices with solar abundance ratios have been transformed into those for non solar abundance ratios. The algorithms in use are not unique, thus leading to uncertain results (see TC04 for more details).
- Passing now from individual stars to star clusters, reduced here to single stellar populations (SSPs) and galaxies (manifolds of SSPs), the derivation of theoretical indices (and spectra, magnitudes, and broad-band colours) is even more complicated because other ingredients intervene: (i) the construction of realistic isochrones for SSPs including all evolutionary phases, even the unusual ones that are known to appear at very high metallicities (see Bressan et al. 1994, and TC04); (ii) the initial mass function; (iii) and finally, in the case of galaxies, the past history of star formation and chemical enrichment weighing the contribution from stellar populations of different ages and chemical compositions (see e.g. Bressan et al. 1994, for all details). It is worth noting here that galaxy indices are almost always compared to SSP indices, thus neglecting the mix of stellar populations and missing important contributions from some peculiar components. For instance an old SSP of very high metallicity and/or a very old SSP of extremely low metal content would possess strong Hβ thus mimicking a young SSP of normal metallicity (see TC04 for more details). Integrated indices for model galaxies have been occasionally calculated and used (Tantalo 1998), but never systematically applied to this kind of analysis. This is a point that should be carefully investigated and kept in mind when comparing data with theory.

If for solar abundance ratios the dependence of the indices on age and metallicity is currently on rather solid ground except for the effect of some unusual phases of stellar evolution, the same does not happen for non-solar abundance ratios, because it is still highly controversial how some indices (Hβ, in particular) at a given age and total metallicity would respond to changes in the abundance ratios. According to TC04, SSPs of the same age and metallicity but with different degrees of enhancement in α-elements may have significantly different Hβ; in short, keeping age and metallicity constant, Hβ should increase with the increasing degree of enhancement (see the discussion in Sect. 4.2 for more details). Based on this, Tantalo & Chiosi (2004b) suggested an alternative, complementary interpretation of the large scatter in Hβ shown by early-type galaxies of the local universe in two-indices diagnostic planes like Hβ versus [MgFe]. In summary: (i) most probably the majority of galaxies (those with H$\beta \leq 2$) are very old objects of the same age (say approximately 13 Gyr) but with a different degree of enhancement; (ii) only for galaxies with H$\beta > 2$, the presence of secondary star-forming activity ought to be invoked. High-resolution synthetic spectra for stars with a good coverage of gravity, effective temperature, chemical composition, and degree of enhancement in α-element can greatly alleviate the above difficulties and shed light on these important issues. In principle, indices can be straightforwardly calculated from the spectra with no need of $\mathcal{FF}$s, $\mathcal{RF}$s, and suitable algorithms to take the α-element enhancement into account. In this paper, we limit ourselves to presenting new $\mathcal{RF}$s and a simple correction algorithm. Full exploitation of the possibilities offered by the high-resolution spectra is left to a forthcoming study.

The plan of the paper is as follows. Section 2 deals with the theory of absorption-line indices, the definition of enhancement, and the dependence of the $\mathcal{FF}$s of the Lick system on the main stellar parameters, comments on the fact that they are based on solar-scaled chemical compositions and briefly describes the $\mathcal{FF}$s by Borges et al. (1995) in which the effect of enhancing α-elements is taken into account for some indices. Section 3 briefly reviews the method of the $\mathcal{RF}$s by Tripicco & Bell (1995) and the current algorithms that are adopted to transfer

solar-scaled indices into the corresponding ones with α-enhancement. Section 4 presents the library of synthetic spectra in use and our new $\mathcal{RF}$s for many types of star all across the entire HR diagram. The indices and $\mathcal{RF}$s are calculated for both original (1 Å) and the Lick (around 8 Å) resolution of the spectra. The new $\mathcal{RF}$s (and indices) are strictly equivalent to those of Tripicco & Bell (1995). Together with the classical $\mathcal{FF}$s, they can be used to pass from solar to α-enhanced mixtures. Section 5 presents the indices for SSPs at varying metallicity, degree of enhancement, and age. After briefly summarising the index definition for SSPs, the library of stellar spectra with medium resolution that are specifically used to this purpose, and the sources of stellar models and isochrones, the new indices are presented and compared to those in previous studies. Section 6 compares the new indices with the data for globular clusters. Finally, Sect. 7 contains some concluding remarks.

2. Theory of absorption-line indices

In this section we deal with the theory of absorption-line indices. We summarize their definition for a single star (Sect. 2.1) and present two different methods for enhancing the abundance of α-elements with respect to that of Fe, i.e. at constant or increasing total metallicity, and examines the implications in some detail (Sect. 2.2). We also recall the dependence of the $\mathcal{FF}$s of the Lick system on the main stellar parameters, comments on the fact that they are based on solar-scaled chemical compositions and briefly describes the $\mathcal{FF}$s by Borges et al. (1995) in which the effect of enhancing α-elements is taken into account for some indices (Sect. 2.4).

2.1. Definition

In the Lick system of absorption-line indices (see Burstein et al. 1984; Faber et al. 1985; Worthey et al. 1994), the definition of an index with pass-band $\Delta\lambda$ is different according to whether it is measured in equivalent width (*EW*) or magnitude (Mag):

$$I_1 = \Delta\lambda\left(1 - \frac{F_1}{F_c}\right) \quad (EW) \tag{1}$$

$$I_1 = -2.5\log\left(\frac{F_1}{F_c}\right) \quad (\mathrm{Mag}) \tag{2}$$

where F_1 and F_c are the fluxes in the line and pseudo-continuum, respectively (e.g. see Fig. 5). The flux F_c is calculated at the central wavelength of the absorption-line by interpolating the fluxes in the midpoints of the red and blue pseudo-continua bracketing the line (Worthey et al. 1994). The pass-bands adopted for the 25 indices of the Lick system are taken from Trager et al. (1998, see also Worthey et al. 1994). Because of the finite sampling of the Lick library of template stellar spectra and their different resolution with respect to theoretical spectral libraries currently in usage, Eqs. (1) and/or (2) cannot be applied straightforwardly. As already mentioned, the problem is bypassed by means of the $\mathcal{FF}$s (Worthey et al. 1994).

We also add the index D4000 centred at the 4000 Å break. It is defined as the ratio of the average flux F_ν (in erg s^{-1} cm^{-2} Hz^{-1}) in two bands at the long- and short-wavelength side of the discontinuity (Bruzual 1983), i.e.

$$D4000 = \frac{\lambda_2^{\mathrm{b}} - \lambda_1^{\mathrm{b}}}{\lambda_2^{\mathrm{r}} - \lambda_1^{\mathrm{r}}} \frac{\int_{\lambda_1^{\mathrm{r}}}^{\lambda_2^{\mathrm{r}}} F_\nu \mathrm{d}\lambda}{\int_{\lambda_1^{\mathrm{b}}}^{\lambda_2^{\mathrm{b}}} F_\nu \mathrm{d}\lambda}. \tag{3}$$

The blue and red pass-bands are from 3750 to 3950 Å and 4050 to 4250 Å, respectively.

2.2. α-enhanced chemical compositions

As pointed out by Bressan (2005, private communication), the current definition of enhancement in α-elements of a chemical mixture is not univocal and may be a source of uncertainty when comparing results from different authors and in particular when using synthetic spectra with α-enhanced chemical compositions. The problem can be reduced to the statement: enhancing of α-elements can be made either at constant or at varying total metallicity Z.

2.2.1. Enhancement at constant Z

Let us take a certain mixture of elements with total metallicity Z (sum of all elements heavier than He), then denote with N_j the number density of the generic element j with mass abundance X_j ($N_j = \rho N_0 X_j/\mathcal{A}_j$, where ρ is the mass density, N_0 the Avogadro number, and $\mathcal{A}_j$ the mass number), and define the quantity A_j as

$$A_j = \log\left(\frac{N_j}{N_{\mathrm{H}}}\right) + 12. \tag{4}$$

Ignoring elements from H to He, in this mixture $\sum_j X_j = Z$ by definition. The abundance by mass with respect to Fe is given by

$$\left[\frac{X_j}{X_{\mathrm{Fe}}}\right] = \log\left(\frac{X_j}{X_{\mathrm{Fe}}}\right) - \log\left(\frac{X_j}{X_{\mathrm{Fe}}}\right)_\odot, \tag{5}$$

or in terms of A_j, by

$$\left[\frac{X_j}{X_{\mathrm{Fe}}}\right] = \left(A_j - A_j^\odot\right) - \left(A_{\mathrm{Fe}} - A_{\mathrm{Fe}}^\odot\right). \tag{6}$$

Keeping the number density of Fe, i.e. $(A_{\mathrm{Fe}} - A_{\mathrm{Fe}}^\odot) = 0$ constant and changing other elements (enhancement), we obtain

$$A_j^{\mathrm{enh}} = \left[\frac{X_j}{X_{\mathrm{Fe}}}\right] + A_j^\odot. \tag{7}$$

Inserting the adopted $[X_j/X_{\mathrm{Fe}}]$ and the solar values for $A_j^\odot$ by Grevesse & Sauval (1998), respectively, from Eq. (4), we can calculate the new abundances by mass for any pattern of α-enhanced elements. In general, the sum of the X_j will be different from Z. The mass abundance must therefore be re-scaled to the true value X'_j given by

$$X'_j = \frac{X_j}{\sum X_j}. \tag{8}$$

Finally we may define the "total enhancement factor" Γ_Z as

$$\Gamma_Z = -\log\left(\frac{X'_{\mathrm{Fe}}}{X_{\mathrm{Fe}}^\odot}\right), \tag{9}$$

from which we immediately obtain the relationship between Γ_Z and the new value of the Fe abundance in α-enhanced mixtures:

$$\log\left(\frac{X'_{\mathrm{Fe}}}{X'_{\mathrm{H}}}\right) = \log\left(\frac{X_{\mathrm{Fe}}}{X_{\mathrm{H}}}\right)_\odot + \log\left(\frac{X'_{\mathrm{H}}}{X_{\mathrm{H}}^\odot}\right) - \Gamma_Z. \tag{10}$$

It is worth mentioning that, at given total metallicity Z, different patterns of $[\mathrm{X_j/X_{Fe}}]$ may yield the same total enhancement

Table 1. Abundance ratios for the solar-scaled and α-enhanced mixtures in which enhancement is performed at constant total metallicity.

	$\Gamma_Z = 0$			$\Gamma_Z = 0.25$		
Element	A_{el}	X'_{el}/Z	[X_{el}/Fe]	A_{el}	X'_{el}/Z	[X_{el}/H]
C	8.52	0.1627	0.00	8.52	0.0840	–0.2459
N	7.92	0.0477	0.00	7.92	0.0246	–0.2459
O	8.83	0.4430	0.40	9.23	0.5747	0.1541
Ne	8.08	0.0985	0.40	8.48	0.1277	0.1541
Na	6.33	0.0020	0.00	6.33	0.0010	–0.2459
Mg	7.58	0.0374	0.40	7.98	0.0485	0.1541
Si	7.55	0.0407	0.40	7.95	0.0528	0.1541
S	7.33	0.0280	0.40	7.73	0.0363	0.1541
Ca	6.36	0.0037	0.40	6.76	0.0049	0.1541
Ti	5.02	0.0002	0.40	5.42	0.0003	0.1541
Cr	5.67	0.0010	0.00	5.67	0.0005	–0.2459
Fe	7.50	0.0725	0.00	7.50	0.0374	–0.2459
Ni	6.25	0.0043	0.00	6.25	0.0022	–0.2459

The solar scaled values are taken from Grevesse & Sauval (1998). The enhancement factor [X_{el}/Fe] = +0.4 dex is the same as in Castelli & Kurucz (2004).

factor Γ_Z. This fact strongly influences the procedure for deriving α-enhanced indices because each elemental species leads to a different effect.

Finally, for the sake of comparing the results from enhancing at varying metallicity (see below), we enhance the elements as in Munari et al. (2005) by the ratio [α/Fe] = +0.4 dex and derive the total enhancement factor Γ_Z and the abundances listed in Table 1. This definition of enhancement has already been adopted by Tantalo et al. (1998), Trager et al. (2000b,a), Maraston et al. (2003), Thomas et al. (2003a,b), Thomas & Maraston (2003), and TC04. It is indeed the most popular one for calculating theoretical indices for SSPs.

2.2.2. Enhancement at varying metallicity

Let us relax the condition that X_H, X_{He}, and Z remain constant. By supposing that some elements are increased by the factor $[X_i/X_{Fe}] > 0$, the total metallicity will be greater, the abundance of H and He will be different (decrease), and the condition $\sum X_j = 1$, where j runs over all elements (starting from H), will not be satisfied. In order to recover it, the new abundances are re-scaled by means of the relations

$$N'_j = \frac{N_j}{\sum N_j} \qquad X'_j = \frac{X_j}{\sum X_j}, \tag{11}$$

where once again j runs over all elements. In this case Γ_Z defined in Sect. 2.2.1 can no longer be used to rank the degree of total enhancement because it would vary with the metallicity. We indeed need to find a new, metallicity-independent, definition for the total enhancement factor. Then, Γ_Z can be simply replaced by the ratio proposed earlier by Salaris et al. (1993),

$$\Gamma_\alpha = \left[\frac{\sum X_i^{\alpha,\mathrm{enh}}}{\sum X_j^{\alpha}} \right], \tag{12}$$

where $\sum X_i^{\alpha,\mathrm{enh}}$ is the sum of the abundances of all enhanced elements and $\sum X_j^{\alpha}$ the sum of the abundances for all α-elements that are left unchanged. The square brackets have their usual meaning. Thereinafter Γ_α is used to indicate the global enhancement ratio. Given a set of enhanced elements, Γ_α does not change with the metallicity; it changes, however, with the specific pattern of enhanced elements and degree of enhancement. To a certain extent the same Γ_α may correspond to different patterns of abundances[2].

This definition of enhancement is, for instance, adopted by Castelli & Kurucz (2004) on which the library of synthetic spectra by Munari et al. (2005) is based. The difference brought about by the two definitions is not trivial and leads to different results.

2.3. General remarks

With the first definition (constant metallicity), indices can be simply compared for solar scaled and α-enhanced mixtures with the same Z. With the second one for any degree of enhancement, one has to establish a priori the corresponding total metallicity before making the above comparison. For the sake of illustration we present in Table 2, but limited it to the case of solar composition [$X = 0.7347, Y = 0.248, Z = 0.0170$], how the metallicity Z and abundance of H and He would vary when the some heavy elements are enhanced by +0.4 dex.

The new abundances should be compared with those presented in Table 1 and obtained at constant Z. Due to the effect of enhancement (the same on the same elements), the new chemical parameters become [$X = 0.7219, Y = 0.244, Z = 0.0340$]: the metallicity is almost doubled and the abundances of H and He are slightly decreased. Finally, in Table 3 for all metallicities [M/H] of the Munari et al. (2005) library, we present the relationship between the chemical parameters $[X, Y, Z]$ for solar-scaled mixtures and the corresponding ones for the enhancement [α/Fe] = +0.4 dex ($\Gamma_\alpha = 0.4$). They are indicated as $[X', Y', Z']$.

As in this study we have adopted the Castelli & Kurucz (2004) model atmospheres and the companion Munari et al. (2005) synthetic spectra, we also adopt their definition of enhancement. Throughout this paper, when comparing results for the "same" metallicity and different degree of enhancement, we will make use of the relationship shown in Table 3. It is worth noting that this relationship changes with the adopted degree of enhancement. This is a point to keep in mind when comparing results from different authors and those obtained with the definition of enhancement at constant metallicity. Taking advantage of the fact that the same enhancement factor [α/Fe] is adopted in the Munari et al. (2005) library, we indicate our α-enhanced mixtures simply with $\Gamma_\alpha = 0.4$.

2.4. The Worthey et al. (1994) and Borges et al. (1995) fitting functions

In the following we adopt the Worthey et al. (1994) $\mathcal{FF}$s, extended however to high temperature stars ($T_{\mathrm{eff}} \approx 10\,000$ K) as reported in Longhetti et al. (1998). Recently new $\mathcal{FF}$s have also become available for the λ4000 break by Gorgas et al. (1999) and Ca II triplet by Cenarro et al. (2001). All these $\mathcal{FF}$s depend on stellar effective temperature, gravity, and metallicity ([Fe/H]). They do not explicitly include the effect of α-enhancement.

However, many studies have emphasised that absorption-line indices should also depend on the detailed pattern of chemical abundances (Barbuy 1994; Idiart & de Freitas-Pacheco 1995; Weiss et al. 1995; Borges et al. 1995), in particular when some elements are enhanced with respect to the solar value. Empirical $\mathcal{FF}$s for Mg2 and NaD, in which the effect of enhancement

[2] With the pattern of abundances we have adopted, $\Gamma_\alpha = 0.4$. It also worth noticing that by applying this new definition of enhancement to the previous case we would also obtain $\Gamma_\alpha \sim 0.4$.

Table 2. Abundance ratios for the solar-scaled and α-enhanced mixtures in which enhancement is performed varying the total metallicity Z.

	$\Gamma_\alpha = 0$				$\Gamma_\alpha = 0.4$				
Element	$A_{\rm el}$	$X_{\rm el}$	$X_{\rm el}/Z$	$X_{\rm el}$/H	[$X_{\rm el}$/Fe]	$A_{\rm el}$	$X_{\rm el}$	$X_{\rm el}/Z$	$X_{\rm el}$/H
H	12.00	0.734709	–	1.0000	0.00	12.00	0.721943	–	1.0000
He	10.93	0.248336	–	0.3380	0.00	10.93	0.244022	–	0.3380
C	8.52	0.002899	0.1709	0.0039	0.00	8.52	0.002849	0.0837	0.0039
N	7.92	0.000849	0.0501	0.0012	0.00	7.92	0.000834	0.0245	0.0012
O	8.83	0.007884	0.4650	0.0107	0.40	9.23	0.019460	0.5717	0.0270
Ne	8.08	0.001768	0.1043	0.0024	0.40	8.48	0.004365	0.1282	0.0060
Na	6.33	0.000036	0.0021	0.0000	0.00	6.33	0.000035	0.0010	0.0000
Mg	7.58	0.000674	0.0397	0.0009	0.40	7.98	0.001662	0.0488	0.0023
Si	7.55	0.000726	0.0428	0.0010	0.40	7.95	0.001793	0.0527	0.0025
S	7.33	0.000500	0.0295	0.0007	0.40	7.73	0.001233	0.0362	0.0017
Ca	6.36	0.000067	0.0039	0.0001	0.40	6.76	0.000165	0.0048	0.0002
Ti	5.02	0.000004	0.0002	0.0000	0.40	5.42	0.000009	0.0003	0.0000
Cr	5.67	0.000018	0.0010	0.0000	0.00	5.67	0.000017	0.0005	0.0000
Fe	7.50	0.001287	0.0759	0.0018	0.00	7.50	0.001265	0.0372	0.0018
Ni	6.25	0.000076	0.0045	0.0001	0.00	6.25	0.000075	0.0022	0.0001
	$X = 0.7347$ $Y = 0.248$ $Z = 0.0170$				$X = 0.7219$ $Y = 0.244$ $Z = 0.0340$				

The solar-scaled values are taken from Grevesse & Sauval (1998). The enhancement factor [$X_{\rm el}$/Fe] = +0.4 dex ($\Gamma_\alpha = 0.4$) is the same as in Castelli & Kurucz (2004).

Table 3. Relationship between the chemical composition parameters $[X, Y, Z]$ for solar-scaled and α-enhanced mixtures ($[X', Y', Z']$) according to the definition of Castelli & Kurucz (2004). The data refers to the mixtures in Table 2.

$\Gamma_\alpha = 0$				$\Gamma_\alpha = 0.4$			
X	Y	Z	[M/H]	X'	Y'	Z'	[M/H]$'$
0.7473	0.253	0.0002	–2.0	0.7471	0.253	0.0004	–1.7
0.7470	0.252	0.0005	–1.5	0.7465	0.252	0.0011	–1.2
0.7461	0.252	0.0017	–1.0	0.7448	0.252	0.0035	–0.7
0.7433	0.251	0.0054	–0.5	0.7391	0.250	0.0110	–0.2
0.7347	0.248	0.0170	0.0	0.7219	0.244	0.0340	0.3
0.7087	0.240	0.0517	0.5	0.6725	0.227	0.1003	0.8

This relationship holds true only for the case under consideration. It changes indeed with [α/Fe].

is considered, were presented by Borges et al. (1995). For all other indices, one has to use the Worthey et al. (1994) $\mathcal{FF}$s, in which the effect of enhancement is missing, but for the re-scaling of [Fe/H] given by Eqs. (10) and/or (11). A great deal of the effect of enhancing α-elements is simply lost.

3. The current correcting algorithm: the Tripicco & Bell (1995) response functions

A general method designed to include the effects of enhancement on all indices at once has been suggested by Tripicco & Bell (1995), who introduced the concept of $\mathcal{RF}$s. From model atmospheres and spectra for three prototype stars, i.e. a cool-dwarf star (CD) with $T_{\rm eff} = 4575$ K and $\log g = 4.6$, a turn-off (TO) star with $T_{\rm eff} = 6200$ K and $\log g = 4.1$, and a cool-giant (CG) star with $T_{\rm eff} = 4255$ K and $\log g = 1.9$, they calculate the reference indices I_0 for the solar abundance ratios. Separately, doubling the abundance X_i of the C, N, O, Mg, Fe, Ca, Na, Si, Cr, and Ti in steps of $\Delta[X_i/{\rm H}] = 0.3$ dex, they determine the variation $\Delta I = I_{\rm enh} - I_0$ in units of the observational error σ_0. The indices I_0, the observational error σ_0 and the normalized ΔI are given in Tables 4–6 of Tripicco & Bell (1995).

The definition of the generic $\mathcal{RF}$ to be used for arbitrary variations $\Delta[X_i/{\rm H}]$ is

$$R_{0.3}(X_i) = \frac{1}{I_0}\,\frac{\Delta I}{\Delta[X_i/{\rm H}]}\,0.3.$$

The $\mathcal{RF}$s for cool-dwarfs, cool-giants, and turn-off stars constitute the milestones of the calibration. They are used by Trager et al. (2000b), Thomas et al. (2003a), and TC04 to transfer indices with solar abundance ratios to those enhanced in α-elements by means of two different algorithms. As they are not strictly equivalent, some clarification is needed here.

Without providing a formal justification, Trager et al. (2000b) propose that the fractional variation of an index to changes in the chemical parameters is the same as that for the reference index I_0 according to the relation

$$\frac{\Delta I}{I} = \frac{\Delta I_0}{I_0} = \left\{\prod_i [1 + R_{0.3}(X_i)]^{\frac{[X_i/{\rm H}]}{0.3}}\right\} - 1 \qquad (13)$$

where $R_{0.3}(X_i)$ are the $\mathcal{RF}$s we have defined above. The explanation of relation (13) has been provided by TC04 to which the reader should refer for details. The advantage of this formulation is that no particular constraint is required on the sign of I_0, and the ΔI given by Tripicco & Bell (1995) is straightforwardly used.

A different reasoning was followed by Thomas et al. (2003a). Briefly, they start from the observational hint that in galactic stars Mg2 $\propto \exp([{\rm Mg/H}])$ (see Borges et al. 1995), next assume that all indices depend exponentially on the abundance ratios and introduce the variable $\ln I \propto [X_i/{\rm H}]$, then expand $\ln I$ in the Taylor series, and by replacing the partial derivatives with respect to abundances by the finite incremental ratio of

Tripicco & Bell (1995), they express the fractional variation of an index to changes in the abundance ratios as

$$\frac{\Delta I}{I} = \left\{ \prod_i \exp\left(R_{0.3}(X_i)\right)^{\frac{[X_i/\mathrm{H}]}{0.3}} \right\} - 1. \quad (14)$$

The reader is referred to Thomas et al. (2003a) for the formal derivation of relation (14). Although relations (13) and (14) may look similar, actually they are not so because in the latter the partial derivatives in the Taylor expansion have been replaced by the finite incremental ratios. This topic has been thoroughly discussed in TC04.

As emphasized by Trager et al. (2000b) and Thomas et al. (2003a), Eqs. (13) and (14) while ensuring that the indices tend to zero for small abundances, let them increase with the exponent $[X_i/\mathrm{H}]/0.3$. For abundances higher than $[X_i/\mathrm{H}] = 0.6$ dex, the exponent may became too large and consequently both types of correction may diverge. Second, the use of Eqs. (13) and (14) requires that the sign of the index to be corrected is the same as the corresponding I_0 in Tripicco & Bell (1995). In general this holds good. It may, however, happen that the signs do not coincide. Furthermore, some of the indices I_0 in Tripicco & Bell (1995) are negative so that the $\ln I$ variable cannot be defined and the Taylor expansions can no longer be applied. To overcome this potential difficulty, Thomas et al. (2003a) apply a correcting procedure thereby forcing the negative reference indices I_0 of Tripicco & Bell (1995) to become positive. This occurs in particular for Hβ of cool-dwarf stars (and other indices as well). The argument is that by neglecting non-LTE effects Tripicco & Bell (1995) underestimate the true values of Hβ so that negative values found for temperatures lower than approximately 4500 K should be shifted to higher, positive values (see for instance Fig. 12 in Tripicco & Bell 1995). We suspect that any change to the values tabulated by Tripicco & Bell (1995) may be risky for a number of reasons: (i) the $\mathcal{FF}$s were derived from a set of data that include a significant number of stars with negative values of Hβ; (ii) the incremental ratios by Tripicco & Bell (1995) have been calculated for particular stars (stellar spectra) with assigned $T_{\rm eff}$, $\log g$, and I_0. Changing the reference I_0 while leaving the incremental ratios (partial derivatives) unchanged may not be very safe; (iii) the replacement of the partial derivatives with the Tripicco & Bell (1995) incremental ratios may be risky when dealing with exponential functions; (iv) the corrections found by Thomas et al. (2003a) for a number of indices are quite large; (v) finally, the use of $\ln I$ as a dependent variable requires that only positive values for I_0 are considered.

The application of Eqs. (13) and (14) by TC04 has generated different and highly controversial results for some indices, Hβ in particular, under unusual enhancements in some elements. In brief, TC04 presented grids of indices with α-enhanced abundance ratios. The indices were derived from the Salasnich et al. (2000) stellar models and isochrones with the abundance ratios by Ryan et al. (1991) and corrected by means of Eq. (13) of Trager et al. (2000b). The unusual abundance ratio for Ti ([Ti/Fe] = 0.63, which implies [Ti/H] = 0.2634 when the definition of enhancement at constant Z is adopted), together with the interpolation among the fractional variations of the calibrating stars, yielded Hβ strongly increasing with Γ_Z. This immediately reflected on the ages assigned to galaxies by means of the minimum-distance method of Trager et al. (2000b,a), widely used by TC04. The strong impact of Ti on Hβ is due to the high $\mathcal{RF}$s of this element for cool-dwarfs in the Tripicco & Bell (1995) calibration. After decreasing the ratio [Ti/Fe] to zero as in Trager et al. (2000b) or to 0.3 as in Thomas et al. (2003a), the results by TC04 were in close agreement with those by the other authors. It is worth recalling that the ratio [Ti/H] entering Eqs. (13) and (14) was 0 in Trager et al. (2000b), 0.023 in Thomas et al. (2003a), and nearly 0.2 in TC04 with obvious consequences[3]. The effect was also confirmed by adopting the more recent determinations by Carney (1996) and Habgood (2001) of the [Ti/Fe] in globular clusters that yield $\langle[\mathrm{Ti/Fe}]\rangle \simeq 0.25 \div 0.30$, and by Gratton et al. (2003) for a sample of metal-poor stars with accurate parallaxes, for which they yield $\langle[\mathrm{Ti/Fe}]\rangle \simeq 0.20 \pm 0.05$ (TC04). In any case, the controversy about the correcting technique still remain. It can be reduced to the statement: does Hβ increase (significantly) with [α/Fe] or not? Or, even worse, does it decrease with it? According to Thomas et al. (2003a), there should be no difference in Hβ at increasing [α/Fe]. The analysis below will clarify that this is not the case.

4. The new response functions

In this section we present the $\mathcal{RF}$s we derive from high-resolution spectra and a simple algorithm to pass from solar-scaled to α-enhanced indices. We start by presenting the library of synthetic spectra in use in Sect. 4.1. Second, we calculate indices and $\mathcal{RF}$s. The analysis is made in two steps: (i) adopting the definition of the indices in the Lick system and the Tripicco & Bell (1995) definition of $\mathcal{RF}$s but using the stellar spectra at 1-Å resolution, we derive the indices for the calibrating stars (Sect. 4.2). These indices constitute the backbone of the new grid of Tripicco & Bell (1995)-like $\mathcal{RF}$s given in Sect. 4.3. Owing to the large body of data on the Lick system, it is worth providing indices and $\mathcal{RF}$s from spectra having the same resolution of the Lick system. They are presented in Sect. 4.4.

4.1. The high-resolution spectra

The spectra used in the present analysis are taken from a partial pre-release of the 2500–10 500 Å extensive synthetic spectral library computed by Munari et al. (2005). The spectral library is based on the new grid of ATLAS9 model atmospheres computed by Castelli & Kurucz (2004) for new opacity distribution functions that include, among other characteristics, the replacement of the solar abundances from Anders & Grevesse (1989) with those from Grevesse & Sauval (1998) and the TiO line-list from Kurucz (1993) with that of Schwenke (1998). The Munari et al. (2005) spectral library includes more than 200 000 spectra at resolutions of 20 000 and 2000 (the latter matching the SLOAN spectra), as well as uniform dispersions of 1 Å/pix and 10 Å/pix.

The library covers very large intervals of effective temperature (3500–50 000 K), gravities ($0 \le \log g \le 5.0$), metallicities ($-2.5 \le [Z/Z_\odot] \le 0.5$), microturbulent velocities (0, 1, 2 and 4 km s^{-1}), a dozen rotational velocities, and finally two degrees of enhancement ([α/Fe] = 0. and +0.4 dex). For all other details, see Munari et al. (2005). The library is still under construction. When completed, it will provide a powerful tool for predicting absorption-line indices and exploring their applications. A strictly coordinated library of synthetic spectra is the one published by Zwitter et al. (2004) for the GAIA and RAVE wavelength range, amounting to 183 588 spectra covering a similar parameter space.

In this work we made use of the version at 1 Å/pix with temperature interval 4000–13 000 K, gravity $0 \le \log g \le 5.0$,

[3] Similar considerations apply to all other elements listed in the Tripicco & Bell tabulation.

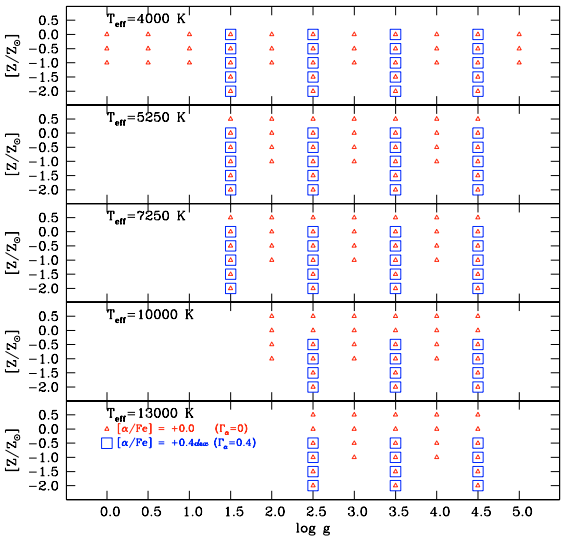

Fig. 1. Typical coverage in the atmospheric parameters, and Γ_α of the 1-Å resolution spectra used in this study. The filled-triangles are for chemical compositions with solar abundance ratios [α/Fe] = 0 (Γ_α = 0), whereas the open-squares are α-enhanced mixtures with [α/Fe] = +0.4 dex (Γ_α = 0.4).

metallicities –2.5 ≤ [$Z/Z_\odot$] ≤ 0.5, null micro-turbulence, and rotational velocities, and with two degrees of enhancement ([α/Fe] = 0. and +0.4 dex, i.e. Γ_α = 0. and 0.4, respectively). It is worth recalling that, for Γ_α = 0.4, the temperature coverage is narrower at high metallicities, i.e. from 4000 to 7250 K for [$Z/Z_\odot$] = 0 and from 10 000 to 13 000 for [$Z/Z_\odot$] = 0.5.

The temperature, gravity, and metallicity coverage of the body of stellar spectra in use here is summarised in Fig. 1 (as already mentioned in the case of the highest metallicity and α-enhanced spectra, the temperature interval is smaller). Each panel is for a different effective temperature, as indicated. The symbols show the combination of metallicity, expressed here in spectroscopic notation as [$Z/Z_\odot$] = log($Z/Z_\odot$), and gravity (log g) for which a spectrum has been calculated. The triangles are for Γ_α = 0, whereas the squares are for Γ_α = 0.4. The parameters span the following ranges: two values of [α/Fe] (or Γ_α), i.e. [α/Fe] = 0 and +0.4 dex; six values of [$Z/Z_\odot$], i.e. –2.0, –1.5, –1.0, –0.5, 0, and 0.5 for [α/Fe] = 0, and five values ([$Z/Z_\odot$] = –2.0, –1.5, –1.0, –0.5, and 0) for [α/Fe] = +0.4 dex; five values of $T_{\rm eff}$, i.e. 4000, 5250, 7250, 10 000, and 13 000 K for most of the spectra, they are reduced to three values (4000, 5250, and 7250 K) for [α/Fe] = +0.4 dex and [$Z/Z_\odot$] = 0; finally eleven values of log g going from 0 to 5.0 in steps of 0.5. The spectral grid is only a sub-set of the original model atmosphere grid. It is, however, fully adequate to the purposes of this study. The range of wavelength in each spectrum goes from 2500 Å to 10 500 Å with a resolution of 1 Å. The flux F_λ is in erg s^{-1} cm^{-2} Å^{-1}. In Fig. 2 for the sake of illustration we show the spectral energy distribution for the model with $T_{\rm eff}$ = 4000 K, log g = 4.5, [$Z/Z_\odot$] = –0.5, micro-turbulence velocity k = 2 km s^{-1}, and Γ_α = 0 (left panel) and 0.4 (right panel). It fairly represents the case of a cool-dwarf star.

4.2. Indices from 1-Å resolution spectra

With the aid of Eqs. (1) and (2) and the pass-bands of Trager et al. (1998), we filter the energy distribution of each star in our grids and derive the indices. They are not strictly equivalent to the Lick system because the spectra in use have 1-Å resolution, whereas those on the Lick system have significantly smaller resolution (approximately 8.4 Å) that also depends on the wavelength interval (see Worthey & Ottaviani 1997, for all details). This case will be considered in detail in Sect. 4.4.

The data for all the set of indices are not displayed, but are partly given in and partly recovered from Tables A.1 through A.5 to be described in Appendix A. We limit ourselves to showing the variation in the index Hβ in Fig. 3 across the HR-diagram for the case with [$Z/Z_\odot$] = –0.5 and with Γ_α = 0 and 0.4. In the same diagram, we also plot two isochrones with the same metal content taken from the Padova Library (Girardi private communication): the ages are 0.01 Gyr and 10 Gyr. The grids of calibrating stars cover most of the HR-diagram in which real stars are found.

4.3. Response functions for 1-Å resolution spectra

We present here the analogue of the Tripicco & Bell (1995) $\mathcal{RF}$s. The only difference is that they cannot be evaluated for separate increases in the abundance of individual species [α_i/Fe] but only for all elements enhanced with respect to the solar value lumped together. However, now the dependence of the $\mathcal{RF}$s on temperature, gravity, metallicity, and enhancement can be evaluated in detail. This was not the case with the Tripicco & Bell (1995) calibration, which depended on three stars with solar metallicity. We start by calculating the differences

$$(\delta I)_{T_{\rm eff},g,[Z/Z_\odot]} = I_{\rm enh} - I_{\rm sol} \qquad (15)$$

taken at fixed log $T_{\rm eff}$, log g, and metallicity ([$Z/Z_\odot$]) and varying Γ_α from 0 to 0.4, whose corresponding indices are indicated as $I_{\rm sol}$ and $I_{\rm enh}$, respectively. The differences for all the sets of values are given in Tables A.1–A.5 for [$Z/Z_\odot$] = –2.0, –1.5, –1.0, –0.5, and 0.

In the ten panels of Fig. 4 we show the case of Hβ. Each panel displays the variation in Hβ with changing log $T_{\rm eff}$ (left panels) and/or log g (right panels). For any metallicity passing from Γ_α = 0 to 0.4, (i) at given log $T_{\rm eff}$ δHβ increases with increasing log g; (ii) at given log g δHβ increases with decreasing log $T_{\rm eff}$. For most cases δHβ is positive, i.e. the index Hβ increases with increasing Γ_α; or, in other words, Hβ for α-enhanced mixtures is greater than the solar case, keeping all other parameters constant. The increase is always significant, approximately 0.1 ÷ 0.2, but it can amount to nearly 1.4 for stars of low $T_{\rm eff}$ and high gravity, roughly in the intervals covered by cool-dwarf and old turn-off stars, which are the most interesting in view of the discussion below.

Why is there such an increase with Γ_α? The answer lies in the relative variation in $F_{\rm l}$ and $F_{\rm c}$. In the case of Hβ (our prototype index), we derive the variation (δI) passing from solar to α-enhanced mixtures. Upon differentiating the index with respect to $F_{\rm l}$ and $F_{\rm c}$ ($\frac{\partial I}{\partial F_{\rm l}} = -\frac{1}{F_{\rm c}}\Delta\lambda$ and $\frac{\partial I}{\partial F_{\rm c}} = \frac{F_{\rm l}}{F_{\rm c}^2}\Delta\lambda$), we obtain

$$(\delta I) = \Delta\lambda \left(\frac{F_{\rm l}}{F_{\rm c}}\right)_{\rm sol} [\Delta\ln F_{\rm c} - \Delta\ln F_{\rm l}] \qquad (16)$$

where $\Delta\ln F_{\rm l}$ and $\Delta\ln F_{\rm c}$ are the differences in the line and continuum fluxes passing from enhanced to solar. Plugging the values of $F_{\rm l}$ and $F_{\rm c}$ as appropriate, it turns out that the index increases with α. What happens is best illustrated in Fig. 5 which, when limited to the case of a typical cool-dwarf with $T_{\rm eff}$ = 4000, log g = 4.5, and [$Z/Z_\odot$] = –0.5 (Z = 0.008), shows how the index Hβ is built up and how it varies, passing from

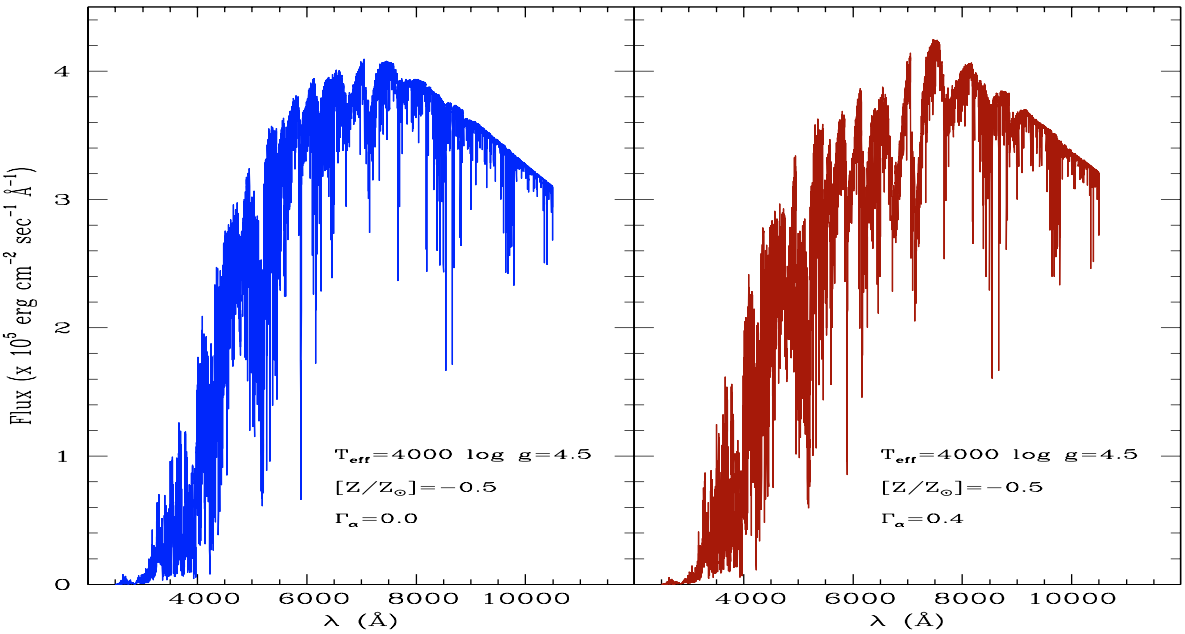

Fig. 2. Two theoretical spectra of the Munari et al. (2005) library. *Left-hand panel*: spectral energy distribution F_λ for the star with $T_{\rm eff}$ = 4000 K, $\log g$ = 4.5, $[Z/Z_\odot]$ = –0.5, Γ_α = 0. The wavelength is in Å. F_λ is in erg s^{-1} cm^{-2} Å^{-1} and the resolution is 1 Å. *Right-hand panel*: the same but for Γ_α = 0.4.

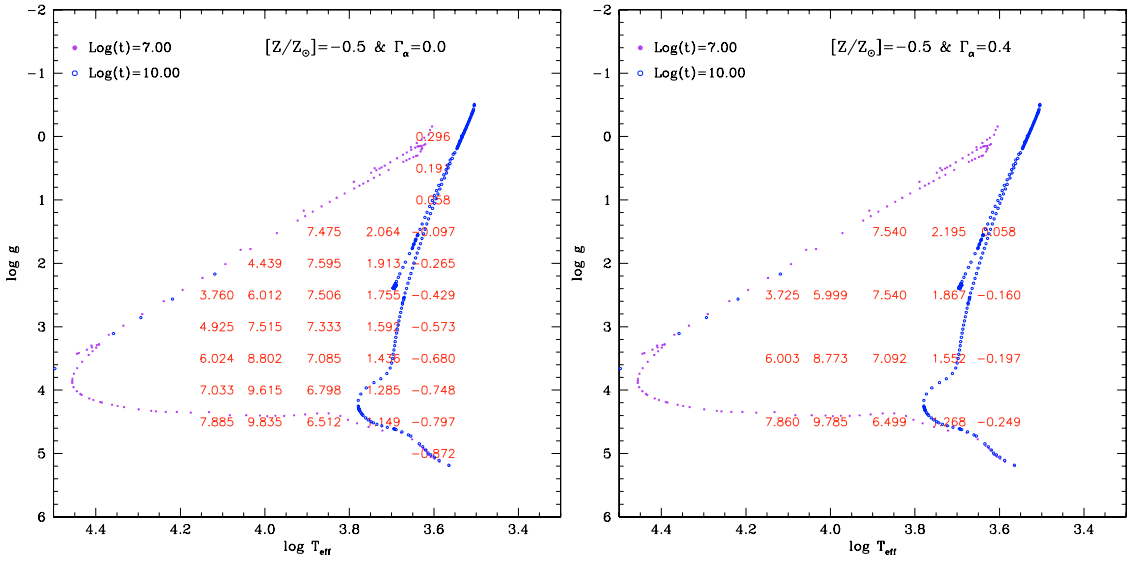

Fig. 3. *Left panel*: variation in Hβ from 1-Å resolution spectra across the HR-diagram in the $\log g$ versus $\log T_{\rm eff}$ plane. Each value of Hβ corresponds to a star (theoretical spectrum) of given $\log g$, $\log T_{\rm eff}$, and $[Z/Z_\odot]$. The case under consideration is for $[Z/Z_\odot]$ = –0.5 and Γ_α = 0. In the same diagram, we also plot two isochrones of the Padova Library with the same metallicity (Z = 0.008) and ages of 0.01 and 10 Gyr. *Right panel*: The same as in the left panel but for Γ_α = 0.4.

Γ_α = 0 to Γ_α = 0.4. First in the bottom panel we display the ratio $F_{\lambda,\rm enh}/F_{\lambda,\odot}$ and the pass-bands defining the index Hβ. The absorption in the α-enhanced spectrum is significantly larger than in the solar-scaled one. The effect is greater in the blue pseudo-continuum and central band than in the red pseudo-continuum. This means that α-enhanced mixtures distort the spectrum in such a way that simple predictions cannot be made. This is due to the contribution of hundreds of molecular and atomic lines falling into the spectral regions over which the index is defined. Second, in the upper panel we show the spectral energy distribution of the solar-scaled and α-enhanced spectra and once more the pass-bands for Hβ. Different symbols indicate the mean fluxes in the three pass-bands and the interpolation of the pseudo-continuum to derive $F_{\rm c}$ in the case of solar-scaled spectrum. The same but for the α-enhanced mixture. The increase of Hβ passing from solar to α-enhanced abundance ratios is straightforward.

With the differences (δI), the equivalent of the Tripicco & Bell (1995) $\mathcal{RF}$s [i.e. $R_{0.3}(X_i)$s] is

$$R_{0.4}(\alpha) = \frac{1}{I_{\rm sol}} \frac{I_{\rm enh} - I_{\rm sol}}{\Delta[\alpha/{\rm Fe}]} 0.4 \qquad (17)$$

where the symbol α reminds the reader that only variations for the all elements enhanced at a time are available (the products in Eqs. (13) and (14) would extend only over one term). Work is in progress to repeat the analysis made by Tripicco & Bell (1995)

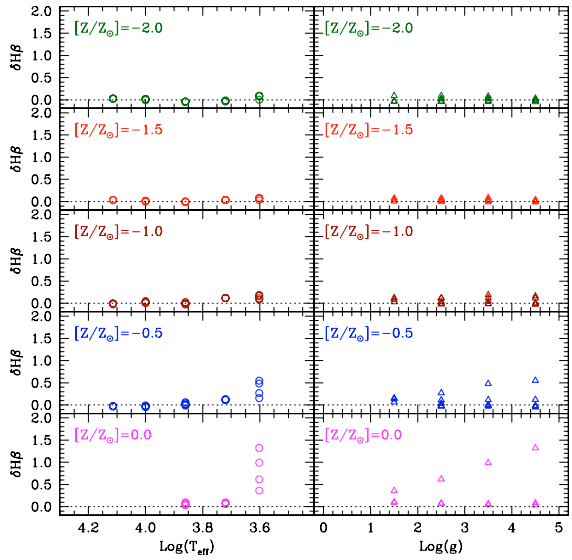

Fig. 4. Variations of the index Hβ derived from 1-Å resolution spectra, passing from solar to α-enhanced chemical mixture. We plot the difference $(\delta I)_{T_{\rm eff},g,[Z/Z_\odot]}$ as a function of the atmospheric parameters as indicated. *Left-hand panels*: for each $\log T_{\rm eff}$, δHβ increases with $\log g$. *Right-hand panels*: for each $\log g$, δHβ decreases with $\log T_{\rm eff}$.

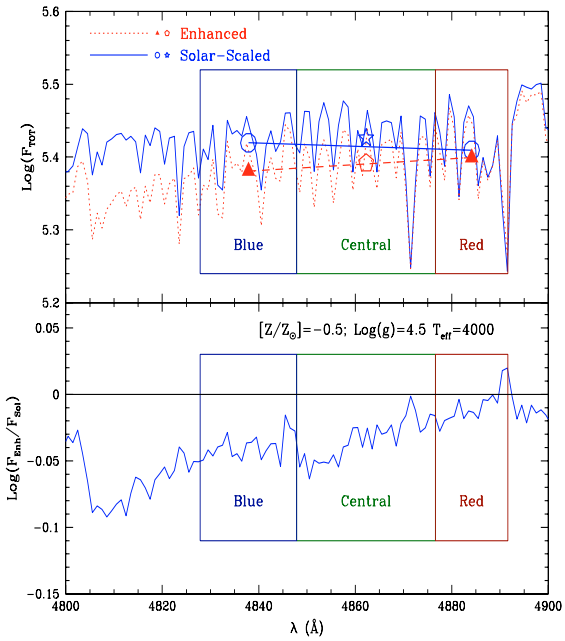

Fig. 5. 1-Å resolution spectra. We show how the index Hβ is built up in a cool-dwarf with $T_{\rm eff}$ = 4000, $\log g$ = 4.5 and $[Z/Z_\odot]$ = −0.5 both for the solar scaled and the total enhancement factor Γ_α = 0.4. The boxes shows the blue, central, and red pass-bands used to define the index Hβ. The bottom panel shows the ratio $F_{\lambda,\rm enh}/F_{\lambda,\odot}$. The absorption in the α-enhanced spectrum is significantly larger than the solar-scaled one. The effect is larger in the blue wing of the pseudo-continuum and central band than in the red pseudo-continuum. The upper panel shows the spectral energy distribution of the solar-scaled (solid line) and α-enhanced (dotted line) spectrum. The open-circles and star show the mean fluxes in the three pass-band and the interpolation of the pseudo-continuum to derive $F_{\rm c}$ in the case of solar-scaled spectrum. The filled-triangles and pentagon are the same for the α-enhanced mixture. The increase in Hβ passing from solar to α-enhanced abundance ratios is straightforward.

exactly, i.e. to provide partial $\mathcal{RF}$s by separately enhancing individual elements at a time. This would improve upon the $\mathcal{RF}$s and yet maintain the $\mathcal{FF}$s until high-resolution spectra becomes a general tool.

Having done that and for the sake of a preliminary investigation of the whole subject, we linearly extrapolate the results obtained for $[Z/Z_\odot]$ = −2.0, −1.5, −1.0, −0.5, and 0 to the higher value of metallicity, i.e. $[Z/Z_\odot]$ = 0.5 for the temperatures lower than 10 000 K and also to $[Z/Z_\odot]$ = 0 and 0.5 for the temperatures of 10 000 and 13 000 K.

The extrapolation is safe, because $(\delta I) = I_{\rm enh} - I_{\rm sol}$ smoothly changes with the metallicity at given $\log T_{\rm eff}$ and $\log g$. This is shown in Fig. 6 but limited to the case of Hβ. The dependence is almost linear and nearly insensitive to gravity for $T_{\rm eff}$ = 5250, 7250, 10 000 and 13 000 K. The case of $T_{\rm eff}$ = 4000 deserves little attention, because δHβ tends to increase with $[Z/Z_\odot]$ and gravity. Adopting the simple linear extrapolation on $[Z/Z_\odot]$, we probably underestimate δHβ for the high metallicities.

4.4. Indices and response functions at the Lick resolution

The 1-Å resolution spectra were degraded to the resolution of the Lick system following the procedure and the FWHM of Worthey & Ottaviani (1997). The new spectral energy distribution of each star in the calibrating grid were filtered to derive the indices and the whole procedure described in Sect. 4.3 was repeated. The data are given in Tables A.6–A.10 of Appendix A. These represent the analogue of Tables A.1 through A.5. As a comparison we show the differences $(\delta I)_{T_{\rm eff},g,[Z/Z_\odot]} = I_{\rm enh} - I_{\rm sol}$ in Fig. 7. In general, the new values of $(\delta I)_{T_{\rm eff},g,[Z/Z_\odot]}$ shares the same trends as in the previous case, but are only slightly smaller. The most noticeable change is for Hβ, whose largest (δI) amounts to 1.1 instead of 1.4 for the case of a cool-dwarf ($T_{\rm eff}$ = 4000, $\log g$ = 4.5) and $[Z/Z_\odot]$ = 0. Also in this case we linearly extrapolate the data to higher values of the metallicity for the sake of the preliminary investigation. Indices and (δI) fully consistent with the Lick system are used in the discussion below.

5. SSP indices from $\mathcal{FF}$s and new $\mathcal{RF}$s

Owing to the large body of data and synthetic indices in the Lick system, it might be worth deriving indices still based on the $\mathcal{FF}$s but in which the old $\mathcal{RF}$s are replaced by the new ones. This means that indices for a solar-scaled mixture are calculated as amply described in TC04, whereas those for $\Gamma_\alpha > 0$ are obtained according to the following equation

$$I_{i,\rm enh} = I_{i,\rm sol} + \delta\mathcal{I}_i \qquad (18)$$

where $I_{i,\rm sol}$ is the solar-scaled index of the generic star in the SSP and $I_{i,\rm enh}$ the same but corrected for enhancement by $\delta\mathcal{I}_i$. This is derived by linearly interpolating the new $\mathcal{RF}$s (listed in Tables A.6–A.10) both in $\log g$ and $\log T_{\rm eff}$ and taking the enhancement-metallicity relationship into account as discussed in Sect. 2.2[4].

5.1. Definition of SSP indices

The integrated indices of SSPs can be derived in the following way. We start from the flux in the absorption-line of the generic star of the SSP, $F_{{\rm l},i}$

$$F_{{\rm l},i} = F_{{\rm c},i}\left(1 - \frac{I_{{\rm l},i}}{\Delta\lambda}\right) \quad (EW) \qquad (19)$$

[4] It is worth recalling that an equivalent procedure would be to use Eq. (13) combined with (17) instead of Eq. (18).

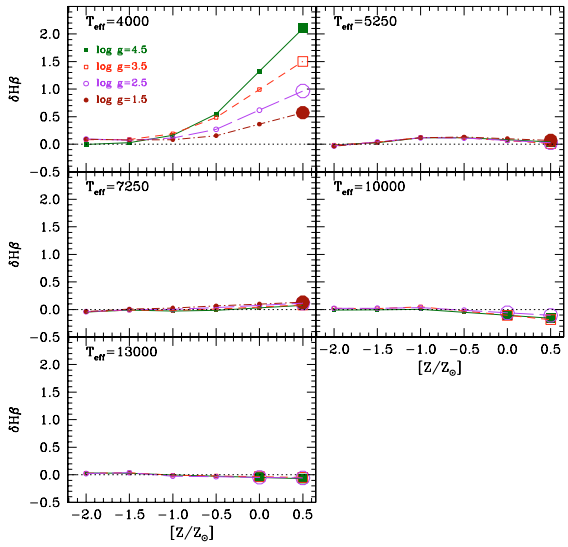

Fig. 6. 1-Å resolution spectra. We show the variation δHβ as a function of the metallicity $[Z/Z_\odot]$ at fixed $\log T_{\rm eff}$ and $\log g$, as indicated. In each panel the big symbols display the value of δHβ linearly extrapolated to the metallicity $[Z/Z_\odot] = 0$ for $T \leq 7250$ K and up to 0.5 for $T = 1000$ and 13 000 K.

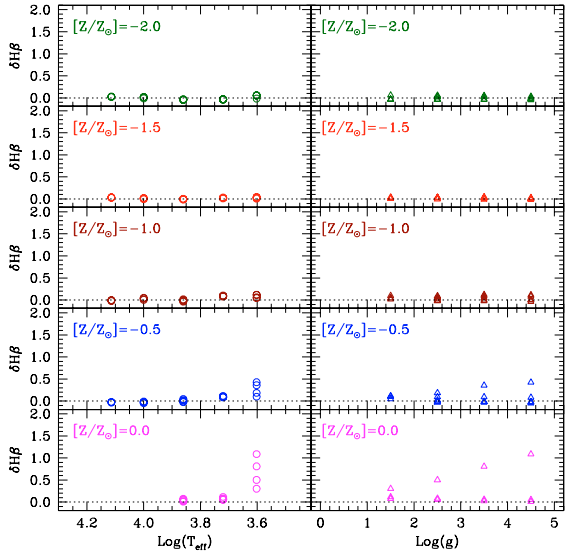

Fig. 7. The same as in Fig. 4 but for spectra degraded to the resolution of the Lick system (see Sect. 4.4). In the various panels we show the variations in the index Hβ passing from solar to α-enhanced chemical mixture. We plot the difference $(\delta I)_{T_{\rm eff},g,[Z/Z_\odot]}$ as a function of the atmospheric parameters, as indicated. *Left-hand panels*: for each $T_{\rm eff}$ δHβ increases with $\log g$. *Right-hand panels*: for each $\log g$ δHβ decreases with $\log T_{\rm eff}$.

$$F_{{\rm l},i} = F_{{\rm c},i} 10^{-0.4 I_{{\rm l},i}} \quad \text{(Mag)} \tag{20}$$

where $I_{{\rm l},i}$ is the index derived from the $\mathcal{FF}$s using the $\log T_{\rm eff}$, $\log g$, and chemical composition of the star, and, in the case of α-enhancement, also corrected according to Eq. (18). $F_{{\rm c},i}$ is the pseudo-continuum flux, $F_{{\rm l},i}$ the flux in the pass-band, and $\Delta\lambda$ is the same as in Eq. (1). Flux $F_{{\rm c},i}$ is calculated by interpolating to the central wavelength of the absorption-line, the fluxes in the midpoints of the red and blue pseudo-continua bracketing the line (Worthey et al. 1994).

To calculate flux $F_{{\rm c},i}$ of a generic star, one needs the theoretical spectrum of the same star. To be able to compare our results based on the new $\mathcal{RF}$s with the old ones by Trager et al. (2000b), Thomas et al. (2003a), and TC04 based on low-resolution spectra, we have to make use of stellar spectra with similar resolution. Therefore we leave aside the library of high-resolution spectra by Munari et al. (2005) and adopt the low-resolution one amalgamated by Girardi et al. (2002) and adopted by TC04. As the backbone of this library are the Kurucz ATLAS9 model atmospheres and stellar spectra, there is partial consistency between the spectra adopted to evaluate the pseudo-continuum and the 1-Å resolution spectra adopted to derive the new $\mathcal{RF}$s.

Once the fluxes $F_{{\rm l},i}$ and $F_{{\rm c},i}$ for a single star are known, the contribution is weighed on the relative number of stars of the same type in the SSP. Therefore the integrated index is given by

$$I_{\rm l}^{\rm SSP} = \Delta\lambda \left(1 - \frac{\sum_i F_{{\rm l},i} N_i}{\sum_i F_{{\rm c},i} N_i}\right) \quad (EW) \tag{21}$$

$$I_{\rm l}^{\rm SSP} = -2.5 \log \left(\frac{\sum_i F_{{\rm l},i} N_i}{\sum_i F_{{\rm c},i} N_i}\right) \quad \text{(Mag)} \tag{22}$$

where N_i is the number of stars in the bin.

When computing actual SSPs, single stars are identified to the isochrone elemental bins defined in such a way that all relevant quantities – i.e. luminosity, $\log T_{\rm eff}$, $\log g$ and mass – vary by small amounts. In particular, the number of stars in an isochrone bin is given by

$$N_i = \int_{m_a}^{m_b} \phi(m) {\rm d}m \tag{23}$$

where m_a and m_b are the minimum and maximum star mass in the bin and $\phi(m)$ is the mass function in number. These are the equations adopted to calculate the indices of SSPs.

Finally, in view of the discussion below, it is worth reminding the reader of the definition of two indices that are commonly used but that do not belong to the original Lick system:

$$\langle {\rm Fe} \rangle = 0.5 \times ({\rm Fe5270} + {\rm Fe5335})$$

$$[{\rm MgFe}] = \sqrt{{\rm Mgb} \times (0.5 \times {\rm Fe5270} + 0.5 \times {\rm Fe5335})}.$$

5.2. Stellar models and isochrones

For the purposes of this study, we adopt the Padova Library of stellar models and companion isochrones according to Girardi et al. (2000). This set of stellar models/isochrones differs from the classical one by Bertelli et al. (1994) for the efficiency of convective overshooting and the prescription for the mass-loss rate along the asymptotic red giant branch (AGB) phase. The stellar models extend from the zero-age mean sequence (ZAMS) up to either the start of the thermally pulsing AGB phase (TP-AGB) or to carbon ignition. No details on the stellar models are given here; they can be found in Girardi et al. (2000, 2002). Suffice it to mention that: (i) in low-mass stars passing from the tip of red giant branch (T-RGB) to the horizontal branch (HB) or clump, mass-loss by stellar winds is included according to the Reimers (1975) rate with $\eta = 0.45$; (ii) the whole TP-AGB phase is included in the isochrones with ages older than 0.1 Gyr according to the algorithm of Girardi & Bertelli (1998) and the mass-loss rate of Vassiliadis & Wood (1993); (iii) four chemical compositions are considered as listed in Table 4.

5.3. Results for SSP indices on the Lick resolution

Going into a detailed description of the dependence of the absorption-line indices for SSPs on age, chemical composition,

Table 4. Chemical composition as a function of metallicity for the SSPs in use.

Z	Y	X
0.008	0.248	0.7440
0.019	0.273	0.7080
0.040	0.320	0.6400
0.070	0.338	0.5430

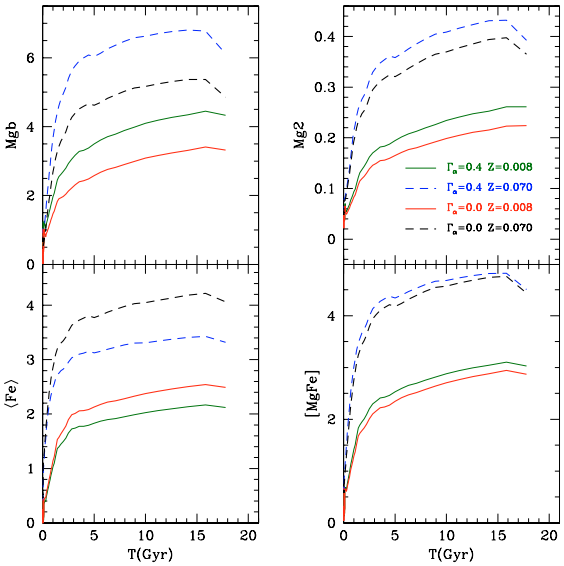

Fig. 8. Indices calculated with the Lick resolution, the old $\mathcal{FF}$s, and the new $\mathcal{RF}$s. The panels show the temporal variation of four different indices.

and Γ_α, is beyond the scope of this study[5]. Suffice it to show the temporal evolution of nine important indices in Figs. 8 and 9, i.e. Mgb, Mg2, ⟨Fe⟩, [MgFe], and the Balmer Lick Hβ, HγF, HδF, HγA, and HδA, for the following combinations of metallicity and Γ_α, namely $Z = 0.008$ (solid lines) and $Z = 0.070$ (broken lines), $\Gamma_\alpha = 0.$ (heavy lines) and $\Gamma_\alpha = 0.4$ (light lines). The age goes from 0.01 to 18 Gyr. These results are very similar, although not identical, to those found by TC04 adopting the same library of stellar spectra, the Worthey et al. (1994) $\mathcal{FF}$s, the old $\mathcal{RF}$s of Tripicco & Bell (1995) and the algorithm of Trager et al. (2000b). Finally, we note that the most controversial result in the studies by TC04 and Tantalo & Chiosi (2004b), i.e. the increase in Hβ with [α/Fe] (and/or Γ_Z and/or Γ_α) at fixed age and metallicity, is recovered by the present analysis.

5.4. Passing from old to new $\mathcal{RF}$s

Comparing the present results with previous ones in literature is not an easy task because the strict analogues do not exist. In brief, the models by Trager et al. (2000b,a), Maraston et al. (2003), Thomas et al. (2003a,b), Thomas & Maraston (2003), and TC04 are calculated with the definition of enhancement at constant Z, the classical $\mathcal{FF}$s of Worthey et al. (1994), the old $\mathcal{RF}$s of Tripicco & Bell (1995), and either Eqs. (13) or (14) to pass from solar-scaled to α-enhanced mixtures. The present models adopt the definition of enhancement at increasing Z, the classical $\mathcal{FF}$s of Worthey et al. (1994), the new $\mathcal{RF}$s calculated

[5] The complete grids of absorption-line indices are available from the authors upon request and/or can be downloaded from the web site `http://dipastro.pd.astro.it/galadriel`

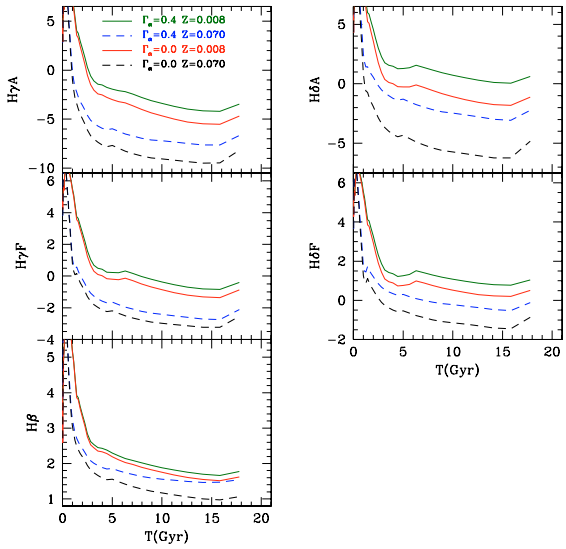

Fig. 9. The same as Fig. 8 but for the Balmer Lick indices.

in this work, and Eq. (18) to pass from solar-scaled to α enhanced indices.

In addition to this, there are differences arising from the quality of the spectra for the calibrating stars adopted by Tripicco & Bell (1995) and Munari et al. (2005). Owing to the many improvements in the physics of stellar atmospheres introduced by Munari et al. (2005) and Castelli & Kurucz (2004), the more recent compilations for the solar abundances and many other details that are summarised in Sect. 4.1, the new $\mathcal{RF}$s likely supersede the old ones.

Despite these major drawbacks, it might be useful to compare the present models, indicated as $I_{N\mathcal{RF}}$, with those calculated with the old procedure, indicated as $I_{O\mathcal{RF}}$. The latter have been explicitly calculated with the abundances listed in Table 1, i.e. by using the same enhancement ([α/Fe] = +0.4 dex) but the definition with constant Z (i.e. $\Gamma = 0.25$ and $\Gamma_\alpha = 0.4$), the Tripicco & Bell (1995) $\mathcal{RF}$s, and Eq. (13).

For the sake of brevity, we compare four indices, namely Hβ, Mgb, ⟨Fe⟩, and Mg2, for three metallicities ($Z = 0.008$, 0.019, and 0.070), and $\Gamma_\alpha = 0$ and 0.4 (the same values hold good for both definitions of total enhancement). This choice for the metallicity will allow us to check cases for which the $\mathcal{RF}$s have been extrapolated. Furthermore, passing from the $I_{O\mathcal{RF}}$ to the $I_{N\mathcal{RF}}$ at given Z, we have also taken into account the correlation between Γ_α and Z (and/or [M/H]) discussed in Sect. 2.2 (see Table 3). The correlations between $I_{O\mathcal{RF}}$ and $I_{N\mathcal{RF}}$ are shown in Fig. 10. In each panel three groups of models are displayed whose metallicity increases, going from bottom-left to top-right, whereas the age increases as indicated. Along each curve the age goes from 1 to 18 Gyr as in Figs. 8 and 9.

For ⟨Fe⟩, there is no significant difference between the two groups: $\mathrm{Mgb}_{N\mathcal{RF}}$ is systematically lower than $\mathrm{Mgb}_{O\mathcal{RF}}$ by 0.2 Å to as much as 0.4 Å with increasing age and/or metallicity; $\mathrm{Mg2}_{N\mathcal{RF}}$ tends to become larger than $\mathrm{Mg2}_{O\mathcal{RF}}$ at increasing age by as much as approximately 15 per cent. We suspect that for both indices the offset is due to differences in the stellar spectra that are difficult to pin down.

Finally, in the case of Hβ there is coincidence independent of the metallicity and definition of enhancement for ages younger than 3 Gyr, whereas $\mathrm{H}\beta_{O\mathcal{RF}}$ is larger than $\mathrm{H}\beta_{N\mathcal{RF}}$ for older ages and the difference increases with metallicity. In the age range where the largest deviation occurs, the maximum

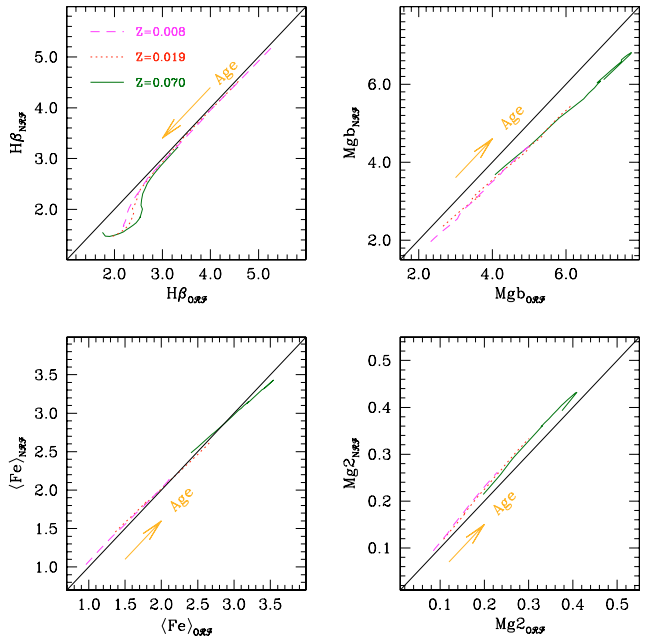

Fig. 10. Indices on the Lick resolution: comparison between Hβ (*top-left panel*), Mgb (*top-right panel*), ⟨Fe⟩ (*bottom-left panel*), and Mg2 (*bottom-right panel*) calculated with the $\mathcal{FF}$s of Worthey et al. (1994), different $\mathcal{RF}$s and different and definition of enhancement. The indices indicated as $I_{O\mathcal{RF}}$ are calculated with the first definition of enhancement ($\Gamma_Z = 0.25$), the old $\mathcal{RF}$s by Tripicco & Bell (1995), and the algorithm of Eq. (13). The indices $I_{N\mathcal{RF}}$ are calculated with the second definition of enhancement ($\Gamma_\alpha = 0.4$), the new $\mathcal{RF}$s, and Eq. (18). Both groups have the same elements enhanced by [α/Fe] = +0.4 dex. The corresponding abundances are given in Tables 1 and 2. Finally, three different metallicities are considered, as indicated.

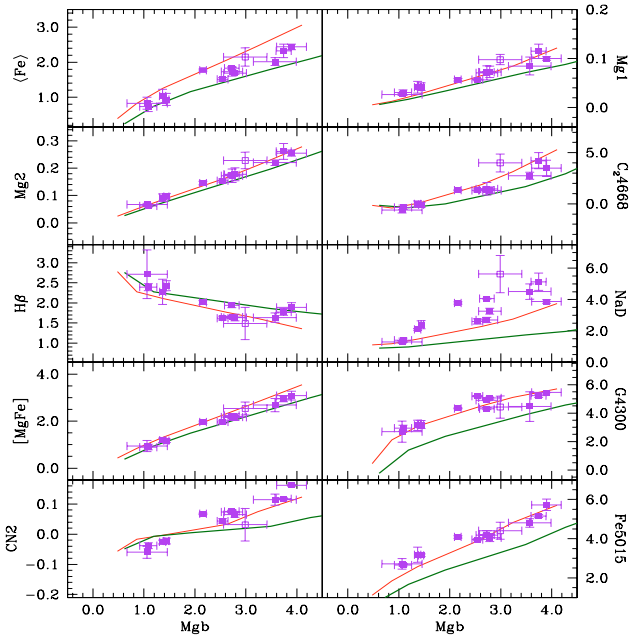

Fig. 11. The Mgb index versus ten different indices on the Lick resolution calculated with the metallicities typical of globular clusters. The thin-solid lines are the models with solar-scaled pattern of abundances, whereas the thick-solid are the models with $\Gamma_\alpha = 0.4$. Along each line, indices of SSPs with the same age (∼12 Gyr) are shown. They differ in the metallicity, which increases along each line from [$Z/Z_\odot$] = −2 ($Z \sim 0.0001$) to 0 ($Z \sim 0.019$), moving from left to right. These models are calculated with the classical $\mathcal{FF}$s and the new $\mathcal{RF}$s. The filled-squares are the globular cluster data, and the open-square is the galactic bulge from Puzia et al. (2002).

difference amounts to approximately 30 per cent. Careful inspection of the data reveals that the difference mostly originates from correcting algorithm in usage when applied to elements for which the $\mathcal{RF}$ is strong. Recalling that the indices $I_{O\mathcal{RF}}$ are calculated with [Ti/Fe] = 0.40 (this corresponds to [Ti/H] = +0.154), one of the elements with the strongest $\mathcal{RF}$ in the Tripicco & Bell (1995) tabulation, the excess of H$\beta_{O\mathcal{RF}}$ over H$\beta_{N\mathcal{RF}}$ is most probably due to the correcting algorithm of Eq. (13) that tends to diverge whenever [X_i/Fe] or [X_i/H]/0.3 and $R_{0.3}(X_i)$ are high (see Eq. (13)). In the case of H$\beta_{N\mathcal{RF}}$, the correction with respect to solar values is smaller (even though sizable) because of the linearity of the algorithm in use. For more details on this subject, the reader is referred to the discussion by TC04.

From this comparison we learn that:

(i) in general, there seems to be overall agreement between the two groups of indices despite the large difference in the definition of enhancement. As the case at increasing Z requires the re-scaling of the metallicity to lower values, the results eventually get close to those at constant Z, which implies a decrease in all elements that are not enhanced (Fe, in particular);

(ii) the new $\mathcal{RF}$s take effects into account that would otherwise be missed, such as the dependence on the metallicity;

(iii) the new $\mathcal{RF}$s for some indices and some stars, e.g. Hβ for cool-dwarfs, have the opposite dependence on Γ_α to the one predicted by Tripicco & Bell (1995). The result stems from the modern physical input of the new spectra.

No better comparison can be made at the present time, because we would need stellar spectra with abundances of elemental species increased one-by-one to derive the strict analogue of the $\mathcal{RF}$s by Tripicco & Bell (1995) and spectra with enhanced composition according to the constant Z scheme. All this is still out of reach for obvious reasons.

6. Comparison with globular clusters

It is worth checking whether the present indices can reproduce the data for the globular clusters. To do so we took the sample of Galactic globular clusters and Bulge compiled by Puzia et al. (2002) for which indices in the Lick system have been measured. To analyse this sample we adopted the isochrones of the Padova Library with the chemical composition typical of the Galactic globular clusters (Girardi et al. 2000), and derived the indices using the classical $\mathcal{FF}$s and the new $\mathcal{RF}$s as described in Sect. 5. The metallicity-enhancement relation was taken into account when comparing indices for solar-scaled and α-enhanced mixtures. The results are shown in Fig. 11 for a number of indices. Each line shows the expected correlation between two indices at fixed age and varying metallicity. The age under consideration is the one that is typical of globular clusters, i.e. 12 Gyr. The metallicity increases from [$Z/Z_\odot$] = −2.0 ($Z \sim 0.0001$) to [$Z/Z_\odot$] = 0 ($Z \sim 0.019$) moving from bottom left to top right. Different symbols indicate the models with solar-scaled pattern of abundances and those with $\Gamma_\alpha = 0.40$. Despite the fact that these indices were not particularly designed to match the globular clusters, the overall agreement is satisfactory. The new indices are of the same quality as those in TC04 and Thomas et al. (2003a). In general, the agreement is better for the solar-scaled

Table 5. Ages, metallicities and [α/Fe] for the sample of Galactic Globular Clusters by Puzia et al. (2002). Columns (2) through (5) are estimates of the parameters based on the colour–magnitude diagrams or spectroscopic measurements; Cols. (6) through (8) are the results derived from the absorption line indices.

NGC	$[Fe/H]_{CG}$	$[\alpha/Fe]^d$	T_{CG}	σ_T	[Z/H]	[α/Fe]	Age
5927	–0.64[a]	—	10.0	0.7[a]	–0.62	0.34	12.6
6218	–1.14[a]	0.35	10.0	0.9[a]	–1.76	0.30	7.9
6284	–1.13[a]	—	9.5	0.4[a]	–1.51	0.37	8.9
6356	–0.89[a]	—	10.0	2.0[b]	–0.94	0.37	12.6
6388	–0.74[a]	—	10.6	2.0[b]	–0.91	0.06	10.0
6528	0.07[b]	0.11	10.0	2.0[b]	–0.03	0.16	12.6
6553	–0.06[b]	0.19	10.0	2.0[b]	–0.03	0.03	12.6
6624	–0.70[b]	—	10.6	1.4[c]	–0.91	0.30	12.6
6637	–0.78[a]	—	9.9	1.1[a]	–1.03	0.37	12.6
6981	–1.21[a]	—	8.7	0.9[a]	–1.74	0.34	10.0

[a] De Angeli et al. (2005); [b] Santos & Piatti (2004); [c] Salaris & Weiss (2002); [d] Pritzl et al. (2005).

mixture even if values of Γ_α in the range of 0 to 0.4 cannot be excluded. The index NaD departs from the observational value in Thomas et al. (2003a), TC04, and here.

To further confirm the quality of the theoretical indices, we derive the ages, metallicities, and enhancement degree from the indices for the sub-set of this sample of globular cluster for which the same parameters are known from the colour–magnitude diagrams.

To this aim, we first select the globular clusters for which the estimate of ages and metallicities (i.e. [Fe/H]) have been derived from the colour–magnitude diagrams (see De Angeli et al. 2005; Santos & Piatti 2004; Salaris & Weiss 2002; Schiavon et al. 2005). Then we consider the current estimates of enhancement (i.e. [α/Fe]) obtained directly from stars and take these as indicators of the total degree of enhancement in each cluster (see Pritzl et al. 2005). Table 5 lists the metal content, degree of enhancement, and age, together with its uncertainty, which we have been able to collect from literature (the sources of data are indicated). These are the values we would like to recover from the indices.

To derive metallicities, degree of enhancement, and age from the indices we adopt the *minimum-distance method* originally proposed by Trager et al. (2000b) and amply described in TC04. Due to the different sensitivity of the adopted indices to each parameter we prefer to use the so-called *recursive minimum-distance method*[6].

Taking advantage of the high sensitivity of $\langle$Fe$\rangle$ and Mg2 to [α/Fe] and their lower sensitivity to age and metallicity, we apply the minimum-distance method to derive [α/Fe] from the plane $\langle$Fe$\rangle$-Mg2 assuming the provisional age $T \sim 13$. This value, briefly indicated as Γ^0_α, is used to construct the functions $H\beta(T, Z, \Gamma^0_\alpha)$, $\langle Fe\rangle(T, Z, \Gamma^0_\alpha)$, and $Mgb(T, Z, \Gamma^0_\alpha)$ and to solve the equations

$$H\beta_{obs} = H\beta(T, Z, \Gamma^0_\alpha)$$

$$\langle Fe\rangle_{obs} = \langle Fe\rangle(T, Z, \Gamma^0_\alpha)$$

$$Mgb_{obs} = Mgb(T, Z, \Gamma^0_\alpha)$$

for the age and metallicity (T and Z). The procedure is iterated until full consistency is achieved.

[6] This method was introduced and applied in the first version of the paper by Tantalo & Chiosi (2004a).

The results of this analysis are shown in Table 5 (Cols. (6) through (8) for the metallicity, [α/Fe], and age). Metallicities, degree of enhancement, and ages derived from indices fully agree with those obtained from the colour–magnitude diagrams. This holds true both for individual clusters and the mean values for the whole sample: $\langle Age\rangle = 11.2 \pm 1.8$, $\langle [Z/H]\rangle = -0.95 \pm 0.62$[7], and $\langle [\alpha/Fe]\rangle = 0.26 \pm 0.13$[8].

7. Discussion and conclusions

We have generated synthetic absorption-line indices in the Lick system based on the recent library of 1-Å resolution spectra calculated by Munari et al. (2005) over a wide range of atmospheric parameters ($\log T_{eff}$, $\log g$, and [Fe/H]), both for solar and α-enhanced abundance ratios in the chemical composition. The main results of this study are:

(i) First we derive a modern version of the so-called $\mathcal{RF}$s of Tripicco & Bell (1995). In contrast to the previous situation in which the $\mathcal{RF}$s were known only for three stars of given $\log T_{eff}$ and $\log g$, now the $\mathcal{RF}$s are given for wide range ranges of $\log T_{eff}$, $\log g$, and [Fe/H] (or $[Z/Z_\odot]$). The $\mathcal{RF}$s vary not only with the type of star but also with the metallicity[9], so the effect of metallicity is important and cannot be neglected. While completing this study, a similar analysis was published by Korn et al. (2005). Strictly following the Tripicco & Bell (1995) approach, they presented the $\mathcal{RF}$s for three stars (a dwarf, a turn-off, and a red giant for six chemical compositions). Their results are similar to ours even if the coverage of the effective temperature-gravity intervals for the reference stars is much narrower.

(ii) With the aid of the new $\mathcal{RF}$s and the $\mathcal{FF}$s of Worthey et al. (1994), indices for SSPs are calculated and compared with the old ones by TC04. Except for the differences caused by the new $\mathcal{RF}$s and the kind of enhancement adopted by TC04 and here, the agreement is good, thus confirming that the method adopted by TC04 to account for the effect of α-enhancement was correct. The present results demonstrate clearly that all indices depend on the enhancement and also that Hβ increases with it as already anticipated by TC04 and contrary to what claimed by Thomas et al. (2003a,b). The same conclusion was marginally reached by Korn et al. (2005) in their recent study.

(iii) The new indices have been compared to those of galactic globular clusters, for which there are independent estimates of age, metallicity, and degree of enhancement, and were used to re-derive these basic parameters by means of the recursive minimum distance method customarily applied to galaxies. The estimates of the three key parameters from the two methods agree with each other, thus suggesting that the indices for SSPs we calculated are correct.

Acknowledgements. This study was financed by the Italian Ministry of Education, University, and Research (MIUR), and the University of Padua under the special contract "Formation and evolution of elliptical galaxies: the age problem".

[7] We pass from [Z/H] to [Fe/H] with the aid of the obvious relation: $[Fe/H] = [Z/H] - \Gamma_Z$, which is $[Fe/H] = [Z/H] - 0.625\Gamma_\alpha$ with the definition of enhancement adopted in this study.

[8] We can directly compare our results with the observed ones due to the fact that the latter are generally the average of the [Mg/Fe], [Si/Fe], [Ca/Fe], and [Ti/Fe] abundance ratios.

[9] The new $\mathcal{RF}$s are given as large 3D-matrices made available on the web page `http://dipastro.pd.astro.it/galadriel`

References

Anders, E., & Grevesse, N. 1989, Geochim. Cosmochim. Acta, 53, 197
Barbuy, B. 1994, ApJ, 430, 218
Bertelli, G., Bressan, A., Chiosi, C., Fagotto, F., & Nasi, E. 1994, A&AS, 106, 275
Borges, C. A., Idiart, T. P., de Freitas-Pacheco, J. A., & Thevein, F. 1995, AJ, 110, 2408
Bressan, A., Chiosi, C., & Fagotto, F. 1994, ApJS, 94, 63
Bressan, A., Chiosi, C., & Tantalo, R. 1996, A&A, 311, 425
Bruzual, G. 1983, ApJ, 273, 205
Burstein, D., Bertola, F., Buson, L. M., Faber, S. M., & Lauer, T. R. 1988, ApJ, 328, 440
Burstein, D., Faber, S. M., Gaskell, C. M., & Krumm, N. 1984, ApJ, 287, 586
Carney, B. 1996, PASP, 108, 900
Castelli, F., & Kurucz, R. L. 2004, in Modelling of Stellar Atmospheres, ed. N. E. Piskunov, W. W. Weiss, & D. F. Gray, IAU Symp., 189
Cenarro, A. J., Cardiel, N., Gorgas, J., et al. 2001, MNRAS, 326, 959
Cenarro, A. J., Gorgas, J., Cardiel, N., Vazdekis, A., & Peletier, R. F. 2002, MNRAS, 329, 863
Chiosi, C., & Carraro, G. 2002, MNRAS, 335, 335
Davies, R. L., Kuntschner, H., Emsellem, E., et al. 2001, ApJ, 548, L33
De Angeli, F., Piotto, G., Cassisi, S., et al. 2005, AJ, 130, 116
Faber, S. M., Friel, E. D., Burstein, D., & Gaskell, C. M. 1985, ApJS, 57, 711
Faber, S. M., Worthey, G., & González, J. J. 1992, in The Stellar Population of Galaxies, ed. B. Barbuy, & A. Renzini (Dordrecht: Kluwer Academic Publishers), IAU Symp., 149, 255
Girardi, L., & Bertelli, G. 1998, MNRAS, 300, 533
Girardi, L., Bressan, A., Bertelli, G., & Chiosi, C. 2000, A&AS, 141, 371
Girardi, L., Bertelli, G., Bressan, A., et al. 2002, A&A, 391, 195
González, J. J. 1993, Ph.D. Thesis, University of California, Santa Cruz
Gorgas, J., Cardiel, N., Pedraz, S., & González, J. J. 1999, A&AS, 139, 29
Gratton, R., Carretta, E., Claudi, R., Lucatello, S., & Barbieri, M. 2003, A&A, 404, 187
Grevesse, N., & Sauval, A. J. 1998, Space Sci. Rev., 85, 161
Habgood, M.-J. 2001, Ph.D. Thesis, Univ. of North Carolina at Chapel Hill
Idiart, T. P., & de Freitas-Pacheco, J. A. 1995, AJ, 109, 2218
Jørgensen, I. 1999, MNRAS, 306, 607
Korn, A. J., Maraston, C., & Thomas, D. 2005, A&A, 438, 685
Kuntschner, H. 1998, Ph.D. Thesis, Univ. of Durham
Kuntschner, H. 2000, MNRAS, 315, 184
Kuntschner, H., & Davies, R. L. 1998, MNRAS, 295, L29
Kuntschner, H., Lucey, J. R., Smith, R. J., Hudsen, M. J., & Davies, R. L. 2001, MNRAS, 323, 615
Kurucz, R. 1993, in The Stellar Populations of Galaxies, ed. B. Barbuy, & A. Renzini (Dordrecht: Kluwer), IAU Symp., 149, 255
Larson, R. B. 1974, MNRAS, 142, 501
Longhetti, M., Rampazzo, R., Bressan, A., & Chiosi, C. 1998, A&AS, 130, 251
Maraston, C., Greggio, L., Renzini, A., et al. 2003, A&A, 400, 823
Matteucci, F. 1994, A&A, 154, 279
Matteucci, F. 1997, Fundam. Cosmic Phys., 17, 283
Matteucci, F., Ponzone, R., & Gibson, B. K. 1998, A&A, 335, 855
Munari, U., Sordo, R., Castelli, F., & Zwitter, T. 2005, A&A, 442, 1127
Poggianti, B., Bridges, T., Mobasher, B., et al. 2001, ApJ, 562, 689
Pritzl, B., Venn, K., & Irwin, M. 2005, AJ, in press
Puzia, T., Saglia, R., Kissler-Patig, M., et al. 2002, A&A, 395, 45
Reimers, D. 1975, Mem. Soc. R. Sci. Liege, Ser. 6, 8, 369
Renzini, A., & Buzzoni, A. 1986, in Spectral Evolution of Galaxies, ed. C. Chiosi, & A. Renzini (Dordecht: Reidel), 213
Ryan, S., Norris, J., & Bessell, M. 1991, AJ, 102, 303
Salaris, M., & Weiss, A. 2002, A&A, 338, 492
Salaris, M., Chieffi, A., & Straniero, O. 1993, ApJ, 414, 580
Salasnich, B., Girardi, L., Weiss, A., & Chiosi, C. 2000, A&A, 361, 1023
Sánchez-Blázquez, P., Peletier, R., Vazdekis, A., et al. 2003, in Rev. Mex. Astron. Astrofis. Conf. Ser., ed. V. Avila-Reese, C. Firmani, C. Frenk, & C. Allen, 17, 192
Santos, J., & Piatti, A. 2004, A&A, 428, 79
Schiavon, R., Rose, J., Courteau, S., & MacArthur, L. 2005, ApJS, 160, 163
Schwenke, D. W. 1998, Faraday Discussion, 109, 321
Tantalo, R. 1998, Ph.D. Thesis, Univ. of Padova
Tantalo, R., & Chiosi, C. 2004a, MNRAS, 353, 917
Tantalo, R., & Chiosi, C. 2004b, MNRAS, 353, 405
Tantalo, R., Chiosi, C., & Bressan, A. 1998, A&A, 333, 419
Thomas, D., & Maraston, C. 2003, A&A, 401, 429
Thomas, D., Maraston, C., & Bender, R. 2003a, MNRAS, 339, 897
Thomas, D., Maraston, C., & Bender, R. 2003b, MNRAS, 343, 279
Trager, S. C., Faber, S. M., Worthey, G., & González, J. J. 2000a, AJ, 120, 165
Trager, S. C., Faber, S. M., Worthey, G., & González, J. J. 2000b, AJ, 119, 1645, (TFWG20)
Trager, S. C., Worthey, G., Faber, S. M., Burstein, D., & Gonzalez, J. J. 1998, ApJS, 116, 1
Tripicco, M. J., & Bell, R. A. 1995, AJ, 110, 3035, (TB95)
Vassiliadis, D. A., & Wood, P. R. 1993, ApJ, 413, 641
Vazdekis, A., Kuntschner, H., Davies, R. L., et al. 2001, ApJ, 551, 127
Weiss, A., Peletier, R. F., & Matteucci, F. 1995, A&A, 296, 73
Worthey, G. 1992, Ph.D. Thesis, Univ. of California
Worthey, G. 1994, ApJS, 95, 107
Worthey, G., Faber, S. M., & González, J. J. 1992, ApJ, 398, 69
Worthey, G., Faber, S. M., González, J. J., & Burstein, D. 1994, ApJS, 94, 687
Worthey, G., & Ottaviani, D. 1997, ApJS, 111, 377
Zwitter, T., Castelli, F., & Munari, U. 2004, A&A, 417, 1055

Online Material

Appendix A:

Tables A.1–A.5 list the new $\mathcal{RF}$s calculated with the 1-Å resolution spectra from Munari et al. (2005) as a function of $T_{\rm eff}$ and $\log g$ and for four different metallicities: $[Z/Z_{\odot}]$ = –2.0, −1.5, –1.0, –0.5. For each index we give the value $I_{\rm sol}$ for the solar abundance ratios and the difference $(\delta I) = I_{\rm enh} - I_{\rm sol}$ between the α-enhanced and the solar case. The corresponding $\mathcal{RF}$s can be derived immediately from relation (17). Tables A.6–A.10 are the same but for the high-resolution spectra degraded to the Lick resolution.

Table A.1. 1-Å resolution spectra: I_{sol} and $I_{enh} - I_{sol}$ for $[Z/Z_\odot] = -2.0$.

T_{eff}	4000								5250							
log g	1.5		2.5		3.5		4.5		1.5		2.5		3.5		4.5	
	I_{sol}	(δI)	I_{sol}	(δI)	I_{sol}	(δI)	I_{sol}	(δI)	I_{sol}	(δI)	I_{sol}	(δI)	I_{sol}	(δI)	I_{sol}	(δI)
CN1	0.043	0.011	0.057	0.034	0.050	0.039	0.047	0.049	–0.025	0.007	–0.029	0.008	–0.035	0.009	–0.041	0.010
CN2	0.092	0.017	0.129	0.042	0.126	0.046	0.143	0.058	0.001	0.007	–0.009	0.009	–0.022	0.009	–0.034	0.012
Ca4227	0.328	0.463	1.272	0.599	2.213	0.411	3.872	0.406	0.095	0.005	0.042	0.055	0.033	0.115	0.135	0.170
G4300	8.302	–0.936	8.620	–1.344	7.356	–1.649	6.386	–1.953	3.053	–0.949	4.441	–1.009	5.746	–0.940	6.863	–1.153
Fe4383	5.127	–1.691	5.742	–1.931	5.221	–1.886	5.448	–1.792	1.079	–0.246	1.067	–0.417	1.270	–0.607	1.700	–0.810
Ca4455	1.208	–0.208	1.253	–0.214	1.082	–0.261	1.141	–0.249	0.341	–0.064	0.302	–0.048	0.278	–0.056	0.276	–0.065
Fe4531	3.218	–0.428	3.025	–0.417	2.611	–0.455	2.678	–0.410	1.276	–0.198	1.131	–0.210	1.002	–0.227	0.888	–0.244
$C_2$4668	0.705	–0.142	0.335	–0.130	–0.029	–0.113	–0.359	–0.059	–0.096	0.046	–0.072	0.034	–0.039	0.029	–0.006	0.041
Hβ	0.129	0.091	–0.085	0.093	–0.212	0.081	–0.296	–0.002	1.666	–0.035	1.389	–0.032	1.167	–0.017	1.046	–0.011
Fe5015	3.714	–0.617	2.826	–0.749	2.068	–0.806	1.432	–0.797	1.435	–0.440	1.372	–0.421	1.285	–0.402	1.136	–0.397
Mg1	0.076	0.008	0.162	0.028	0.188	0.026	0.272	0.041	–0.004	–0.003	–0.003	–0.002	–0.004	–0.002	–0.004	–0.001
Mg2	0.165	0.016	0.303	0.041	0.353	0.032	0.459	0.037	0.022	–0.001	0.026	–0.001	0.036	0.000	0.057	0.001
Mgb	1.966	0.384	3.586	0.600	4.091	0.537	4.374	0.323	0.372	0.146	0.528	0.145	0.959	0.182	1.723	0.232
Fe5270	2.168	–0.268	2.555	–0.344	2.516	–0.465	2.695	–0.586	0.526	–0.099	0.550	–0.107	0.606	–0.138	0.704	–0.204
Fe5335	2.085	–0.373	2.294	–0.426	2.201	–0.528	2.437	–0.645	0.762	–0.146	0.741	–0.163	0.735	–0.196	0.769	–0.256
Fe5406	1.215	–0.253	1.538	–0.321	1.594	–0.405	1.844	–0.520	0.274	–0.126	0.316	–0.117	0.358	–0.119	0.417	–0.147
Fe5709	0.652	–0.160	0.559	–0.152	0.365	–0.156	0.227	–0.118	0.085	–0.071	0.091	–0.074	0.090	–0.074	0.077	–0.071
Fe5782	0.254	–0.143	0.240	–0.140	0.153	–0.110	0.107	–0.073	0.020	–0.022	0.022	–0.024	0.022	–0.025	0.019	–0.024
NaD	1.030	–0.412	1.860	–0.671	2.550	–1.024	4.313	–1.521	0.286	–0.029	0.307	–0.043	0.394	–0.086	0.606	–0.172
TiO1	0.002	0.000	0.002	–0.001	0.000	–0.003	–0.001	–0.005	0.000	–0.001	0.000	0.000	0.000	0.000	–0.001	0.000
TiO2	0.015	–0.006	0.014	–0.006	0.010	–0.010	0.006	–0.012	0.001	–0.002	0.001	–0.002	0.001	–0.001	0.000	–0.001
HδA	–3.633	1.935	–3.861	2.099	–3.422	2.074	–3.158	1.999	0.759	0.274	0.349	0.294	–0.278	0.396	–1.028	0.592
HγA	–7.774	0.850	–9.516	1.408	–8.939	1.993	–9.083	2.373	–1.041	0.937	–2.589	1.048	–4.228	1.060	–5.810	1.377
HδF	–1.682	0.752	–1.887	0.851	–1.685	0.921	–1.473	0.923	1.075	0.206	0.750	0.187	0.344	0.205	–0.046	0.267
Hγ F	–3.023	0.436	–3.953	0.782	–3.831	1.057	–3.823	1.237	0.667	0.413	–0.263	0.495	–1.319	0.537	–2.316	0.724
D4000	2.422	–0.256	2.335	–0.302	2.276	–0.289	2.312	–0.284	1.407	–0.028	1.380	–0.025	1.397	–0.028	1.450	–0.036

T_{eff}	7250								10 000						13 000			
log g	1.5		2.5		3.5		4.5		2.5		3.5		4.5		2.5		3.5		4.5	
	I_{sol}	(δI)	I_{sol}	(δI)	I_{sol}	(δI)	I_{sol}	(δI)	I_{sol}	(δI)	I_{sol}	(δI)	I_{sol}	(δI)	I_{sol}	(δI)	I_{sol}	(δI)	I_{sol}	(δI)
CN1	–0.185	0.000	–0.197	0.000	–0.189	0.000	–0.171	0.000	–0.129	–0.001	–0.235	–0.002	–0.344	–0.001	–0.077	–0.001	–0.149	–0.001	–0.235	–0.002
CN2	–0.093	–0.001	–0.113	0.000	–0.112	0.000	–0.100	0.000	–0.042	–0.001	–0.137	–0.002	–0.258	–0.001	–0.016	0.000	–0.069	–0.001	–0.152	–0.002
Ca4227	0.032	0.005	0.044	0.002	0.052	0.000	0.062	–0.003	0.018	–0.009	0.010	–0.007	0.003	–0.006	0.007	–0.006	0.006	–0.006	0.002	–0.004
G4300	–1.320	0.023	–1.669	0.027	–1.704	0.004	–1.534	–0.024	–0.851	–0.027	–2.462	–0.034	–3.990	–0.013	–0.416	0.003	–1.309	–0.009	–2.598	–0.023
Fe4383	–0.166	–0.158	–0.658	–0.131	–0.860	–0.101	–0.818	–0.065	–0.175	–0.022	–1.023	–0.031	–3.234	–0.040	0.075	–0.009	–0.300	–0.012	–1.318	–0.022
Ca4455	–0.006	–0.047	0.017	–0.039	0.038	–0.023	0.048	–0.012	0.030	–0.009	0.014	–0.009	–0.002	–0.008	0.257	–0.009	0.236	–0.011	0.210	–0.006
Fe4531	0.371	–0.152	0.299	–0.151	0.233	–0.134	0.176	–0.114	0.056	–0.034	0.036	–0.027	0.026	–0.022	0.024	–0.014	0.023	–0.014	0.017	–0.009
$C_2$4668	–0.170	0.068	–0.120	0.060	–0.080	0.048	–0.045	0.032	0.052	0.035	0.047	0.021	–0.024	0.012	0.146	0.029	0.123	0.017	0.099	0.007
Hβ	7.151	–0.036	7.134	–0.040	6.678	–0.042	6.086	–0.044	6.063	0.021	8.825	0.021	9.741	–0.010	3.894	0.023	6.203	0.030	8.037	0.032
Fe5015	0.200	–0.123	0.164	–0.129	0.129	–0.129	0.106	–0.127	0.059	–0.017	0.043	–0.013	–0.034	–0.011	0.133	–0.024	0.087	–0.016	0.046	–0.005
Mg1	0.001	0.001	–0.003	0.001	–0.005	0.001	–0.006	0.001	0.007	0.000	0.004	0.000	–0.007	0.000	0.008	0.000	0.007	0.000	0.003	0.000
Mg2	0.014	0.001	0.011	0.000	0.009	0.000	0.009	–0.001	0.009	0.000	0.008	0.000	–0.001	0.000	0.009	0.000	0.009	0.000	0.006	0.000
Mgb	0.383	0.061	0.384	0.051	0.379	0.037	0.389	0.017	0.066	–0.009	0.070	–0.017	0.079	–0.018	0.034	–0.005	0.035	–0.008	0.028	–0.012
Fe5270	0.024	–0.049	0.052	–0.050	0.078	–0.051	0.097	–0.054	–0.002	0.006	0.002	0.004	0.003	0.001	0.006	0.000	0.007	0.000	0.007	0.000
Fe5335	0.170	–0.077	0.164	–0.089	0.153	–0.095	0.141	–0.096	0.020	–0.014	0.014	–0.011	0.012	–0.010	0.012	–0.008	0.010	–0.007	0.007	–0.004
Fe5406	0.021	–0.025	0.036	–0.029	0.046	–0.033	0.052	–0.037	0.003	–0.002	0.002	–0.002	0.002	–0.001	0.003	–0.002	0.003	–0.002	0.003	–0.002
Fe5709	0.003	–0.002	0.004	–0.005	0.005	–0.006	0.005	–0.006	0.002	0.000	0.002	0.000	0.002	0.000	0.002	0.000	0.002	0.000	0.002	0.000
Fe5782	0.002	–0.002	0.002	–0.002	0.002	–0.002	0.002	–0.002	0.001	–0.001	0.001	0.000	0.001	–0.001	0.001	0.000	0.002	0.000	0.001	0.000
NaD	0.145	–0.035	0.155	–0.032	0.159	–0.029	0.162	–0.029	–0.031	–0.002	–0.013	–0.004	0.000	–0.009	–0.136	0.001	–0.102	0.001	–0.075	0.000
TiO1	0.002	0.000	0.001	0.000	0.001	0.000	0.001	0.000	0.003	0.000	0.003	0.000	0.003	0.000	0.003	0.000	0.003	0.000	0.003	0.000
TiO2	0.003	0.000	0.002	0.000	0.002	0.000	0.001	0.000	0.003	0.000	0.003	0.000	0.003	0.000	0.004	0.000	0.004	0.000	0.004	0.000
HδA	8.941	0.071	9.384	0.031	8.968	0.021	8.118	0.004	6.543	0.041	11.170	0.050	15.360	0.030	4.197	0.031	7.510	0.044	11.130	0.060
HγA	8.708	0.039	9.262	–0.004	8.958	–0.011	8.143	–0.019	6.628	0.043	11.270	0.070	15.520	0.020	4.152	0.029	7.445	0.043	11.140	0.070
HδF	7.587	0.036	7.484	0.018	6.995	0.012	6.332	0.002	5.935	0.032	9.009	0.034	10.460	0.000	3.837	0.027	6.380	0.035	8.434	0.043
HγF	7.366	0.015	7.354	–0.009	6.920	–0.018	6.286	–0.028	5.969	0.024	8.880	0.026	10.300	0.010	3.885	0.023	6.304	0.030	8.291	0.039
D4000	1.217	-0.005	1.276	–0.006	1.295	–0.005	1.294	–0.006	1.080	0.000	1.199	0.002	1.377	0.002	1.017	0.001	1.084	0.001	1.187	0.003

Table A.2. 1-Å resolution spectra: I_{sol} and $I_{enh} - I_{sol}$ for $[Z/Z_\odot] = -1.5$.

T_{eff}	4000								5250							
log g	1.5		2.5		3.5		4.5		1.5		2.5		3.5		4.5	
	I_{sol}	(δI)	I_{sol}	(δI)	I_{sol}	(δI)	I_{sol}	(δI)	I_{sol}	(δI)	I_{sol}	(δI)	I_{sol}	(δI)	I_{sol}	(δI)
CN1	0.082	−0.002	0.088	0.017	0.072	0.027	0.051	0.034	−0.032	0.004	−0.039	0.007	−0.043	0.009	−0.046	0.013
CN2	0.150	0.004	0.178	0.020	0.171	0.033	0.158	0.039	−0.006	0.005	−0.018	0.009	−0.029	0.013	−0.038	0.019
Ca4227	1.041	1.281	2.400	1.191	3.824	1.104	5.133	0.925	0.160	0.093	0.055	0.174	0.050	0.285	0.250	0.431
G4300	8.389	−0.915	8.376	−1.272	7.356	−1.213	5.699	−1.130	5.157	−0.723	6.424	−0.884	7.216	−0.936	8.064	−1.280
Fe4383	6.349	−1.553	7.111	−2.000	6.858	−1.811	6.265	−1.683	1.685	−0.188	1.888	−0.362	2.329	−0.654	2.985	−0.981
Ca4455	1.751	−0.131	1.843	−0.166	1.691	−0.104	1.538	−0.110	0.580	−0.065	0.515	−0.042	0.465	−0.020	0.459	−0.012
Fe4531	4.012	−0.278	3.818	−0.306	3.482	−0.220	3.317	−0.191	2.032	−0.038	1.877	−0.030	1.713	−0.036	1.584	−0.058
$C_2$4668	1.390	−0.159	0.795	−0.042	0.246	0.187	−0.242	0.273	−0.018	0.109	−0.011	0.088	0.014	0.069	0.041	0.071
Hβ	0.093	0.075	−0.200	0.073	−0.395	0.084	−0.476	0.028	1.787	0.034	1.464	0.041	1.213	0.037	1.056	0.029
Fe5015	4.747	−0.618	3.736	−0.613	2.934	−0.462	2.134	−0.407	2.497	−0.088	2.376	−0.085	2.256	−0.095	2.119	−0.124
Mg1	0.131	0.025	0.230	0.029	0.279	0.048	0.331	0.061	0.001	−0.002	0.001	−0.001	0.000	0.000	0.001	0.004
Mg2	0.241	0.044	0.397	0.054	0.482	0.086	0.531	0.089	0.030	0.003	0.038	0.007	0.057	0.013	0.093	0.025
Mgb	2.632	0.754	4.334	0.916	5.007	1.219	4.601	0.974	0.308	0.220	0.626	0.326	1.360	0.511	2.590	0.811
Fe5270	2.849	−0.207	3.231	−0.330	3.331	−0.360	3.278	−0.411	0.872	0.070	0.890	0.067	0.983	0.038	1.180	−0.020
Fe5335	2.840	−0.276	3.056	−0.412	3.011	−0.438	2.944	−0.536	1.110	−0.027	1.115	−0.031	1.150	−0.049	1.258	−0.093
Fe5406	1.687	−0.199	2.042	−0.331	2.174	−0.347	2.204	−0.414	0.403	−0.046	0.457	−0.054	0.541	−0.067	0.672	−0.095
Fe5709	0.952	−0.060	0.830	−0.065	0.613	−0.055	0.378	−0.056	0.210	−0.022	0.220	−0.023	0.220	−0.023	0.203	−0.022
Fe5782	0.491	−0.119	0.468	−0.141	0.339	−0.123	0.220	−0.100	0.055	−0.013	0.061	−0.014	0.062	−0.014	0.058	−0.013
NaD	1.563	−0.371	2.744	−0.687	3.994	−0.848	5.614	−1.226	0.332	−0.039	0.379	−0.056	0.542	−0.105	0.910	−0.191
TiO1	0.006	0.002	0.005	0.004	0.005	0.009	0.002	0.008	0.000	0.000	0.000	0.000	0.000	0.000	0.000	0.000
TiO2	0.025	−0.003	0.024	0.001	0.022	0.010	0.014	0.009	0.004	0.000	0.003	0.000	0.003	0.000	0.002	0.000
HδA	−5.011	1.931	−5.262	2.142	−4.782	1.878	−3.510	1.581	0.258	0.242	−0.193	0.328	−0.932	0.496	−1.945	0.749
HγA	−9.139	0.687	−10.690	1.384	−10.540	1.410	−9.443	1.597	−2.950	0.706	−4.475	0.910	−5.746	1.038	−7.302	1.487
HδF	−2.400	0.530	−2.641	0.721	−2.425	0.729	−1.727	0.709	0.774	0.193	0.489	0.214	0.094	0.270	−0.382	0.369
HγF	−3.279	0.392	−4.072	0.711	−4.115	0.749	−3.576	0.772	−0.039	0.368	−1.045	0.523	−1.959	0.629	−2.947	0.883
D4000	- 2.633	−0.215	2.571	−0.302	2.548	−0.287	2.448	−0.250	1.487	0.012	1.456	0.005	1.484	−0.005	1.565	−0.019

T_{eff}	7250								10 000						13 000					
log g	1.5		2.5		3.5		4.5		2.5		3.5		4.5		2.5		3.5		4.5	
	I_{sol}	(δI)	I_{sol}	(δI)	I_{sol}	(δI)	I_{sol}	(δI)	I_{sol}	(δI)	I_{sol}	(δI)	I_{sol}	(δI)	I_{sol}	(δI)	I_{sol}	(δI)	I_{sol}	(δI)
CN1	−0.181	0.001	−0.195	0.001	−0.188	0.001	−0.171	0.001	−0.127	−0.001	−0.232	−0.001	−0.343	0.000	−0.075	−0.001	−0.146	−0.001	−0.233	−0.001
CN2	−0.088	0.001	−0.110	0.001	−0.110	0.001	−0.099	0.000	−0.041	−0.001	−0.134	−0.001	−0.256	0.000	−0.015	0.000	−0.067	−0.001	−0.150	−0.001
Ca4227	0.061	0.020	0.070	0.016	0.080	0.013	0.094	0.014	0.033	−0.005	0.022	−0.001	0.016	0.006	0.016	−0.003	0.015	−0.003	0.008	−0.002
G4300	−1.061	0.102	−1.396	0.114	−1.435	0.117	−1.296	0.114	−0.799	0.012	−2.396	0.010	−3.966	0.025	−0.415	−0.004	−1.284	−0.014	−2.571	−0.016
Fe4383	0.124	−0.045	−0.457	−0.052	−0.740	−0.049	−0.769	−0.046	−0.139	−0.005	−0.970	−0.014	−3.164	−0.022	0.087	0.003	−0.279	−0.002	−1.288	−0.010
Ca4455	0.016	0.011	0.031	0.000	0.061	−0.011	0.090	−0.016	0.001	−0.002	−0.013	−0.006	−0.030	−0.009	0.228	−0.007	0.207	−0.008	0.184	−0.011
Fe4531	0.661	−0.021	0.558	−0.029	0.457	−0.034	0.374	−0.037	0.113	−0.016	0.081	−0.012	0.062	−0.010	0.046	−0.004	0.046	−0.006	0.032	−0.004
$C_2$4668	−0.277	0.102	−0.210	0.080	−0.144	0.057	−0.080	0.040	−0.007	0.023	0.011	0.015	−0.043	0.011	0.096	0.022	0.094	0.011	0.083	0.005
Hβ	7.225	0.006	7.213	−0.003	6.761	−0.009	6.170	−0.012	6.015	0.023	8.781	0.015	9.752	−0.005	3.833	0.038	6.134	0.039	7.986	0.027
Fe5015	0.402	−0.035	0.377	−0.039	0.345	−0.041	0.319	−0.040	0.038	−0.050	0.041	−0.041	−0.022	−0.034	0.091	−0.051	0.049	−0.053	0.019	−0.046
Mg1	−0.001	0.001	−0.005	0.001	−0.007	0.001	−0.007	0.000	0.007	0.000	0.004	0.000	−0.007	0.000	0.007	0.000	0.007	0.000	0.003	0.000
Mg2	0.018	0.001	0.015	0.001	0.013	0.001	0.013	0.002	0.010	0.000	0.008	0.001	0.001	0.001	0.009	0.000	0.009	0.000	0.006	0.000
Mgb	0.473	0.071	0.460	0.075	0.448	0.079	0.484	0.102	0.081	0.013	0.108	0.021	0.143	0.028	0.043	−0.007	0.050	−0.006	0.047	−0.005
Fe5270	0.110	0.030	0.140	0.033	0.168	0.033	0.193	0.030	−0.012	0.007	−0.005	0.006	0.000	0.005	0.006	0.002	0.006	0.002	0.007	0.002
Fe5335	0.318	−0.012	0.325	−0.014	0.318	−0.015	0.304	−0.014	0.042	−0.004	0.032	−0.003	0.027	−0.002	0.025	0.003	0.020	0.000	0.014	0.000
Fe5406	0.046	−0.033	0.078	−0.028	0.100	−0.022	0.114	−0.017	0.007	0.000	0.005	0.000	0.004	0.000	0.006	0.001	0.006	0.001	0.005	0.001
Fe5709	0.006	0.004	0.011	0.004	0.014	0.003	0.015	0.003	0.002	0.000	0.002	0.000	0.002	0.000	0.002	0.000	0.002	0.000	0.002	0.000
Fe5782	0.005	−0.001	0.005	−0.001	0.005	−0.001	0.005	−0.001	0.003	−0.001	0.002	−0.001	0.002	0.000	0.002	−0.001	0.002	−0.001	0.002	−0.001
NaD	0.204	−0.025	0.208	−0.023	0.207	−0.022	0.211	−0.023	−0.027	−0.002	−0.005	−0.003	0.015	−0.006	−0.136	−0.002	−0.102	−0.001	−0.075	−0.001
TiO1	0.002	0.000	0.002	0.000	0.001	0.000	0.001	0.000	0.003	0.000	0.003	0.000	0.003	0.000	0.003	0.000	0.003	0.000	0.003	0.000
TiO2	0.003	0.000	0.002	0.000	0.002	0.000	0.001	0.000	0.003	0.000	0.003	0.000	0.003	0.000	0.004	0.000	0.004	0.000	0.004	0.000
HδA	8.793	0.025	9.333	0.014	8.945	0.016	8.122	0.020	6.439	0.035	11.040	0.040	15.300	0.010	4.092	0.042	7.384	0.058	11.030	0.060
HγA	8.480	−0.025	9.105	−0.041	8.839	−0.052	8.074	−0.056	6.535	0.014	11.160	0.020	15.470	−0.010	4.072	0.045	7.340	0.056	11.050	0.060
HδF	7.516	0.019	7.457	0.017	6.984	0.019	6.336	0.020	5.851	0.026	8.936	0.019	10.450	−0.010	3.742	0.036	6.279	0.042	8.366	0.029
HγF	7.326	0.017	7.349	0.004	6.935	−0.007	6.320	−0.012	5.915	0.020	8.826	0.016	10.300	−0.010	3.819	0.041	6.229	0.043	8.238	0.030
D4000	1.234	0.004	1.293	0.003	1.311	0.003	1.311	0.003	1.079	0.001	1.197	0.002	1.376	0.001	1.017	−0.001	1.082	0.001	1.185	0.001

Table A.3. 1-Å resolution spectra: I_{sol} and $I_{enh} - I_{sol}$ for $[Z/Z_\odot] = -1.0$.

T_{eff}	4000								5250							
log g	1.5		2.5		3.5		4.5		1.5		2.5		3.5		4.5	
	I_{sol}	(δI)	I_{sol}	(δI)	I_{sol}	(δI)	I_{sol}	(δI)	I_{sol}	(δI)	I_{sol}	(δI)	I_{sol}	(δI)	I_{sol}	(δI)
CN1	0.135	–0.035	0.120	–0.009	0.090	0.010	0.045	0.024	–0.042	0.004	–0.043	0.002	–0.041	0.002	–0.040	0.006
CN2	0.222	–0.034	0.226	–0.010	0.212	0.006	0.164	0.022	–0.017	0.007	–0.022	0.006	–0.024	0.007	–0.025	0.013
Ca4227	2.303	1.585	3.863	1.269	5.836	0.849	6.731	0.690	0.209	0.214	0.037	0.349	0.053	0.491	0.441	0.628
G4300	8.401	–0.815	8.144	–1.093	7.652	–1.107	5.594	–0.631	7.032	–0.867	7.585	–0.727	7.819	–0.699	8.264	–0.965
Fe4383	7.784	–1.785	8.451	–2.249	8.915	–2.474	7.486	–1.979	2.710	–0.531	3.193	–0.819	3.800	–1.187	4.728	–1.719
Ca4455	2.336	–0.178	2.440	–0.210	2.460	–0.199	2.109	–0.145	0.849	–0.076	0.782	–0.066	0.731	–0.043	0.747	–0.031
Fe4531	4.905	–0.269	4.668	–0.313	4.577	–0.309	4.168	–0.206	3.000	–0.205	2.874	–0.221	2.712	–0.238	2.604	–0.285
$C_2$4668	2.269	–0.398	1.376	0.007	0.722	0.522	0.103	0.744	0.512	–0.146	0.478	–0.157	0.436	–0.147	0.377	–0.093
Hβ	0.031	0.082	–0.326	0.114	–0.593	0.189	–0.669	0.163	1.870	0.119	1.539	0.116	1.247	0.120	1.027	0.118
Fe5015	5.780	–0.627	4.799	–0.553	4.258	–0.374	3.256	–0.238	4.109	–0.313	3.888	–0.300	3.713	–0.336	3.618	–0.454
Mg1	0.195	0.019	0.286	0.022	0.370	0.030	0.399	0.055	0.010	–0.003	0.009	–0.003	0.008	0.000	0.009	0.007
Mg2	0.331	0.047	0.482	0.057	0.624	0.075	0.630	0.102	0.045	0.002	0.056	0.008	0.085	0.017	0.142	0.035
Mgb	3.380	0.979	4.998	1.164	6.022	1.365	5.153	1.310	0.306	0.292	0.795	0.456	1.852	0.711	3.595	1.099
Fe5270	3.586	–0.319	3.870	–0.426	4.204	–0.523	4.004	–0.465	1.485	–0.023	1.521	–0.049	1.690	–0.121	2.041	–0.241
Fe5335	3.744	–0.415	3.899	–0.584	4.054	–0.732	3.670	–0.693	1.650	–0.110	1.738	–0.148	1.873	–0.215	2.138	–0.329
Fe5406	2.272	–0.311	2.584	–0.444	2.894	–0.534	2.728	–0.489	0.706	–0.118	0.772	–0.135	0.918	–0.190	1.188	–0.290
Fe5709	1.324	–0.059	1.161	–0.064	0.950	–0.066	0.607	–0.049	0.488	–0.086	0.499	–0.090	0.500	–0.095	0.479	–0.099
Fe5782	0.833	–0.189	0.775	–0.223	0.626	–0.243	0.401	–0.201	0.136	–0.023	0.150	–0.027	0.155	–0.030	0.153	–0.032
NaD	2.448	–0.602	3.908	–0.982	6.147	–1.512	7.656	–1.691	0.423	–0.078	0.513	–0.114	0.765	–0.185	1.309	–0.301
TiO1	0.011	0.004	0.011	0.010	0.016	0.022	0.012	0.025	0.002	0.000	0.002	0.000	0.002	0.000	0.001	0.000
TiO2	0.039	–0.001	0.038	0.010	0.045	0.029	0.035	0.035	0.009	–0.001	0.008	–0.001	0.007	–0.001	0.006	–0.001
HδA	–7.093	2.637	–6.977	2.633	–6.823	2.498	–4.447	1.569	–0.614	0.543	–1.117	0.743	–1.995	1.060	–3.473	1.628
HγA	–10.740	0.837	–11.950	1.510	–12.810	1.840	–10.640	1.435	–4.985	0.993	–5.887	0.920	–6.744	1.017	–8.246	1.565
HδF	–3.441	0.650	–3.515	0.799	–3.443	0.907	–2.226	0.679	0.342	0.310	0.139	0.344	–0.224	0.434	–0.844	0.652
HγF	–3.662	0.448	–4.236	0.666	–4.582	0.740	–3.715	0.551	–0.751	0.502	–1.488	0.518	–2.161	0.574	–3.076	0.836
D4000	2.938	–0.247	2.847	–0.345	2.905	–0.392	2.655	–0.281	1.649	–0.010	1.617	–0.035	1.662	–0.064	1.790	–0.108

T_{eff}	7250								10 000						13 000					
log g	1.5		2.5		3.5		4.5		2.5		3.5		4.5		2.5		3.5		4.5	
	I_{sol}	(δI)	I_{sol}	(δI)	I_{sol}	(δI)	I_{sol}	(δI)	I_{sol}	(δI)	I_{sol}	(δI)	I_{sol}	(δI)	I_{sol}	(δI)	I_{sol}	(δI)	I_{sol}	(δI)
CN1	–0.173	0.000	–0.191	0.001	–0.184	0.000	–0.169	0.000	–0.125	0.000	–0.229	0.000	–0.342	0.001	–0.073	0.001	–0.144	0.000	–0.231	0.000
CN2	–0.080	0.000	–0.106	0.001	–0.106	0.000	–0.097	0.000	–0.039	0.001	–0.131	0.000	–0.255	0.002	–0.013	0.000	–0.065	0.000	–0.148	0.001
Ca4227	0.122	0.003	0.121	0.007	0.123	0.010	0.141	0.016	0.049	–0.010	0.044	–0.008	0.051	–0.004	0.041	–0.014	0.040	–0.015	0.029	–0.013
G4300	–0.758	0.142	–1.086	0.147	–1.093	0.128	–0.933	0.107	–0.729	0.058	–2.310	0.059	–3.928	0.077	–0.431	0.008	–1.281	0.011	–2.554	0.013
Fe4383	0.328	0.079	–0.313	0.049	–0.620	0.005	–0.694	–0.036	–0.057	–0.015	–0.861	–0.029	–3.055	–0.017	0.137	–0.016	–0.228	–0.010	–1.241	0.001
Ca4455	0.155	–0.008	0.133	–0.006	0.125	–0.007	0.140	–0.015	–0.025	0.006	–0.037	–0.001	–0.055	–0.008	0.221	–0.019	0.204	–0.024	0.178	–0.028
Fe4531	1.166	–0.092	1.040	–0.087	0.896	–0.090	0.772	–0.098	0.229	–0.045	0.183	–0.041	0.155	–0.041	0.104	–0.019	0.105	–0.024	0.081	–0.022
$C_2$4668	–0.301	0.109	–0.262	0.097	–0.208	0.079	–0.127	0.058	–0.155	0.074	–0.096	0.060	–0.118	0.052	–0.019	0.062	0.007	0.041	0.031	0.024
Hβ	7.340	0.027	7.346	0.002	6.903	–0.015	6.320	–0.028	5.968	0.033	8.721	0.048	9.760	0.003	3.830	–0.024	6.103	–0.008	7.948	–0.003
Fe5015	1.061	–0.242	1.057	–0.248	1.006	–0.243	0.952	–0.234	0.026	–0.087	0.036	–0.073	–0.015	–0.066	0.069	–0.082	0.019	–0.093	–0.009	–0.090
Mg1	–0.002	0.000	–0.005	0.000	–0.007	0.000	–0.008	0.000	0.006	0.000	0.003	0.000	–0.008	0.001	0.007	0.000	0.007	0.000	0.003	0.000
Mg2	0.024	–0.001	0.021	0.000	0.018	0.000	0.020	0.002	0.010	0.001	0.010	0.001	0.003	0.001	0.009	0.000	0.009	0.000	0.007	0.000
Mgb	0.463	0.119	0.443	0.134	0.446	0.154	0.548	0.211	0.085	0.048	0.149	0.053	0.221	0.044	0.026	0.002	0.043	0.006	0.057	0.004
Fe5270	0.387	–0.016	0.405	0.004	0.410	0.020	0.419	0.032	–0.010	0.004	–0.011	0.011	–0.003	0.011	0.008	0.002	0.009	0.003	0.009	0.004
Fe5335	0.593	–0.069	0.628	–0.067	0.635	–0.061	0.630	–0.055	0.088	–0.011	0.078	–0.014	0.078	–0.016	0.061	0.002	0.051	–0.004	0.037	–0.005
Fe5406	0.129	–0.071	0.181	–0.073	0.223	–0.069	0.251	–0.061	0.023	–0.005	0.015	–0.002	0.012	–0.001	0.019	–0.003	0.020	–0.002	0.016	–0.001
Fe5709	0.023	0.004	0.040	0.001	0.051	–0.003	0.056	–0.007	0.000	0.002	0.001	0.001	0.002	0.001	0.001	0.002	0.001	0.002	0.002	0.001
Fe5782	0.014	–0.002	0.014	–0.002	0.013	–0.001	0.013	–0.001	0.008	–0.005	0.005	–0.002	0.003	–0.001	0.007	–0.005	0.007	–0.005	0.005	–0.003
NaD	0.244	–0.015	0.241	–0.013	0.237	–0.014	0.247	–0.018	–0.017	–0.006	0.012	–0.007	0.047	–0.014	–0.138	–0.002	–0.106	0.000	–0.078	0.001
TiO1	0.003	0.000	0.002	0.000	0.002	0.000	0.001	0.000	0.003	0.000	0.003	0.000	0.003	0.000	0.004	0.000	0.004	0.000	0.004	0.000
TiO2	0.004	0.000	0.004	0.000	0.003	0.000	0.002	0.000	0.004	0.000	0.004	0.000	0.003	0.000	0.004	0.000	0.004	0.000	0.004	0.000
HδA	8.520	0.091	9.237	0.041	8.883	0.043	8.110	0.055	6.347	0.001	10.910	0.020	15.250	–0.030	4.058	–0.048	7.329	–0.035	10.970	–0.030
HγA	8.217	–0.044	8.955	–0.067	8.707	–0.058	7.983	–0.050	6.427	–0.028	11.020	–0.010	15.420	–0.060	4.061	–0.036	7.297	–0.028	10.990	–0.020
HδF	7.345	0.095	7.368	0.071	6.920	0.071	6.304	0.072	5.775	0.005	8.850	0.026	10.420	0.000	3.703	–0.033	6.221	–0.018	8.304	–0.010
HγF	7.294	0.021	7.374	–0.007	6.977	–0.017	6.384	–0.022	5.864	0.005	8.764	0.021	10.290	–0.010	3.825	–0.033	6.206	–0.018	8.201	–0.009
D4000	1.264	0.005	1.323	0.004	1.340	0.002	1.341	0.003	1.079	0.000	1.196	0.001	1.378	–0.001	1.016	–0.001	1.081	0.000	1.183	0.000

Table A.4. 1-Å resolution spectra: I_{sol} and $I_{enh} - I_{sol}$ for $[Z/Z_\odot] = -0.5$.

T_{eff}	4000								5250							
log g	1.5		2.5		3.5		4.5		1.5		2.5		3.5		4.5	
	I_{sol}	(δI)	I_{sol}	(δI)	I_{sol}	(δI)	I_{sol}	(δI)	I_{sol}	(δI)	I_{sol}	(δI)	I_{sol}	(δI)	I_{sol}	(δI)
CN1	0.185	–0.068	0.151	–0.039	0.099	–0.012	0.030	0.014	–0.027	–0.016	–0.021	–0.020	–0.019	–0.018	–0.022	–0.011
CN2	0.284	–0.070	0.267	–0.045	0.235	–0.024	0.164	0.005	0.000	–0.012	0.004	–0.016	0.005	–0.014	0.003	–0.004
Ca4227	4.300	1.463	5.563	1.079	7.370	0.508	8.053	0.327	0.104	0.544	–0.081	0.706	–0.010	0.848	0.605	0.963
G4300	8.423	–0.636	8.049	–0.877	7.884	–0.959	6.068	–0.184	7.898	–0.571	8.050	–0.484	8.039	–0.538	8.219	–0.820
Fe4383	9.299	–2.023	9.703	–2.495	10.640	–3.086	9.187	–2.427	3.774	–0.769	4.371	–1.052	5.023	–1.403	6.104	–2.018
Ca4455	2.945	–0.197	3.024	–0.213	3.204	–0.267	2.847	–0.187	1.178	–0.054	1.133	–0.071	1.118	–0.078	1.176	–0.077
Fe4531	6.042	–0.260	5.709	–0.362	5.819	–0.518	5.348	–0.312	3.951	–0.320	3.826	–0.346	3.683	–0.385	3.597	–0.439
$C_2$4668	3.171	–0.498	2.070	0.433	1.529	1.473	0.943	2.030	1.527	–0.495	1.490	–0.551	1.304	–0.487	1.047	–0.327
Hβ	–0.097	0.155	–0.429	0.270	–0.680	0.483	–0.797	0.548	2.064	0.131	1.755	0.112	1.436	0.116	1.149	0.119
Fe5015	7.168	–0.487	6.287	–0.351	6.154	–0.177	5.004	0.237	5.867	–0.413	5.495	–0.388	5.216	–0.441	5.107	–0.630
Mg1	0.258	0.006	0.330	0.006	0.419	0.002	0.465	0.035	0.027	–0.008	0.027	–0.009	0.024	–0.004	0.026	0.009
Mg2	0.432	0.046	0.568	0.052	0.728	0.047	0.751	0.092	0.070	0.000	0.085	0.007	0.124	0.021	0.203	0.045
Mgb	4.242	1.326	5.729	1.398	6.816	1.346	5.959	1.421	0.489	0.324	1.105	0.562	2.487	0.898	4.763	1.329
Fe5270	4.333	–0.450	4.473	–0.554	4.927	–0.718	4.839	–0.570	2.241	–0.089	2.280	–0.139	2.482	–0.221	2.927	–0.348
Fe5335	4.798	–0.616	4.829	–0.833	5.076	–1.135	4.618	–1.009	2.292	–0.155	2.472	–0.222	2.701	–0.323	3.097	–0.474
Fe5406	2.952	–0.449	3.187	–0.570	3.595	–0.730	3.421	–0.598	1.024	–0.150	1.121	–0.175	1.304	–0.241	1.673	–0.370
Fe5709	1.768	–0.080	1.545	–0.088	1.320	–0.097	0.925	–0.041	0.854	–0.112	0.847	–0.117	0.834	–0.124	0.801	–0.132
Fe5782	1.224	–0.250	1.103	–0.316	0.912	–0.400	0.627	–0.384	0.300	–0.039	0.326	–0.048	0.335	–0.055	0.337	–0.063
NaD	3.782	–0.942	5.376	–1.401	8.272	–2.283	10.170	–2.429	0.604	–0.136	0.738	–0.189	1.093	–0.283	1.855	–0.438
TiO1	0.019	0.012	0.025	0.028	0.043	0.049	0.042	0.064	0.002	0.001	0.002	0.001	0.002	0.001	0.002	0.001
TiO2	0.059	0.010	0.066	0.035	0.091	0.066	0.086	0.089	0.015	–0.002	0.013	–0.002	0.012	–0.002	0.011	–0.002
HδA	–9.627	3.438	–8.909	3.245	–8.914	3.206	–6.115	1.728	–1.726	0.898	–2.217	1.185	–3.101	1.576	–4.768	2.248
HγA	–12.710	0.960	–13.440	1.620	–14.850	2.250	–12.740	1.290	–6.216	0.779	–6.763	0.764	–7.451	0.973	–8.910	1.639
HδF	–4.793	0.902	–4.506	0.975	–4.404	1.113	–3.000	0.722	–0.016	0.310	–0.109	0.351	–0.402	0.466	–1.066	0.732
HγF	–4.253	0.517	–4.545	0.632	–4.960	0.688	–4.198	0.307	–1.043	0.438	–1.582	0.432	–2.147	0.526	–2.979	0.801
D4000	3.370	–0.298	3.158	–0.379	3.235	–0.471	2.936	–0.324	1.894	–0.034	1.821	–0.055	1.857	–0.089	2.017	–0.155

T_{eff}	7250								10 000						13 000					
log g	1.5		2.5		3.5		4.5		2.5		3.5		4.5		2.5		3.5		4.5	
	I_{sol}	(δI)	I_{sol}	(δI)	I_{sol}	(δI)	I_{sol}	(δI)	I_{sol}	(δI)	I_{sol}	(δI)	I_{sol}	(δI)	I_{sol}	(δI)	I_{sol}	(δI)	I_{sol}	(δI)
CN1	–0.164	–0.002	–0.188	0.000	–0.183	0.001	–0.171	0.002	–0.123	0.002	–0.228	0.003	–0.341	0.004	–0.070	0.001	–0.141	0.001	–0.227	0.001
CN2	–0.071	–0.001	–0.102	0.001	–0.103	0.001	–0.098	0.001	–0.037	0.002	–0.129	0.003	–0.253	0.004	–0.011	0.001	–0.062	0.001	–0.144	0.001
Ca4227	0.179	–0.004	0.165	0.013	0.159	0.026	0.185	0.044	0.043	–0.003	0.046	0.002	0.070	–0.001	0.057	–0.013	0.056	–0.013	0.047	–0.015
G4300	–0.385	0.181	–0.707	0.169	–0.679	0.133	–0.466	0.082	–0.622	0.107	–2.186	0.124	–3.831	0.138	–0.442	0.002	–1.256	0.017	–2.502	0.023
Fe4383	0.474	0.158	–0.194	0.126	–0.488	0.055	–0.549	–0.050	0.027	0.009	–0.723	–0.016	–2.892	0.010	0.200	–0.019	–0.154	–0.008	–1.142	0.001
Ca4455	0.345	–0.017	0.305	–0.024	0.260	–0.021	0.229	–0.016	–0.048	0.004	–0.062	–0.004	–0.081	–0.016	0.199	–0.009	0.187	–0.017	0.160	–0.025
Fe4531	1.769	–0.132	1.655	–0.113	1.476	–0.096	1.302	–0.095	0.373	–0.055	0.320	–0.057	0.286	–0.066	0.179	–0.020	0.183	–0.028	0.149	–0.029
$C_2$4668	–0.189	0.068	–0.174	0.051	–0.173	0.050	–0.131	0.050	–0.363	0.109	–0.252	0.096	–0.225	0.091	–0.195	0.103	–0.147	0.075	–0.080	0.051
Hβ	7.475	0.065	7.506	0.034	7.085	0.007	6.512	–0.013	6.012	–0.013	8.802	–0.029	9.835	–0.050	3.760	–0.035	6.024	–0.021	7.885	–0.025
Fe5015	2.144	–0.429	2.125	–0.411	2.005	–0.383	1.876	–0.357	0.028	–0.118	0.031	–0.104	–0.010	–0.104	0.059	–0.098	–0.019	–0.115	–0.068	–0.122
Mg1	0.001	–0.002	–0.003	–0.002	–0.006	–0.002	–0.007	–0.002	0.007	0.000	0.003	0.000	–0.009	0.001	0.008	–0.001	0.007	–0.001	0.003	0.000
Mg2	0.030	–0.002	0.026	–0.001	0.025	0.001	0.029	0.003	0.012	0.001	0.012	0.001	0.005	0.001	0.009	0.000	0.009	0.000	0.007	0.000
Mgb	0.361	0.176	0.340	0.202	0.403	0.234	0.666	0.328	0.113	0.079	0.214	0.073	0.297	0.059	–0.031	0.021	0.005	0.027	0.045	0.029
Fe5270	0.753	0.004	0.776	0.027	0.772	0.047	0.773	0.068	0.037	–0.014	0.019	0.002	0.028	0.008	0.026	–0.003	0.029	0.000	0.024	0.007
Fe5335	0.856	–0.058	0.941	–0.058	0.994	–0.051	1.036	–0.035	0.134	0.005	0.139	–0.005	0.157	–0.015	0.114	0.013	0.092	0.007	0.073	0.001
Fe5406	0.269	–0.088	0.326	–0.093	0.378	–0.094	0.426	–0.085	0.064	–0.018	0.043	–0.009	0.034	–0.003	0.049	–0.009	0.054	–0.009	0.043	–0.003
Fe5709	0.063	0.009	0.106	0.000	0.131	–0.009	0.142	–0.018	–0.004	0.005	–0.001	0.003	0.002	0.003	–0.002	0.005	–0.001	0.004	0.000	0.003
Fe5782	0.038	–0.007	0.038	–0.005	0.037	–0.003	0.037	–0.002	0.022	–0.013	0.013	–0.007	0.008	–0.004	0.017	–0.014	0.018	–0.014	0.013	–0.010
NaD	0.284	–0.017	0.278	–0.021	0.276	–0.026	0.303	–0.038	0.016	–0.020	0.055	–0.021	0.100	–0.027	–0.126	–0.013	–0.097	–0.010	–0.071	–0.007
TiO1	0.003	0.000	0.003	0.000	0.002	0.000	0.002	0.000	0.005	0.000	0.004	0.000	0.003	0.000	0.005	0.000	0.005	0.000	0.005	0.000
TiO2	0.006	0.000	0.005	–0.001	0.004	–0.001	0.003	0.000	0.005	0.000	0.004	0.000	0.004	0.000	0.004	0.000	0.004	0.000	0.004	0.000
HδA	8.149	0.156	9.134	0.076	8.816	0.071	8.145	0.074	6.211	–0.026	10.810	–0.050	15.170	–0.100	3.907	–0.063	7.156	–0.057	10.790	–0.050
HγA	7.962	–0.101	8.821	–0.107	8.567	–0.070	7.856	–0.017	6.290	–0.086	10.910	–0.110	15.340	–0.170	3.948	–0.043	7.146	–0.048	10.830	–0.060
HδF	7.113	0.172	7.253	0.133	6.843	0.122	6.284	0.116	5.693	–0.022	8.820	–0.030	10.420	–0.050	3.578	–0.043	6.089	–0.034	8.191	–0.030
HγF	7.270	0.008	7.414	–0.018	7.030	–0.021	6.447	–0.012	5.817	–0.021	8.768	–0.040	10.310	–0.060	3.750	–0.040	6.115	–0.032	8.122	–0.030
D4000	1.307	0.011	1.368	0.009	1.383	0.007	1.386	0.007	1.081	–0.001	1.198	–0.001	1.381	–0.005	1.014	0.000	1.078	0.000	1.178	0.000

Table A.5. 1-Å resolution spectra: I_{sol} and $I_{enh} - I_{sol}$ for $[Z/Z_{\odot}] = 0.0$.

T_{eff}	4000								5250							
log g	1.5		2.5		3.5		4.5		1.5		2.5		3.5		4.5	
	I_{sol}	(δI)	I_{sol}	(δI)	I_{sol}	(δI)	I_{sol}	(δI)	I_{sol}	(δI)	I_{sol}	(δI)	I_{sol}	(δI)	I_{sol}	(δI)
CN1	0.217	–0.091	0.172	–0.067	0.101	–0.038	0.011	–0.005	0.040	–0.070	0.044	–0.071	0.039	–0.064	0.024	–0.049
CN2	0.321	–0.093	0.292	–0.074	0.240	–0.052	0.158	–0.019	0.072	–0.068	0.078	–0.069	0.075	–0.062	0.064	–0.045
Ca4227	6.577	0.874	7.137	0.647	8.055	0.300	8.432	0.090	–0.177	1.077	–0.282	1.232	–0.092	1.349	0.819	1.404
G4300	8.600	–0.339	8.095	–0.599	7.883	–0.690	6.955	–0.079	8.237	–0.176	8.215	–0.205	8.086	–0.325	8.044	–0.593
Fe4383	10.690	–2.075	10.630	–2.600	11.420	–3.313	11.040	–3.199	4.687	–0.765	5.353	–1.059	6.143	–1.485	7.492	–2.252
Ca4455	3.584	–0.245	3.610	–0.257	3.793	–0.327	3.638	–0.344	1.581	–0.044	1.525	–0.066	1.556	–0.101	1.678	–0.131
Fe4531	7.479	–0.284	6.877	–0.456	6.893	–0.766	6.770	–0.793	4.954	–0.445	4.813	–0.477	4.684	–0.525	4.651	–0.598
$C_2$4668	4.429	–0.705	3.297	1.105	3.275	2.817	3.061	4.161	3.499	–1.371	3.402	–1.448	2.862	–1.201	2.172	–0.787
Hβ	–0.282	0.363	–0.416	0.617	–0.406	0.992	–0.500	1.324	2.335	0.100	2.057	0.069	1.732	0.064	1.394	0.081
Fe5015	9.264	–0.257	8.431	–0.094	8.513	0.092	7.735	0.678	7.815	–0.519	7.273	–0.494	6.883	–0.573	6.739	–0.830
Mg1	0.313	–0.018	0.356	–0.020	0.411	–0.029	0.494	–0.020	0.065	–0.026	0.064	–0.026	0.056	–0.016	0.056	0.006
Mg2	0.546	0.039	0.651	0.030	0.769	0.005	0.844	0.012	0.115	–0.008	0.131	0.001	0.179	0.021	0.283	0.051
Mgb	5.377	1.756	6.634	1.538	7.380	1.237	6.719	1.133	0.817	0.470	1.494	0.773	3.221	1.178	6.049	1.538
Fe5270	5.108	–0.615	5.052	–0.716	5.394	–0.901	5.649	–0.878	3.167	–0.174	3.207	–0.250	3.429	–0.331	3.943	–0.445
Fe5335	5.999	–0.883	5.788	–1.179	5.826	–1.600	5.614	–1.712	3.177	–0.239	3.432	–0.324	3.752	–0.444	4.281	–0.635
Fe5406	3.690	–0.552	3.812	–0.648	4.154	–0.817	4.233	–0.789	1.395	–0.168	1.555	–0.210	1.795	–0.283	2.245	–0.423
Fe5709	2.229	–0.111	1.926	–0.133	1.638	–0.142	1.276	–0.077	1.349	–0.126	1.304	–0.129	1.262	–0.134	1.209	–0.146
Fe5782	1.631	–0.301	1.390	–0.420	1.064	–0.562	0.756	–0.645	0.567	–0.040	0.606	–0.058	0.618	–0.071	0.627	–0.092
NaD	5.637	–1.480	7.003	–2.014	9.514	–3.029	11.970	–3.856	0.947	–0.221	1.117	–0.288	1.582	–0.400	2.609	–0.602
TiO1	0.038	0.031	0.061	0.058	0.102	0.086	0.120	0.110	0.000	0.002	0.002	0.002	0.002	0.001	0.003	0.001
TiO2	0.099	0.035	0.128	0.073	0.181	0.104	0.202	0.134	0.020	–0.003	0.019	–0.003	0.017	–0.003	0.016	–0.004
HδA	–12.470	4.156	–10.890	3.826	–10.490	3.661	–8.413	2.324	–3.616	1.733	–4.036	2.078	–4.828	2.485	–6.483	3.176
HγA	–15.470	1.110	–15.280	1.720	–16.180	2.340	–15.480	1.640	–7.064	0.432	–7.541	0.597	–8.221	0.943	–9.693	1.742
HδF	–6.436	1.389	–5.616	1.349	–5.096	1.341	–3.864	0.994	–0.468	0.405	–0.490	0.481	–0.697	0.602	–1.324	0.880
HγF	–5.294	0.681	–5.126	0.633	–5.272	0.545	–4.960	0.129	–1.180	0.396	–1.662	0.434	–2.177	0.549	–2.919	0.824
D4000	3.942	–0.395	3.480	–0.410	3.420	–0.473	3.223	–0.395	2.186	–0.013	2.059	–0.041	2.077	–0.086	2.262	–0.176

T_{eff}	7250							
log g	1.5		2.5		3.5		4.5	
	I_{sol}	(δI)	I_{sol}	(δI)	I_{sol}	(δI)	I_{sol}	(δI)
CN1	–0.155	–0.004	–0.188	–0.001	–0.183	0.000	–0.177	0.002
CN2	–0.063	–0.002	–0.103	0.000	–0.103	0.001	–0.102	0.002
Ca4227	0.324	–0.066	0.274	–0.022	0.241	0.020	0.270	0.063
G4300	0.030	0.217	–0.280	0.166	–0.139	0.091	0.182	–0.007
Fe4383	0.463	0.248	–0.182	0.198	–0.352	0.107	–0.352	–0.048
Ca4455	0.558	–0.032	0.508	–0.051	0.446	–0.056	0.390	–0.052
Fe4531	2.486	–0.222	2.433	–0.206	2.261	–0.184	2.062	–0.159
$C_2$4668	–0.073	0.094	–0.014	0.055	–0.022	0.042	–0.026	0.049
Hβ	7.576	0.099	7.679	0.074	7.305	0.045	6.765	0.032
Fe5015	3.734	–0.651	3.671	–0.601	3.439	–0.546	3.209	–0.501
Mg1	0.005	–0.004	0.001	–0.004	–0.003	–0.003	–0.006	–0.003
Mg2	0.039	–0.004	0.034	–0.002	0.033	0.001	0.041	0.005
Mgb	0.280	0.168	0.237	0.216	0.375	0.291	0.888	0.441
Fe5270	1.246	0.023	1.312	0.037	1.323	0.064	1.352	0.104
Fe5335	1.176	–0.062	1.315	–0.050	1.446	–0.042	1.604	–0.019
Fe5406	0.510	–0.136	0.550	–0.120	0.584	–0.100	0.644	–0.078
Fe5709	0.157	0.010	0.241	–0.006	0.287	–0.019	0.307	–0.030
Fe5782	0.096	–0.016	0.097	–0.010	0.095	–0.005	0.094	–0.002
NaD	0.352	–0.037	0.346	–0.048	0.351	–0.059	0.413	–0.082
TiO1	0.004	0.000	0.003	0.000	0.003	0.000	0.003	0.000
TiO2	0.009	–0.001	0.008	–0.001	0.007	–0.001	0.006	–0.001
HδA	7.635	0.195	9.043	0.106	8.728	0.085	8.206	0.104
HγA	7.725	–0.231	8.786	–0.194	8.413	–0.110	7.676	0.031
HδF	6.810	0.215	7.155	0.164	6.776	0.138	6.306	0.137
HγF	7.249	–0.048	7.494	–0.053	7.096	–0.043	6.517	0.003
D4000	1.371	0.023	1.439	0.020	1.449	0.016	1.458	0.014

Table A.6. Spectra degraded to the Lick resolution: I_{sol} and $I_{enh} - I_{sol}$ for $[Z/Z_{\odot}] = -2.0$.

T_{eff}	4000								5250							
log g	1.5		2.5		3.5		4.5		1.5		2.5		3.5		4.5	
	I_{sol}	(δI)	I_{sol}	(δI)	I_{sol}	(δI)	I_{sol}	(δI)	I_{sol}	(δI)	I_{sol}	(δI)	I_{sol}	(δI)	I_{sol}	(δI)
CN1	0.013	0.014	0.022	0.036	0.018	0.042	0.018	0.053	–0.032	0.008	–0.037	0.010	–0.044	0.011	–0.051	0.013
CN2	0.057	0.018	0.086	0.042	0.086	0.048	0.103	0.059	–0.013	0.008	–0.022	0.010	–0.034	0.011	–0.046	0.014
Ca4227	0.233	0.314	0.870	0.405	1.559	0.245	2.759	0.240	0.101	–0.005	0.095	0.025	0.123	0.066	0.228	0.102
G4300	7.895	–0.940	8.195	–1.339	6.921	–1.623	5.957	–1.885	2.689	–0.938	4.085	–1.002	5.413	–0.942	6.552	–1.149
Fe4383	4.497	–1.440	5.123	–1.643	4.775	–1.640	5.085	–1.614	1.016	–0.210	1.025	–0.365	1.242	–0.539	1.671	–0.728
Ca4455	0.765	–0.146	0.803	–0.167	0.668	–0.202	0.671	–0.204	0.222	–0.062	0.196	–0.046	0.178	–0.050	0.173	–0.058
Fe4531	2.854	–0.328	2.748	–0.314	2.433	–0.379	2.545	–0.358	1.019	–0.147	0.926	–0.151	0.845	–0.167	0.771	–0.194
$C_2$4668	0.701	–0.131	0.331	–0.104	0.034	–0.072	–0.217	–0.049	0.032	0.030	0.036	0.023	0.040	0.016	0.042	0.025
Hβ	0.237	0.060	0.049	0.057	–0.097	0.053	–0.198	–0.013	1.671	–0.036	1.424	–0.036	1.221	–0.028	1.108	–0.029
Fe5015	3.121	–0.432	2.263	–0.553	1.659	–0.589	1.170	–0.570	1.217	–0.355	1.154	–0.335	1.069	–0.318	0.924	–0.308
Mg1	0.075	0.008	0.162	0.028	0.188	0.026	0.271	0.042	–0.004	–0.003	–0.003	–0.002	–0.004	–0.002	–0.004	–0.001
Mg2	0.165	0.017	0.303	0.042	0.353	0.034	0.459	0.039	0.022	–0.001	0.026	–0.001	0.036	0.000	0.056	0.001
Mgb	1.996	0.333	3.599	0.560	4.096	0.494	4.431	0.292	0.361	0.131	0.515	0.132	0.937	0.171	1.681	0.227
Fe5270	1.895	–0.262	2.244	–0.336	2.209	–0.430	2.382	–0.520	0.484	–0.080	0.500	–0.093	0.541	–0.124	0.621	–0.183
Fe5335	1.756	–0.295	1.986	–0.355	1.954	–0.456	2.197	–0.571	0.615	–0.102	0.606	–0.117	0.616	–0.148	0.672	–0.206
Fe5406	1.099	–0.247	1.362	–0.308	1.394	–0.371	1.595	–0.461	0.276	–0.109	0.311	–0.104	0.345	–0.107	0.394	–0.134
Fe5709	0.561	–0.121	0.478	–0.118	0.310	–0.124	0.189	–0.092	0.077	–0.063	0.084	–0.067	0.083	–0.067	0.072	–0.064
Fe5782	0.200	–0.130	0.191	–0.129	0.120	–0.102	0.083	–0.066	0.014	–0.018	0.015	–0.020	0.015	–0.020	0.013	–0.018
NaD	0.991	–0.398	1.818	–0.662	2.510	–1.012	4.250	–1.504	0.278	–0.031	0.299	–0.045	0.387	–0.088	0.601	–0.175
TiO1	0.002	0.000	0.002	–0.001	0.000	–0.004	–0.001	–0.005	0.000	0.000	0.000	0.000	0.000	0.000	0.000	0.000
TiO2	0.014	–0.006	0.013	–0.006	0.009	–0.010	0.005	–0.012	0.001	–0.002	0.001	–0.001	0.000	–0.001	0.000	–0.001
HδA	–3.253	1.805	–3.441	1.949	–3.017	1.918	–2.701	1.851	0.851	0.215	0.413	0.248	–0.226	0.358	–0.962	0.551
HγA	–8.226	1.061	–9.946	1.640	–9.170	2.170	–9.156	2.499	–1.062	0.979	–2.646	1.110	–4.342	1.143	–5.971	1.482
HδF	–1.607	0.694	–1.777	0.775	–1.616	0.842	–1.463	0.859	0.979	0.206	0.697	0.185	0.329	0.201	–0.033	0.257
HγF	–2.862	0.398	–3.692	0.718	–3.563	0.977	–3.549	1.164	0.608	0.416	–0.280	0.489	–1.272	0.518	–2.189	0.682
D4000	2.428	–0.257	2.336	–0.300	2.275	–0.286	2.305	–0.281	1.408	–0.028	1.382	–0.026	1.399	–0.028	1.453	–0.037

T_{eff}	7250								10 000						13 000					
log g	1.5		2.5		3.5		4.5		2.5		3.5		4.5		2.5		3.5		4.5	
	I_{sol}	(δI)	I_{sol}	(δI)	I_{sol}	(δI)	I_{sol}	(δI)	I_{sol}	(δI)	I_{sol}	(δI)	I_{sol}	(δI)	I_{sol}	(δI)	I_{sol}	(δI)	I_{sol}	(δI)
CN1	–0.183	0.000	–0.194	0.000	–0.186	0.000	–0.169	0.001	–0.128	–0.001	–0.230	–0.002	–0.335	–0.001	–0.077	–0.001	–0.147	–0.001	–0.230	–0.002
CN2	–0.121	–0.001	–0.136	0.000	–0.133	0.000	–0.120	0.000	–0.073	–0.001	–0.162	–0.002	–0.269	–0.001	–0.039	–0.001	–0.094	–0.001	–0.170	–0.002
Ca4227	0.033	0.004	0.043	0.000	0.049	–0.002	0.057	–0.004	0.011	–0.005	0.006	–0.005	0.001	–0.005	0.005	–0.004	0.004	–0.003	0.001	–0.002
G4300	–1.751	0.027	–2.028	0.029	–2.019	0.011	–1.828	–0.014	–1.284	–0.026	–2.806	–0.032	–4.113	–0.012	–0.729	–0.002	–1.655	–0.012	–2.841	–0.022
Fe4383	–0.278	–0.133	–0.768	–0.104	–0.955	–0.076	–0.897	–0.045	–0.224	–0.023	–1.179	–0.034	–3.441	–0.042	0.047	–0.008	–0.383	–0.013	–1.480	–0.023
Ca4455	–0.019	–0.031	–0.002	–0.029	0.015	–0.020	0.025	–0.014	0.020	–0.006	0.008	–0.006	–0.004	–0.005	0.191	–0.007	0.177	–0.008	0.158	–0.005
Fe4531	0.235	–0.103	0.201	–0.106	0.167	–0.099	0.135	–0.091	0.042	–0.020	0.027	–0.018	0.020	–0.015	0.021	–0.011	0.020	–0.010	0.015	–0.007
$C_2$4668	–0.097	0.054	–0.067	0.042	–0.046	0.029	–0.025	0.017	0.062	0.025	0.053	0.015	–0.021	0.007	0.151	0.023	0.126	0.013	0.100	0.005
Hβ	6.907	–0.029	6.887	–0.036	6.453	–0.042	5.891	–0.047	5.909	0.020	8.482	0.020	9.361	–0.009	3.818	0.021	5.999	0.029	7.712	0.032
Fe5015	0.189	–0.108	0.147	–0.111	0.110	–0.110	0.086	–0.108	0.080	–0.021	0.053	–0.017	–0.030	–0.015	0.156	–0.025	0.107	–0.019	0.059	–0.010
Mg1	0.000	0.001	–0.003	0.001	–0.005	0.001	–0.006	0.001	0.007	0.000	0.004	0.000	–0.008	0.000	0.008	0.000	0.007	0.000	0.003	0.000
Mg2	0.015	0.001	0.012	0.000	0.009	0.000	0.009	–0.001	0.009	0.000	0.007	0.000	–0.001	–0.001	0.009	0.000	0.009	0.000	0.006	0.000
Mgb	0.365	0.055	0.367	0.048	0.364	0.038	0.375	0.019	0.066	–0.009	0.069	–0.017	0.077	–0.018	0.034	–0.006	0.035	–0.009	0.027	–0.012
Fe5270	0.056	–0.049	0.073	–0.052	0.087	–0.052	0.096	–0.054	0.006	–0.001	0.006	–0.001	0.006	–0.001	0.008	–0.002	0.009	–0.002	0.009	–0.002
Fe5335	0.103	–0.059	0.108	–0.068	0.109	–0.072	0.110	–0.074	0.007	–0.004	0.006	–0.004	0.006	–0.004	0.007	–0.004	0.006	–0.003	0.005	–0.002
Fe5406	0.023	–0.025	0.037	–0.030	0.048	–0.035	0.054	–0.039	0.003	–0.002	0.002	–0.001	0.003	–0.001	0.003	–0.001	0.003	–0.002	0.003	–0.002
Fe5709	0.002	–0.002	0.004	–0.004	0.005	–0.005	0.005	–0.006	0.002	0.000	0.002	0.000	0.002	0.000	0.002	0.000	0.002	0.000	0.002	0.000
Fe5782	0.001	–0.001	0.001	–0.001	0.001	–0.001	0.001	–0.001	0.001	0.000	0.001	0.000	0.001	0.000	0.001	0.000	0.001	0.000	0.001	0.000
NaD	0.145	–0.035	0.155	–0.031	0.158	–0.029	0.161	–0.029	–0.010	–0.002	0.000	–0.004	0.008	–0.009	–0.061	0.000	–0.045	0.000	–0.032	0.000
TiO1	0.002	0.000	0.001	0.000	0.001	0.000	0.001	0.000	0.003	0.000	0.003	0.000	0.003	0.000	0.003	0.000	0.003	0.000	0.003	0.000
TiO2	0.002	0.000	0.002	0.000	0.001	0.000	0.001	0.000	0.003	0.000	0.003	0.000	0.003	0.000	0.004	0.000	0.004	0.000	0.004	0.000
HδA	8.835	0.059	9.232	0.023	8.813	0.017	7.981	0.002	6.479	0.041	10.950	0.060	14.940	0.040	4.138	0.032	7.383	0.044	10.870	0.070
HγA	8.611	0.045	9.141	0.004	8.837	–0.004	8.035	–0.016	6.592	0.041	11.140	0.050	15.250	0.020	4.136	0.028	7.380	0.042	10.980	0.070
HδF	6.919	0.039	6.849	0.022	6.414	0.015	5.819	0.004	5.481	0.029	8.200	0.032	9.638	0.007	3.579	0.026	5.834	0.032	7.693	0.039
HγF	6.912	0.018	6.924	–0.002	6.532	–0.013	5.946	–0.023	5.633	0.025	8.329	0.028	9.775	0.002	3.685	0.022	5.917	0.028	7.794	0.036
D4000	1.218	–0.005	1.276	–0.005	1.296	–0.005	1.295	–0.006	1.080	0.000	1.200	0.002	1.379	0.002	1.017	0.001	1.084	0.002	1.188	0.003

Table A.7. Spectra degraded to the Lick resolution: I_{sol} and $I_{enh} - I_{sol}$ for $[Z/Z_{\odot}] = -1.5$.

T_{eff}	4000								5250							
log g	1.5		2.5		3.5		4.5		1.5		2.5		3.5		4.5	
	I_{sol}	(δI)	I_{sol}	(δI)	I_{sol}	(δI)	I_{sol}	(δI)	I_{sol}	(δI)	I_{sol}	(δI)	I_{sol}	(δI)	I_{sol}	(δI)
CN1	0.044	–0.001	0.045	0.019	0.032	0.029	0.018	0.036	–0.043	0.005	–0.050	0.008	–0.056	0.010	–0.062	0.015
CN2	0.103	0.004	0.124	0.022	0.119	0.034	0.110	0.040	–0.023	0.006	–0.035	0.009	–0.046	0.013	–0.055	0.019
Ca4227	0.712	0.947	1.647	0.904	2.696	0.858	3.685	0.750	0.167	0.060	0.132	0.112	0.160	0.189	0.333	0.286
G4300	7.975	–0.906	7.981	–1.261	6.930	–1.184	5.296	–1.114	4.722	–0.735	6.014	–0.901	6.843	–0.958	7.698	–1.289
Fe4383	5.618	–1.315	6.364	–1.718	6.253	–1.586	5.807	–1.522	1.560	–0.156	1.746	–0.314	2.175	–0.580	2.819	–0.878
Ca4455	1.145	–0.104	1.220	–0.150	1.083	–0.118	0.919	–0.125	0.375	–0.067	0.331	–0.048	0.295	–0.031	0.286	–0.028
Fe4531	3.592	–0.194	3.490	–0.212	3.271	–0.139	3.178	–0.119	1.644	0.000	1.543	0.012	1.436	0.010	1.364	–0.013
$C_2$4668	1.260	–0.200	0.669	–0.076	0.205	0.141	–0.154	0.214	0.139	0.073	0.131	0.059	0.131	0.046	0.129	0.052
Hβ	0.191	0.040	–0.055	0.030	–0.244	0.044	–0.346	0.008	1.784	0.025	1.508	0.030	1.295	0.024	1.163	0.012
Fe5015	3.827	–0.480	2.839	–0.441	2.212	–0.282	1.681	–0.219	2.157	–0.033	2.042	–0.031	1.923	–0.036	1.780	–0.054
Mg1	0.130	0.024	0.228	0.029	0.278	0.047	0.330	0.061	0.001	–0.002	0.000	–0.001	0.000	0.000	0.001	0.004
Mg2	0.240	0.045	0.396	0.055	0.481	0.087	0.531	0.090	0.030	0.003	0.037	0.006	0.056	0.013	0.092	0.025
Mgb	2.700	0.717	4.411	0.866	5.070	1.162	4.700	0.927	0.304	0.205	0.613	0.309	1.323	0.489	2.510	0.776
Fe5270	2.506	–0.199	2.848	–0.314	2.925	–0.332	2.886	–0.370	0.797	0.074	0.813	0.068	0.892	0.040	1.056	–0.010
Fe5335	2.358	–0.229	2.600	–0.361	2.621	–0.397	2.602	–0.486	0.889	–0.003	0.904	–0.006	0.951	–0.022	1.073	–0.062
Fe5406	1.501	–0.199	1.787	–0.313	1.882	–0.325	1.897	–0.381	0.398	–0.040	0.444	–0.050	0.515	–0.064	0.630	–0.091
Fe5709	0.795	–0.044	0.691	–0.048	0.507	–0.038	0.306	–0.037	0.189	–0.017	0.201	–0.019	0.203	–0.020	0.187	–0.019
Fe5782	0.410	–0.097	0.396	–0.120	0.283	–0.107	0.179	–0.089	0.042	–0.009	0.046	–0.009	0.046	–0.010	0.043	–0.009
NaD	1.476	–0.365	2.658	–0.686	3.910	–0.850	5.509	–1.219	0.315	–0.041	0.363	–0.058	0.528	–0.108	0.896	–0.196
TiO1	0.006	0.002	0.005	0.004	0.005	0.009	0.002	0.008	0.000	0.000	0.000	0.000	0.000	0.000	0.000	0.000
TiO2	0.024	–0.003	0.022	0.001	0.020	0.010	0.013	0.009	0.003	0.000	0.003	0.000	0.002	0.000	0.001	0.000
HδA	–4.426	1.808	–4.614	1.978	–4.138	1.733	–2.917	1.447	0.448	0.207	–0.055	0.303	–0.816	0.480	–1.801	0.732
HγA	–9.712	0.893	-11.250	1.628	–10.870	1.582	–9.519	1.710	–2.999	0.748	–4.609	0.983	–5.964	1.141	–7.568	1.621
HδF	–2.268	0.501	–2.465	0.659	–2.297	0.663	–1.709	0.650	0.663	0.180	0.422	0.197	0.071	0.246	–0.367	0.336
HγF	–3.104	0.372	–3.798	0.670	–3.817	0.713	–3.313	0.744	–0.097	0.371	–1.043	0.514	–1.883	0.605	–2.780	0.837
D4000	2.636	–0.215	2.567	–0.299	2.539	–0.284	2.436	–0.246	1.489	0.011	1.459	0.003	1.488	–0.007	1.569	–0.019

T_{eff}	7250								10 000						13 000			
log g	1.5		2.5		3.5		4.5		2.5		3.5		4.5		2.5		3.5		4.5	
	I_{sol}	(δI)	I_{sol}	(δI)	I_{sol}	(δI)	I_{sol}	(δI)	I_{sol}	(δI)	I_{sol}	(δI)	I_{sol}	(δI)	I_{sol}	(δI)	I_{sol}	(δI)	I_{sol}	(δI)
CN1	–0.180	0.001	–0.193	0.001	–0.186	0.001	–0.169	0.001	–0.125	–0.001	–0.227	–0.001	–0.333	0.000	–0.075	–0.001	–0.145	–0.001	–0.228	–0.001
CN2	–0.116	0.001	–0.134	0.001	–0.132	0.001	–0.120	0.001	–0.071	–0.001	–0.159	–0.001	–0.267	0.000	–0.037	0.000	–0.092	–0.001	–0.168	–0.001
Ca4227	0.056	0.016	0.065	0.012	0.073	0.009	0.083	0.010	0.020	–0.003	0.014	0.000	0.010	0.005	0.010	–0.002	0.010	–0.002	0.005	–0.001
G4300	–1.536	0.096	–1.803	0.106	–1.797	0.107	–1.632	0.104	–1.233	0.009	–2.747	0.009	–4.093	0.022	–0.717	–0.008	–1.625	–0.016	–2.813	–0.016
Fe4383	–0.005	–0.017	–0.583	–0.028	–0.842	–0.031	–0.847	–0.033	–0.185	0.001	–1.120	–0.009	–3.370	–0.015	0.059	0.003	–0.361	–0.002	–1.449	–0.010
Ca4455	–0.011	–0.005	0.002	–0.012	0.025	–0.019	0.047	–0.023	–0.003	–0.004	–0.014	–0.006	–0.027	–0.009	0.169	–0.006	0.154	–0.007	0.138	–0.009
Fe4531	0.437	0.000	0.379	–0.007	0.324	–0.015	0.282	–0.023	0.075	–0.010	0.056	–0.009	0.044	–0.008	0.039	–0.002	0.037	–0.004	0.026	–0.003
$C_2$4668	–0.172	0.092	–0.122	0.070	–0.077	0.047	–0.034	0.032	0.019	0.016	0.027	0.011	–0.033	0.008	0.113	0.017	0.104	0.007	0.087	0.003
Hβ	6.965	0.005	6.958	–0.003	6.534	–0.009	5.978	–0.012	5.860	0.023	8.441	0.015	9.371	–0.005	3.758	0.037	5.933	0.037	7.664	0.026
Fe5015	0.370	–0.015	0.332	–0.020	0.294	–0.023	0.266	–0.025	0.086	–0.033	0.068	–0.028	–0.009	–0.023	0.150	–0.029	0.102	–0.033	0.056	–0.030
Mg1	–0.001	0.001	–0.005	0.001	–0.007	0.000	–0.007	0.000	0.007	0.000	0.004	0.000	–0.008	0.000	0.007	0.000	0.007	0.000	0.003	0.000
Mg2	0.018	0.001	0.015	0.001	0.013	0.001	0.013	0.002	0.010	0.000	0.009	0.000	0.001	0.001	0.009	0.000	0.009	0.000	0.006	0.000
Mgb	0.441	0.062	0.431	0.065	0.423	0.070	0.460	0.094	0.082	0.011	0.107	0.019	0.141	0.026	0.044	–0.008	0.050	–0.006	0.047	–0.005
Fe5270	0.140	0.028	0.161	0.030	0.178	0.031	0.191	0.029	0.006	0.003	0.007	0.003	0.007	0.003	0.011	0.000	0.012	0.000	0.011	0.001
Fe5335	0.221	0.002	0.233	0.001	0.236	0.001	0.235	0.001	0.013	0.002	0.012	0.002	0.012	0.002	0.014	0.005	0.009	0.003	0.007	0.002
Fe5406	0.052	–0.027	0.084	–0.025	0.105	–0.022	0.118	–0.020	0.006	0.001	0.005	0.000	0.005	0.000	0.005	0.000	0.006	0.001	0.005	0.001
Fe5709	0.005	0.004	0.010	0.004	0.013	0.003	0.014	0.003	0.001	0.000	0.002	0.000	0.002	0.000	0.002	0.000	0.002	0.000	0.002	0.000
Fe5782	0.003	–0.001	0.003	0.000	0.003	0.000	0.003	0.000	0.002	–0.001	0.002	0.000	0.001	0.000	0.002	–0.001	0.002	–0.001	0.002	0.000
NaD	0.203	–0.027	0.206	–0.026	0.204	–0.025	0.208	–0.026	–0.006	–0.002	0.007	–0.003	0.023	–0.006	–0.061	–0.002	–0.044	–0.001	–0.032	–0.001
TiO1	0.002	0.000	0.002	0.000	0.001	0.000	0.001	0.000	0.003	0.000	0.003	0.000	0.003	0.000	0.003	0.000	0.003	0.000	0.003	0.000
TiO2	0.003	0.000	0.002	0.000	0.002	0.000	0.001	0.000	0.003	0.000	0.003	0.000	0.003	0.000	0.004	0.000	0.004	0.000	0.004	0.000
HδA	8.707	0.017	9.191	0.010	8.795	0.013	7.988	0.017	6.382	0.034	10.840	0.030	14.890	0.010	4.039	0.043	7.264	0.057	10.780	0.060
HγA	8.382	–0.010	8.985	–0.028	8.721	–0.040	7.970	–0.045	6.501	0.016	11.030	0.020	15.200	–0.010	4.057	0.045	7.276	0.056	10.900	0.050
HδF	6.840	0.018	6.816	0.015	6.399	0.016	5.819	0.018	5.404	0.022	8.132	0.018	9.622	–0.001	3.491	0.032	5.742	0.036	7.629	0.027
HγF	6.864	0.020	6.908	0.006	6.534	–0.003	5.967	–0.010	5.577	0.021	8.274	0.015	9.765	–0.002	3.621	0.040	5.845	0.040	7.742	0.030
D4000	1.235	0.004	1.293	0.004	1.312	0.003	1.311	0.004	1.079	0.001	1.198	0.002	1.378	0.001	1.017	–0.001	1.083	0.001	1.186	0.001

Table A.8. Spectra degraded to the Lick resolution: I_{sol} and $I_{enh} - I_{sol}$ for $[Z/Z_\odot] = -1.0$.

T_{eff}	4000								5250							
log g	1.5		2.5		3.5		4.5		1.5		2.5		3.5		4.5	
	I_{sol}	(δI)	I_{sol}	(δI)	I_{sol}	(δI)	I_{sol}	(δI)	I_{sol}	(δI)	I_{sol}	(δI)	I_{sol}	(δI)	I_{sol}	(δI)
CN1	0.089	–0.033	0.071	–0.005	0.041	0.014	0.006	0.027	–0.057	0.006	–0.059	0.004	–0.060	0.005	–0.063	0.010
CN2	0.164	–0.033	0.162	–0.007	0.146	0.011	0.108	0.026	–0.038	0.008	–0.044	0.007	–0.047	0.008	–0.051	0.014
Ca4227	1.588	1.239	2.708	1.028	4.224	0.745	4.968	0.642	0.220	0.143	0.138	0.237	0.177	0.336	0.473	0.433
G4300	8.022	–0.816	7.811	–1.098	7.276	–1.097	5.214	–0.651	6.567	–0.913	7.165	–0.782	7.436	–0.750	7.872	–0.991
Fe4383	7.025	–1.573	7.648	–1.999	8.145	–2.227	6.902	–1.811	2.438	–0.437	2.846	–0.690	3.420	–1.028	4.332	–1.523
Ca4455	1.554	–0.148	1.637	–0.193	1.606	–0.202	1.290	–0.159	0.535	–0.064	0.485	–0.052	0.448	–0.035	0.457	–0.035
Fe4531	4.418	–0.201	4.273	–0.220	4.314	–0.210	4.024	–0.117	2.440	–0.110	2.362	–0.120	2.258	–0.132	2.214	–0.174
$C_2$4668	2.017	–0.448	1.141	–0.060	0.559	0.426	0.093	0.632	0.637	–0.164	0.584	–0.171	0.528	–0.155	0.455	–0.099
Hβ	0.122	0.044	–0.177	0.062	–0.412	0.122	–0.507	0.113	1.857	0.100	1.584	0.093	1.351	0.090	1.184	0.079
Fe5015	4.545	–0.476	3.591	–0.351	3.172	–0.107	2.530	0.017	3.545	–0.211	3.335	–0.196	3.156	–0.217	3.032	–0.300
Mg1	0.192	0.019	0.283	0.022	0.367	0.029	0.396	0.054	0.009	–0.003	0.009	–0.003	0.008	0.000	0.009	0.007
Mg2	0.328	0.047	0.480	0.058	0.622	0.077	0.629	0.103	0.045	0.002	0.056	0.008	0.084	0.017	0.140	0.035
Mgb	3.513	0.925	5.151	1.078	6.175	1.249	5.304	1.227	0.325	0.272	0.799	0.430	1.816	0.674	3.485	1.040
Fe5270	3.181	–0.301	3.433	–0.399	3.710	–0.474	3.524	–0.413	1.354	–0.015	1.398	–0.042	1.551	–0.109	1.851	–0.211
Fe5335	3.079	–0.346	3.274	–0.506	3.471	–0.646	3.186	–0.618	1.315	–0.063	1.402	–0.096	1.543	–0.158	1.809	–0.260
Fe5406	2.015	–0.297	2.258	–0.409	2.499	–0.487	2.335	–0.444	0.665	–0.102	0.725	–0.124	0.856	–0.180	1.099	–0.277
Fe5709	1.085	–0.042	0.952	–0.045	0.777	–0.040	0.488	–0.022	0.434	–0.074	0.449	–0.078	0.453	–0.083	0.436	–0.087
Fe5782	0.733	–0.157	0.689	–0.193	0.551	–0.215	0.343	–0.180	0.110	–0.014	0.120	–0.017	0.124	–0.019	0.120	–0.021
NaD	2.289	–0.581	3.759	–0.967	5.984	–1.490	7.476	–1.664	0.384	–0.070	0.476	–0.107	0.730	–0.180	1.275	–0.301
TiO1	0.010	0.004	0.011	0.010	0.016	0.022	0.012	0.025	0.002	0.000	0.002	0.000	0.002	0.000	0.002	0.000
TiO2	0.037	–0.001	0.036	0.010	0.043	0.029	0.033	0.035	0.008	–0.001	0.007	–0.001	0.006	–0.001	0.005	–0.001
HδA	–6.301	2.469	–6.111	2.418	–5.889	2.268	–3.680	1.409	–0.279	0.483	–0.835	0.681	–1.718	0.983	–3.116	1.512
HγA	–11.530	1.120	–12.670	1.810	–13.320	2.100	–10.760	1.567	–5.153	1.089	–6.153	1.043	–7.083	1.164	–8.627	1.745
HδF	–3.226	0.622	–3.284	0.747	–3.251	0.836	–2.193	0.621	0.239	0.273	0.069	0.309	–0.252	0.393	–0.819	0.590
HγF	–3.459	0.434	–3.955	0.647	–4.248	0.729	–3.435	0.557	–0.821	0.509	–1.477	0.505	–2.064	0.541	–2.879	0.780
D4000	2.935	–0.242	2.836	–0.339	2.884	–0.382	2.637	–0.275	1.652	–0.012	1.621	–0.037	1.667	–0.066	1.795	–0.109

T_{eff}	7250								10 000						13 000					
log g	1.5		2.5		3.5		4.5		2.5		3.5		4.5		2.5		3.5		4.5	
	I_{sol}	(δI)	I_{sol}	(δI)	I_{sol}	(δI)	I_{sol}	(δI)	I_{sol}	(δI)	I_{sol}	(δI)	I_{sol}	(δI)	I_{sol}	(δI)	I_{sol}	(δI)	I_{sol}	(δI)
CN1	–0.174	0.000	–0.191	0.001	–0.185	0.001	–0.170	0.001	–0.124	0.000	–0.225	0.000	–0.333	0.001	–0.074	0.001	–0.143	0.000	–0.226	0.000
CN2	–0.109	–0.001	–0.130	0.001	–0.129	0.000	–0.119	0.000	–0.069	0.000	–0.157	0.000	–0.267	0.002	–0.036	0.000	–0.091	0.000	–0.167	0.000
Ca4227	0.090	0.009	0.095	0.011	0.101	0.011	0.118	0.014	0.030	–0.006	0.028	–0.004	0.036	–0.002	0.026	–0.008	0.025	–0.009	0.018	–0.008
G4300	–1.295	0.140	–1.553	0.143	–1.514	0.122	–1.324	0.098	–1.163	0.047	–2.665	0.049	–4.058	0.066	–0.722	0.007	–1.613	0.007	–2.792	0.009
Fe4383	0.212	0.087	–0.434	0.054	–0.724	0.008	–0.772	–0.035	–0.096	–0.004	–1.003	–0.018	–3.254	–0.007	0.103	–0.010	–0.312	–0.005	–1.401	0.004
Ca4455	0.076	–0.032	0.064	–0.026	0.062	–0.023	0.074	–0.027	–0.024	0.000	–0.034	–0.005	–0.049	–0.010	0.164	–0.016	0.152	–0.019	0.134	–0.022
Fe4531	0.820	–0.057	0.743	–0.047	0.651	–0.046	0.578	–0.053	0.131	–0.021	0.110	–0.021	0.100	–0.026	0.079	–0.008	0.076	–0.013	0.060	–0.014
$C_2$4668	–0.173	0.094	–0.144	0.085	–0.104	0.067	–0.040	0.043	–0.093	0.053	–0.050	0.042	–0.083	0.037	0.025	0.044	0.041	0.026	0.051	0.013
Hβ	7.068	0.016	7.086	–0.006	6.680	–0.023	6.139	–0.036	5.808	0.034	8.380	0.049	9.377	0.004	3.754	–0.024	5.902	–0.006	7.628	–0.003
Fe5015	0.946	–0.173	0.913	–0.175	0.851	–0.171	0.793	–0.166	0.118	–0.066	0.096	–0.053	0.020	–0.045	0.180	–0.059	0.123	–0.068	0.071	–0.066
Mg1	–0.002	0.000	–0.005	0.000	–0.008	0.000	–0.008	0.000	0.006	0.000	0.003	0.000	–0.009	0.001	0.007	0.000	0.007	0.000	0.003	0.000
Mg2	0.024	–0.001	0.021	0.000	0.018	0.000	0.020	0.002	0.011	0.001	0.010	0.001	0.003	0.001	0.010	0.000	0.010	0.000	0.007	0.000
Mgb	0.424	0.105	0.405	0.121	0.409	0.141	0.512	0.197	0.091	0.041	0.151	0.047	0.219	0.040	0.034	–0.002	0.049	0.002	0.061	0.002
Fe5270	0.386	–0.003	0.401	0.014	0.404	0.027	0.407	0.036	0.025	–0.005	0.017	0.001	0.019	0.003	0.024	–0.005	0.025	–0.003	0.021	–0.001
Fe5335	0.439	–0.030	0.469	–0.025	0.480	–0.019	0.486	–0.013	0.029	0.005	0.030	0.003	0.036	0.001	0.028	0.013	0.019	0.007	0.014	0.004
Fe5406	0.131	–0.055	0.182	–0.060	0.222	–0.062	0.250	–0.060	0.018	–0.002	0.014	–0.001	0.014	–0.002	0.015	–0.003	0.017	–0.002	0.014	0.000
Fe5709	0.020	0.004	0.037	0.001	0.048	–0.003	0.053	–0.006	0.000	0.001	0.001	0.001	0.002	0.001	0.000	0.001	0.001	0.001	0.001	0.001
Fe5782	0.008	0.000	0.007	0.001	0.007	0.002	0.007	0.002	0.007	–0.004	0.004	–0.002	0.003	–0.001	0.006	–0.004	0.006	–0.004	0.004	–0.003
NaD	0.240	–0.019	0.235	–0.019	0.231	–0.020	0.241	–0.024	0.007	–0.007	0.026	–0.008	0.056	–0.015	–0.058	–0.004	–0.043	–0.003	–0.030	–0.002
TiO1	0.002	0.000	0.002	0.000	0.002	0.000	0.001	0.000	0.003	0.000	0.003	0.000	0.003	0.000	0.004	0.000	0.004	0.000	0.004	0.000
TiO2	0.004	0.000	0.003	0.000	0.002	0.000	0.002	0.000	0.004	0.000	0.003	0.000	0.003	0.000	0.004	0.000	0.004	0.000	0.004	0.000
HδA	8.471	0.076	9.119	0.029	8.749	0.034	7.986	0.046	6.301	0.000	10.720	0.020	14.840	–0.020	4.007	–0.044	7.212	–0.031	10.720	–0.020
HγA	8.134	–0.029	8.847	–0.056	8.599	–0.048	7.888	–0.040	6.397	–0.025	10.890	0.000	15.150	–0.060	4.048	–0.034	7.235	–0.027	10.840	–0.030
HδF	6.664	0.087	6.718	0.065	6.328	0.063	5.782	0.063	5.327	0.009	8.049	0.025	9.594	–0.004	3.453	–0.030	5.686	–0.016	7.572	–0.011
HγF	6.822	0.025	6.920	–0.001	6.560	–0.009	6.013	–0.015	5.518	0.012	8.207	0.023	9.754	–0.012	3.618	–0.025	5.815	–0.012	7.704	–0.007
D4000	1.265	0.005	1.324	0.004	1.342	0.001	1.342	0.003	1.079	0.000	1.197	0.001	1.380	–0.001	1.016	–0.001	1.082	–0.001	1.184	0.000

Table A.9. Spectra degraded to the Lick resolution: I_{sol} and $I_{enh} - I_{sol}$ for $[Z/Z_{\odot}] = -0.5$.

T_{eff}	4000								5250							
log g	1.5		2.5		3.5		4.5		1.5		2.5		3.5		4.5	
	I_{sol}	(δI)	I_{sol}	(δI)	I_{sol}	(δI)	I_{sol}	(δI)	I_{sol}	(δI)	I_{sol}	(δI)	I_{sol}	(δI)	I_{sol}	(δI)
CN1	0.133	–0.066	0.096	–0.035	0.043	–0.007	–0.015	0.017	–0.046	–0.014	–0.042	–0.017	–0.042	–0.016	–0.050	–0.007
CN2	0.219	–0.068	0.196	–0.041	0.160	–0.017	0.097	0.010	–0.027	–0.012	–0.024	–0.015	–0.025	–0.013	–0.031	–0.003
Ca4227	3.043	1.256	4.016	0.969	5.538	0.528	6.193	0.408	0.147	0.385	0.063	0.493	0.145	0.590	0.592	0.676
G4300	8.116	–0.652	7.797	–0.897	7.596	–0.977	5.725	–0.235	7.432	–0.648	7.634	–0.563	7.659	–0.609	7.824	–0.863
Fe4383	8.648	–1.884	8.943	–2.309	9.779	–2.851	8.436	–2.257	3.393	–0.654	3.847	–0.888	4.441	–1.204	5.499	–1.786
Ca4455	1.982	–0.171	2.043	–0.205	2.104	–0.253	1.777	–0.187	0.721	–0.038	0.689	–0.047	0.678	–0.054	0.718	–0.066
Fe4531	5.498	–0.224	5.246	–0.267	5.487	–0.375	5.179	–0.172	3.257	–0.197	3.175	–0.214	3.084	–0.245	3.062	–0.292
$C_2$4668	2.816	–0.561	1.734	0.319	1.257	1.285	0.799	1.806	1.593	–0.501	1.516	–0.551	1.317	–0.483	1.060	–0.320
Hβ	–0.001	0.099	–0.286	0.184	–0.505	0.358	–0.618	0.426	2.014	0.117	1.761	0.096	1.513	0.091	1.302	0.084
Fe5015	5.683	–0.346	4.839	–0.125	4.804	0.179	3.995	0.612	5.049	–0.302	4.696	–0.274	4.419	–0.310	4.262	–0.447
Mg1	0.254	0.006	0.326	0.006	0.414	0.001	0.462	0.034	0.026	–0.008	0.026	–0.009	0.024	–0.004	0.025	0.009
Mg2	0.428	0.047	0.564	0.053	0.724	0.049	0.748	0.094	0.069	0.000	0.084	0.007	0.122	0.021	0.200	0.045
Mgb	4.466	1.231	5.954	1.267	7.027	1.175	6.158	1.290	0.539	0.308	1.131	0.539	2.457	0.856	4.623	1.252
Fe5270	3.864	–0.417	3.986	–0.504	4.375	–0.635	4.278	–0.485	2.024	–0.078	2.080	–0.123	2.274	–0.198	2.663	–0.304
Fe5335	3.935	–0.517	4.025	–0.714	4.300	–0.981	3.952	–0.881	1.828	–0.100	2.001	–0.162	2.228	–0.253	2.613	–0.386
Fe5406	2.608	–0.410	2.782	–0.517	3.106	–0.660	2.927	–0.544	0.977	–0.155	1.056	–0.179	1.219	–0.247	1.547	–0.371
Fe5709	1.439	–0.053	1.265	–0.056	1.090	–0.054	0.754	0.004	0.744	–0.094	0.745	–0.099	0.738	–0.107	0.711	–0.114
Fe5782	1.114	–0.218	1.010	–0.281	0.832	–0.362	0.557	–0.348	0.255	–0.023	0.275	–0.029	0.282	–0.035	0.283	–0.043
NaD	3.532	–0.904	5.149	–1.365	8.010	–2.219	9.862	–2.349	0.528	–0.116	0.663	–0.172	1.021	–0.269	1.785	–0.431
TiO1	0.018	0.012	0.025	0.028	0.043	0.049	0.043	0.064	0.002	0.001	0.003	0.001	0.003	0.001	0.003	0.001
TiO2	0.057	0.010	0.064	0.034	0.089	0.065	0.084	0.089	0.012	–0.002	0.011	–0.002	0.010	–0.002	0.009	–0.002
HδA	–8.662	3.224	–7.875	2.993	–7.731	2.893	–5.120	1.537	–1.283	0.851	–1.801	1.115	–2.666	1.468	–4.210	2.074
HγA	–13.790	1.350	–14.360	1.990	–15.550	2.590	–12.960	1.470	–6.562	0.932	–7.170	0.920	–7.913	1.149	–9.410	1.856
HδF	–4.454	0.851	–4.217	0.916	–4.183	1.042	–2.959	0.661	–0.124	0.272	–0.204	0.321	–0.466	0.431	–1.070	0.670
HγF	–3.993	0.502	–4.241	0.631	–4.596	0.709	–3.871	0.367	–1.149	0.454	–1.591	0.426	–2.058	0.498	–2.784	0.753
D4000	3.357	–0.288	3.137	–0.367	3.203	–0.455	2.910	–0.315	1.897	–0.035	1.826	–0.057	1.863	–0.091	2.022	–0.156

T_{eff}	7250								10 000						13 000					
log g	1.5		2.5		3.5		4.5		2.5		3.5		4.5		2.5		3.5		4.5	
	I_{sol}	(δI)	I_{sol}	(δI)	I_{sol}	(δI)	I_{sol}	(δI)	I_{sol}	(δI)	I_{sol}	(δI)	I_{sol}	(δI)	I_{sol}	(δI)	I_{sol}	(δI)	I_{sol}	(δI)
CN1	–0.168	–0.001	–0.191	0.001	–0.185	0.002	–0.174	0.003	–0.122	0.002	–0.224	0.003	–0.332	0.004	–0.071	0.001	–0.140	0.001	–0.222	0.001
CN2	–0.102	–0.001	–0.129	0.001	–0.128	0.001	–0.121	0.002	–0.067	0.002	–0.155	0.002	–0.265	0.004	–0.034	0.001	–0.087	0.001	–0.163	0.001
Ca4227	0.105	0.012	0.110	0.020	0.118	0.026	0.148	0.036	0.024	0.000	0.031	0.003	0.054	–0.002	0.036	–0.007	0.035	–0.007	0.029	–0.009
G4300	–0.966	0.163	–1.219	0.152	–1.146	0.117	–0.901	0.066	–1.073	0.098	–2.564	0.113	–3.980	0.126	–0.711	0.003	–1.576	0.014	–2.737	0.020
Fe4383	0.365	0.164	–0.321	0.129	–0.608	0.058	–0.652	–0.045	0.014	0.018	–0.843	–0.002	–3.078	0.025	0.159	–0.007	–0.235	0.000	–1.296	0.007
Ca4455	0.184	–0.042	0.164	–0.043	0.139	–0.037	0.122	–0.031	–0.043	–0.001	–0.055	–0.008	–0.071	–0.018	0.150	–0.009	0.141	–0.016	0.121	–0.022
Fe4531	1.289	–0.084	1.228	–0.061	1.111	–0.042	0.995	–0.036	0.208	–0.022	0.181	–0.025	0.171	–0.035	0.127	–0.002	0.121	–0.008	0.099	–0.012
$C_2$4668	–0.049	0.045	–0.040	0.036	–0.045	0.040	–0.014	0.041	–0.274	0.086	–0.178	0.073	–0.163	0.070	–0.118	0.075	–0.083	0.049	–0.036	0.030
Hβ	7.192	0.046	7.239	0.019	6.858	–0.007	6.332	–0.024	5.838	–0.010	8.453	–0.026	9.447	–0.050	3.683	–0.034	5.825	–0.021	7.566	–0.023
Fe5015	1.890	–0.307	1.832	–0.284	1.701	–0.259	1.573	–0.239	0.182	–0.095	0.140	–0.076	0.062	–0.069	0.236	–0.076	0.156	–0.090	0.082	–0.091
Mg1	0.000	–0.002	–0.003	–0.002	–0.006	–0.002	–0.008	–0.002	0.006	0.000	0.003	0.000	–0.009	0.001	0.008	–0.001	0.007	0.000	0.003	0.000
Mg2	0.031	–0.002	0.026	–0.001	0.024	0.001	0.028	0.003	0.013	0.001	0.013	0.001	0.006	0.001	0.010	–0.001	0.010	0.000	0.007	0.000
Mgb	0.326	0.157	0.303	0.182	0.363	0.215	0.617	0.309	0.126	0.065	0.217	0.062	0.292	0.051	–0.010	0.012	0.022	0.019	0.056	0.023
Fe5270	0.706	0.021	0.739	0.040	0.743	0.056	0.746	0.074	0.076	–0.017	0.056	–0.005	0.059	0.000	0.048	–0.010	0.053	–0.007	0.045	–0.001
Fe5335	0.663	–0.014	0.733	–0.013	0.780	–0.006	0.823	0.012	0.053	0.023	0.067	0.015	0.089	0.008	0.060	0.025	0.040	0.020	0.030	0.014
Fe5406	0.249	–0.059	0.301	–0.067	0.350	–0.074	0.398	–0.075	0.050	–0.010	0.039	–0.006	0.038	–0.005	0.039	–0.008	0.046	–0.007	0.039	–0.002
Fe5709	0.057	0.008	0.097	–0.001	0.121	–0.009	0.132	–0.016	–0.004	0.003	–0.001	0.002	0.003	0.002	–0.004	0.003	–0.003	0.003	–0.001	0.002
Fe5782	0.024	–0.001	0.025	0.001	0.025	0.002	0.025	0.003	0.017	–0.010	0.010	–0.005	0.006	–0.003	0.013	–0.012	0.015	–0.011	0.011	–0.008
NaD	0.273	–0.021	0.262	–0.024	0.259	–0.029	0.287	–0.041	0.041	–0.020	0.070	–0.022	0.109	–0.028	–0.042	–0.015	–0.031	–0.013	–0.020	–0.009
TiO1	0.003	0.000	0.003	0.000	0.002	0.000	0.002	0.000	0.004	0.000	0.004	0.000	0.003	0.000	0.005	0.000	0.005	0.000	0.005	0.000
TiO2	0.005	0.000	0.004	0.000	0.003	0.000	0.003	0.000	0.004	0.000	0.004	0.000	0.003	0.000	0.004	0.000	0.004	0.000	0.004	0.000
HδA	8.153	0.134	9.056	0.054	8.718	0.049	8.049	0.052	6.187	–0.030	10.630	–0.050	14.780	–0.090	3.863	–0.060	7.049	–0.052	10.550	–0.040
HγA	7.891	–0.083	8.721	–0.092	8.466	–0.057	7.762	–0.005	6.265	–0.079	10.790	–0.100	15.070	–0.150	3.942	–0.042	7.089	–0.046	10.680	–0.060
HδF	6.433	0.152	6.596	0.115	6.240	0.104	5.749	0.098	5.246	–0.017	8.015	–0.026	9.580	–0.042	3.335	–0.038	5.563	–0.031	7.464	–0.028
HγF	6.787	0.016	6.948	–0.008	6.600	–0.011	6.062	–0.002	5.471	–0.017	8.204	–0.035	9.765	–0.062	3.540	–0.030	5.724	–0.025	7.624	–0.026
D4000	1.308	0.011	1.370	0.008	1.384	0.007	1.388	0.006	1.081	–0.001	1.199	–0.001	1.383	–0.005	1.014	0.000	1.078	0.000	1.179	0.000

Table A.10. Spectra degraded to the Lick resolution: I_{sol} and $I_{enh} - I_{sol}$ for $[Z/Z_{\odot}] = 0.0$.

T_{eff}	4000								5250							
log g	1.5		2.5		3.5		4.5		1.5		2.5		3.5		4.5	
	I_{sol}	(δI)	I_{sol}	(δI)	I_{sol}	(δI)	I_{sol}	(δI)	I_{sol}	(δI)	I_{sol}	(δI)	I_{sol}	(δI)	I_{sol}	(δI)
CN1	0.159	–0.083	0.113	–0.059	0.043	–0.029	–0.041	0.003	0.013	–0.065	0.016	–0.066	0.009	–0.059	–0.011	–0.042
CN2	0.249	–0.089	0.215	–0.068	0.160	–0.043	0.081	–0.011	0.038	–0.065	0.041	–0.066	0.036	–0.058	0.019	–0.041
Ca4227	4.836	0.905	5.351	0.691	6.274	0.369	6.772	0.193	–0.078	0.800	–0.093	0.888	0.077	0.957	0.727	1.004
G4300	8.386	–0.407	7.929	–0.640	7.685	–0.704	6.668	–0.096	7.790	–0.337	7.828	–0.361	7.739	–0.465	7.684	–0.693
Fe4383	10.310	–2.175	10.040	–2.614	10.610	–3.229	10.130	–3.096	4.344	–0.773	4.787	–0.995	5.464	–1.365	6.752	–2.094
Ca4455	2.425	–0.207	2.450	–0.235	2.511	–0.280	2.330	–0.280	0.954	–0.039	0.924	–0.056	0.950	–0.090	1.035	–0.129
Fe4531	6.957	–0.325	6.431	–0.404	6.574	–0.616	6.594	–0.589	4.134	–0.296	4.041	–0.323	3.959	–0.368	3.980	–0.433
$C_2$4668	3.960	–0.748	2.820	0.966	2.833	2.543	2.713	3.776	3.511	–1.397	3.339	–1.450	2.776	–1.192	2.097	–0.770
Hβ	–0.173	0.304	–0.316	0.502	–0.325	0.810	–0.393	1.088	2.238	0.117	2.013	0.081	1.762	0.062	1.521	0.053
Fe5015	7.587	–0.114	6.828	0.190	7.055	0.549	6.562	1.242	6.708	–0.409	6.195	–0.378	5.810	–0.435	5.597	–0.624
Mg1	0.307	–0.018	0.350	–0.020	0.405	–0.029	0.488	–0.021	0.063	–0.026	0.062	–0.026	0.054	–0.015	0.054	0.006
Mg2	0.539	0.041	0.645	0.032	0.764	0.007	0.840	0.014	0.113	–0.008	0.129	0.001	0.176	0.021	0.278	0.052
Mgb	5.687	1.544	6.901	1.312	7.574	1.012	6.907	0.940	0.913	0.434	1.551	0.732	3.199	1.110	5.872	1.430
Fe5270	4.552	–0.561	4.509	–0.637	4.814	–0.768	5.037	–0.712	2.833	–0.155	2.890	–0.221	3.113	–0.295	3.573	–0.385
Fe5335	4.924	–0.735	4.811	–0.999	4.906	–1.365	4.761	–1.465	2.525	–0.141	2.781	–0.230	3.098	–0.344	3.607	–0.515
Fe5406	3.234	–0.541	3.310	–0.633	3.571	–0.789	3.614	–0.773	1.341	–0.219	1.464	–0.259	1.672	–0.336	2.068	–0.477
Fe5709	1.811	–0.066	1.585	–0.078	1.373	–0.074	1.075	–0.003	1.145	–0.100	1.114	–0.106	1.083	–0.112	1.042	–0.123
Fe5782	1.508	–0.305	1.293	–0.412	0.990	–0.541	0.691	–0.615	0.486	–0.025	0.519	–0.039	0.531	–0.049	0.542	–0.066
NaD	5.270	–1.398	6.679	–1.925	9.161	–2.892	11.510	–3.652	0.807	–0.173	0.980	–0.243	1.450	–0.362	2.479	–0.574
TiO1	0.037	0.031	0.061	0.058	0.102	0.085	0.121	0.110	0.000	0.002	0.002	0.002	0.003	0.001	0.003	0.001
TiO2	0.097	0.035	0.125	0.073	0.178	0.104	0.199	0.134	0.017	–0.002	0.016	–0.003	0.015	–0.003	0.013	–0.003
HδA	–11.400	3.928	–9.785	3.582	–9.208	3.343	–7.163	2.076	–3.064	1.684	–3.477	2.000	–4.210	2.351	–5.700	2.951
HγA	–16.830	1.650	–16.380	2.190	–17.000	2.720	–15.860	1.880	–7.634	0.707	–8.119	0.849	–8.830	1.200	–10.330	2.034
HδF	–5.890	1.204	–5.226	1.193	–4.875	1.223	–3.860	0.902	–0.594	0.366	–0.620	0.449	–0.811	0.569	–1.385	0.820
HγF	–4.936	0.677	–4.765	0.656	–4.866	0.608	–4.535	0.247	–1.322	0.423	–1.693	0.437	–2.099	0.527	–2.729	0.782
D4000	3.914	–0.378	3.449	–0.393	3.384	–0.456	3.190	–0.382	2.191	–0.014	2.065	–0.043	2.082	–0.086	2.264	–0.173

T_{eff}	7250							
log g	1.5		2.5		3.5		4.5	
	I_{sol}	(δI)	I_{sol}	(δI)	I_{sol}	(δI)	I_{sol}	(δI)
CN1	–0.162	–0.002	–0.194	0.001	–0.189	0.002	–0.183	0.004
CN2	–0.097	–0.002	–0.132	0.001	–0.131	0.002	–0.129	0.004
Ca4227	0.166	–0.019	0.158	0.005	0.160	0.028	0.208	0.051
G4300	–0.564	0.183	–0.811	0.136	–0.639	0.066	–0.285	–0.032
Fe4383	0.340	0.226	–0.363	0.186	–0.538	0.097	–0.524	–0.062
Ca4455	0.302	–0.053	0.278	–0.067	0.246	–0.069	0.212	–0.066
Fe4531	1.851	–0.101	1.851	–0.091	1.747	–0.078	1.615	–0.060
$C_2$4668	0.077	0.021	0.123	–0.003	0.109	–0.001	0.103	0.018
Hβ	7.290	0.076	7.404	0.053	7.067	0.026	6.579	0.009
Fe5015	3.292	–0.479	3.185	–0.428	2.945	–0.378	2.718	–0.337
Mg1	0.004	–0.004	0.000	–0.004	–0.003	–0.003	–0.006	–0.003
Mg2	0.040	–0.004	0.034	–0.002	0.032	0.000	0.041	0.005
Mgb	0.261	0.140	0.216	0.190	0.345	0.266	0.832	0.416
Fe5270	1.140	0.047	1.224	0.053	1.257	0.071	1.298	0.107
Fe5335	0.929	0.021	1.054	0.023	1.170	0.029	1.314	0.051
Fe5406	0.453	–0.099	0.487	–0.091	0.521	–0.085	0.583	–0.081
Fe5709	0.143	0.006	0.221	–0.008	0.265	–0.020	0.284	–0.030
Fe5782	0.071	–0.007	0.076	–0.003	0.078	0.000	0.078	0.002
NaD	0.321	–0.027	0.308	–0.035	0.310	–0.044	0.374	–0.067
TiO1	0.003	0.000	0.003	0.000	0.003	0.000	0.003	0.000
TiO2	0.007	–0.001	0.006	–0.001	0.005	–0.001	0.004	–0.001
HδA	7.723	0.170	9.030	0.082	8.694	0.060	8.163	0.079
HγA	7.643	–0.176	8.669	–0.146	8.301	–0.069	7.566	0.069
HδF	6.132	0.181	6.486	0.134	6.154	0.111	5.744	0.111
HγF	6.743	–0.027	7.010	–0.034	6.649	–0.025	6.118	0.018
D4000	1.372	0.022	1.441	0.019	1.450	0.016	1.459	0.014